Master's thesis

NTNU
Norwegian University of Science and Technology
Faculty of Information Technology and Electrical Engineering
Department of Engineering Cybernetics

Jonas Åsnes Sagild

Track Level Fusion of Radar and AIS for Autonomous Surface Vessels

Master's thesis in Cybernetics and Robotics
Supervisor: Edmund Førland Brekke
Co-supervisor: Audun Gullikstad Hem
June 2021

NTNU
Kunnskap for en bedre verden

Jonas Åsnes Sagild

Track Level Fusion of Radar and AIS for Autonomous Surface Vessels

Master's thesis in Cybernetics and Robotics
Supervisor: Edmund Førland Brekke
Co-supervisor: Audun Gullikstad Hem
June 2021

Norwegian University of Science and Technology
Faculty of Information Technology and Electrical Engineering
Department of Engineering Cybernetics

NTNU
Norwegian University of
Science and Technology

Abstract

This thesis concerns the track level approach to the fusion of Automatic Identification System (AIS) messages and radar measurements. A complete track level approach to AIS-radar fusion is developed, consisting of solutions to the track-to-track association and the track-to-track fusion problems.

Track-to-track association is typically solved by a hypothesis test, which requires information from the covariances of the estimates. Unfortunately, covariance information is not always available from the individual tracking systems. An alternative approach that can be used in such cases is a counting technique, where the number of good matches is used as a test statistic. This thesis compares the counting technique with a conventional hypothesis test by simulations using a complete multi-target tracking system. Furthermore, since the data association of the radar tracking system inevitably makes it nontrivial to decide on a ground truth, we also propose a ground truth assessment scheme using a sliding window approach. The results indicate that the counting technique performs at par with the hypothesis test under certain tracking conditions.

Further, the complete AIS-radar track level multi-target tracking system is compared to a measurement level tracking system. The results suggest that the track level approach is a bit less consistent but perform better in terms of positional error.

Sammendrag

Denne oppgaven omhandler "track level"-metoden (spornivåtilnærmingen) for sammenslåing av "Automatic Identification System (AIS)"-meldinger og radarmålinger. En fullstendig tilnærming på spornivå til AIS-radarfusjon har blitt utviklet, bestående av løsninger på spor-til-spor-tilknytning og spor-til-spor-sammenslåingsproblemer.

Spor-til-spor-tilknytning løses vanligvis ved en hypotesetest som krever kovariansinformasjon fra estimatene. Dessverre er kovariansinformasjon ikke alltid tilgjengelig fra de enkelte sporingssystemene. En alternativ tilnærming som kan brukes i slike tilfeller er en telleteknikk hvor antall gode treff brukes som en teststatistikk. Denne oppgaven sammenligner telleteknikken med en konvensjonell hypotesetest ved simuleringer av et fullstendig fler-måls sporingssytem system. Da datatilknytningen til radarsporingssystemet gjør det vanskelig å bestemme seg for en "ground truth", foreslås også en ny måte å evaluere "ground truth" ved hjelp av en glidende vindu-tilnærming. Resultatene indikerer at telleteknikken presterer like godt som hypotesetesten under visse sporingsforhold.

Videre sammenlignes AIS-radar spornivåtilnærmingen med en målesnivåstilnærming. Resultatene antyder at spornivåtilnærmingen er litt mindre konsistent, men fungerer bedre når det gjelder posisjonsfeil.

Preface

This thesis constitutes my master's degree in Cybernetic and Robotics at the Norwegian University of Science and Technology during spring 2021. Supervised by Associate Professor Edmund F. Brekke and with close cooperation with PhD student Audun G. Hem, this thesis summarizes my findings and proposal of a track level multi-target tracker for the fusion of AIS and radar for an autonomous surface vessel.

The reader is assumed to have previous knowledge in target-tracking and probability theory, but the necessary knowledge will be presented.

I want to thank my main supervisor, Associate Professor Edmund F. Brekke, for valuable guidance whenever needed. He has motivated me to pursue a career within autonomous systems, and I am grateful for all I've learned thanks to him. Furthermore, I want to thank my co-supervisor, Audun G. Hem, who have always been quick to help when technical problems arise.

Contents

Figures

Tables

Acronyms

cc

Table 1: Linguistic abbreviations and acronyms.

Symbol	Meaning
DOF	Degree Of Freedom
ASV	Autonomous Surface Vessel
GPS	Global Positioning System
HT	Hypothesis Test
CT	Counting Technique
AIS	Automatic Identification System
IMU	Inertial Measurement Unit
EKF	Extended Kalman Filter
COLREG	The international regulations for preventing collisions at sea
w.r.t	with respect to
s.t.	subject to / such that
e.g.	*exempli gratia* (for example)
i.e.	*id est* (in other words)
etc.	*et cetera* (and so on)
Q.E.D	*Quod Erat Demonstrandum* (which was to be demonstrated)
KF	Kalman Filter
GNNS	Global Navigation Satellite System
PDAF	Probabilistic Data Association Filter
IPDA	Integrated Probabilistic Data Association Filter
JPDA	Joint Probabilistic Data Association Filter
JIPDA	Joint Integrated Probabilistic Data Association Filter
NNF	Nearest Neighbour Filter
GNFF	Global Nearest Neighbour Filter
PMBM	Poisson Multi-Bernoulli Mixture
IMM	Interacting Multiple Models
CV	Constant Velocity
CT	Coordinated-Turn
RRANSAC	Recursive Random Sample Consensus
COLAV	Collision Avoidance
ROC	Receiver Operating Characteristics

T2T	Track-to-Track
T2TA	Track-to-Track Association
T2TF	Track-to-Track Fusion
M2T	Measurement-to-Track
FPR	False-Positive Rate
FNR	False-Negative Rate
OSAP	Optimal Subpattern Assignment
RMSE	Root-Mean Squared Error
ANEES	Average Normalized Estimation Error Squared
VIMMJIPDA	Visibility Interacting Multiple Models Joint Integrated Probabilistic Data Association
MMSI	Maritime Mobile Service Identity

Nomenclature

$\chi^2_n(\alpha)$	The χ^2 distribution with n degrees of freedom evaluated at α
$\mathbb{E}[x]$	The expectation of the random variable x
${}^m\hat{\mathbf{x}}^i_k$	The state estimate of target i from tracker m at timestep k
${}^m\tilde{\mathbf{x}}^i_k$	The state estimation error of target i from tracker m at timestep k
${}^m\mathbf{P}^i_k$	The covariance of ${}^m\hat{\mathbf{x}}^i_k$
${}^m\mathbf{x}^i_k$	The state of target i from tracker m at timestep k
${}^m\mathbf{z}_k$	Measurement received from sensor m at timestep k
$\mathbf{F}$	The state transition matrix
$\mathbf{H}$	The measurement matrix
$p_{\boldsymbol{\sigma}}(x)$	Probability density function of the vector or scalar variable $\boldsymbol{\sigma}$ evaluated at x

Chapter 1

Introduction

1.1 Motivation

Autonomous surface vessels (ASVs) need to observe their surroundings to operate at sea safely. Therefore, knowing the whereabouts of ships in proximity and predicting their positions in the future is essential for collision avoidance (COLAV). And to do so, a robust multi-target tracking (MTT) system must be developed.

MTT for ASVs has typically been solved using radars in combination with cameras and lidars. Another source of information that can provide valuable information is the automatic identification system (AIS). At sea, larger vessels are required to transmit their own positions using the AIS. Fusing the information from a radar with the information from the AIS can enhance the estimates.

There exist different architectures for the fusion of information from multiple sources. A fundamental divide goes between measurement level fusion and track level fusion. In the former approach, all measurements are fed to a centralized tracking algorithm. In the latter approach, state estimates from local tracking algorithms are fused.

The track level approach has a modular structure that allows for simply adding or upgrading individual trackers without substantial change to the tracking algorithms. This permits the usage of robustly tested radar trackers to be combined with AIS trackers straightforwardly and is the main motivation for pursuing the track level approach to AIS-Radar fusion.

1.2 Problem Formulation

This thesis concerns the fusion of AIS and radar for multi-target tracking using the track level approach. The main question of this thesis is whether a track level approach to the fusion of AIS and radar is viable. To answer this, we need to develop a track level multi-target tracking system.

The track level approach can be split into associating tracks that originate from the same target, called the track-to-track association (T2TA) problem, and

the problem of fusion of tracks that originate from the same target, called the track-to-track fusion (T2TF) problem. To develop a complete track level approach to the fusion of AIS and radar, both the problem of T2TF and T2TA needs to be solved.

T2TF was the topic of the author's pre-project thesis. Main results from the pre-project thesis will be presented in this thesis, as its results are relevant for the selection of T2TF approaches in the complete tracking system.

Conventional solutions to the T2TA problem consists of a hypothesis test, which requires covariance information of the estimates. Unfortunately, it is not always available. When using track estimates from marine radars, covariance or any other information related to the probabilistic nature of the state estimates is typically not available. As this thesis wishes to develop a tracking system where the individual trackers can be swapped or upgraded easily, the question of whether there is a non-probabilistic approach to T2TA must be answered.

Such a method should be compared to the commonly used hypothesis test. The output of multi-target trackers should be used when evaluating the approaches to make the analysis relevant to the fusion of AIS and radar.

Potential loss of accuracy compared to the measurement-level approach will also have to be considered. It is known that the measurement-level approach is theoretically superior, and it should be examined whether this holds in the practical setting of fusion of Radar and AIS.

To summarize, the objectives of this thesis are

1. Develop a non-probabilistic approach to T2TA.
2. Compare said non-probabilistic approach to the conventional probabilistic approach.
3. Develop a complete track level multi-target tracking system fusing AIS messages and radar measurements.
4. Compare said tracking system to a measurement level tracking system.

1.3 Background and Related Work

This thesis concerns the track-to-track approach to the fusion of AIS and Radar. The work spans several topics, such as fusion of AIS and radar, track-to-track association (T2TA) and evaluation of T2TA, and track-to-track fusion (T2TF). The topics intertwine, but the author finds it easiest to present relevant work within the individual topics and note specifically work that covers several topics.

1.3.1 Track-to-Track Fusion

Traditionally, the motivation for T2TF was the reduced communication bandwidth required to fuse information from various sensors. In a distributed surveillance system, where "sensing" is done at different locations, communicating all measurements to a central fusion centre could be problematic due to communication

constraints. Communicating updated estimates at desired intervals would reduce the information sent from local sensors to the fusion centre. Later advances in autonomous technology have led to an increased interest in T2TF. In [1] the authors argue that T2TF is preferable for use in highly automated driver assistance functions for cars due to its modularity and flexibility. Other applications are the fusion of surveillance radar with radio transponders in airport geofencing [2].

T2TF have been extensively studied. Chong describes an optimal fusion formula when the systems are deterministic, i.e. the process model is perfect and given, and sensors are assumed synchronised and i.i.d noises [3]. The process noise is not negligible and the formulas presented is approximates of the optimal fusion. In [4] they assume that the estimation error of the two tracks are independent, which Bar-Shalom show is not the case [5]. Bar-Shalom showed that two tracks originating from the same target are dependent due to their common process noise. He also derived the cross-covariance of two tracks originating from the same target. Later, the fusion of two estimates accounting for the dependence due to the common process noise was derived [6]. In [7], they show that [6] makes an assumption that is not met and that the results are optimal only in the maximum likelihood sense. Another way of performing T2TF is the information matrix fusion (IMF), which is a special case of T2TF with memory. It was first proposed in [4], and has the advantage of not requiring the calculation of the cross-covariance, which simplifies the implementation. Moreover, IMF is optimal when the fusion is performed for each new measurement [8]. In [9], Tian and Bar-Shalom generalize the optimal synchronous T2TF algorithm for the asynchronous T2TF problem. They also present an IMF for the fusion of asynchronous tracks with time delays.

1.3.2 Track-to-Track Association and Evaluation of Track-to-Track Association

T2TA is typically solved by means of a hypothesis test. The single-scan T2TA test accounting for the dependence due to the common process noise was derived in [5]. The test was later generalized to multiple frames by Tian and Bar-Shalom [10]. Tian and Bar-Shalom also showed that, counter intuitively, the optimal sliding-window hypothesis test has not necessarily more power. In practice, the cross-covariance can be difficult to calculate and is as a result often ignored. Several papers have been published on the effect of including and ignoring the cross-covariance. For similar sensors [11], for dissimilar sensors [12] and the case when the state space of the trackers are dissimilar [13].

A frequent challenge in practical applications is the lack of covariances or any other information that describe the probabilistic nature of the state estimates beyond the state estimates themselves. Consequently, there is a need for reliable association schemes that only use state estimates. The simplest possible approach that seems feasible for this is a counting technique that associates tracks that have a sufficient number of close matches in some non-probabilistic sense. This is similar

to the well-known M-of-N track initiation scheme [11], and the Recursive Random Sample and Consensus (RRANSAC) method for data association in multi-target tracking [14]. Such a technique is called the counting technique and is available in the Stone Soup Library [15]. Independently of this, it was used in the track-to-track fusion system of [2].

Current work on T2TA evaluation does not deal with the output of multi-target tracking systems, which have integral challenges due to false alarms, wrong associations, misdetections and delayed track initialization. Further, the scenarios examined typically concerns single-target tracking, or two-target tracking, often moving in parallel lines [16, 17]. Other relevant work concerns the evaluation of T2TA of tracks from more than two sensors [18, 19].

1.3.3 Fusion of AIS and Radar

Tracking systems based on radar measurements and AIS messages have been proposed in various forms. Gaglione et al. uses radar and AIS data and formulates a detection-estimation problem that they solve using a Belief Propagation message scheme [20]. Liland uses a logic-based initialisation scheme and a Track Oriented Multi Hypothesis Tracker utilising both radar measurements and AIS messages [21]. Habtemariam et al. proposes a Joint Probabilistic Data Association tracking algorithm which fuses radar and AIS data, and solves the problem of AIS measurements arriving unpredictably by a probabilistic AIS-to-track assignment technique [22]. Several papers have been published on fusion of Radar and AIS for purpose of maritime surveillance, e.g. [23], [24] and [25]. However, typical land based coastal radars are used, in addition to e.g. synthetic aperture radar and over-the-horizon radar [26]. Most recently, the VIMMJIPDA of [27] was further developed to include AIS messages [28].

No work is known to the author on T2TF of Radar and AIS for use in ASVs. Work has been published on T2TF of radar and AIS for Electronic Chart Display and Information System [29]. They apply two fusion methods, first, assuming a deterministic system, as in e.g. [4], and secondly, by inclusion of an approximation of the cross-covariance, as suggested in [11] and [30]. Their analysis of the two methods is limited to comparing the course estimation when different measurement noise levels are used, and no analysis of consistency is presented.

1.4 Main Contributions

One of the main contributions of this thesis is to compare the counting technique with the conventional hypothesis test for the application of radar-AIS fusion. This work was recently submitted to the Fusion 2021 conference [31]. The evaluation is done by means of simulations, using a complete multi-target tracking system based on Joint Integrated Data Association (JIPDA), whose detailed description can be found in [27, 28].

The evaluation of T2TA using a complete multi-target tracking system leads to a second contribution, which concerns how ground truth is assessed in such a simulation approach. When track-to-track fusion is simulated for a single track, ground truth assessment is trivial. One can simply compare the simulated trajectory with its estimates. But when the tracks come from a multi-target tracking algorithm with data association, things are not so simple. The tracking output may suffer from late initialization and track swaps and track-loss, which may be both of a temporary or of a permanent nature. To assess the ground truth of a track, we propose a sliding window approach where the origin of the measurements used to update the track the n last timesteps vote for the ground truth.

Another contribution of this thesis is to compare a complete AIS-radar track level multi-target tracking system with the measurement level approach, exemplified by the VIMMJIPDA AIS-Radar described in [28].

1.5 Outline of the Thesis

This thesis consists of four parts. The first, Part I, presents some background theory on commonly used tracking methods, in addition to an introduction to radar and AIS. Part II consists of 5 chapters related to T2TA. Chapter 4 presents two approaches to T2TA, one probabilistic and one non-probabilistic. Chapter 5 discusses potential approaches to determining ground truth of tracks from MTTs. A sliding window approach to the problem is suggested. In Chapter 6 and Chapter 7, the experimental setup and results comparing the two T2TA approaches are presented. Part III contains mathematical formulations and a comparison of three approaches to T2TF. Most of the work on T2TF is from the author's pre-thesis. Part IV compares the developed tracker with a measurement level tracker. Chapter 16 concludes the thesis and gives recommendations for further work.

Part I

Background Theory

Chapter 2

Target Tracking

Tracking is the process of estimating the state of objects that we detect with sensors. At its core is filtering techniques, such as the Kalman filter, which allows us to predict the state in the future and update the prediction when new measurements arrive. One of the main challenges is data association, e.g. associating measurements with tracks or associating tracks with tracks. There are several complicating factors of target tracking, such as track initialisation, misdetections and false alarms.

2.1 Filtering

2.1.1 The Kalman Filter

The Kalman filter can be derived in several ways. One approach is to derive it from a Bayesian perspective, which is shown in [32]. Another approach is by minimizing the trace of the covariance matrix as done in ch. 4 of [33]. In this section, the general formulas for the linear Kalman filter will be shown.

Kalman filtering consists of two steps, a prediction step and an update step. The prediction step is based on a kinematic model (often called a Markov model, transition model or plant model), describing how the state changes with time. The update step is based on a measurement model, which relates the measurements to the state.

We assume a kinematic model, measurement model and initial estimate as

$$\begin{aligned} \mathbf{x}_k &= \mathbf{F}\mathbf{x}_{k-1} + \mathbf{v}_k & \mathbf{v}_k &\sim \mathcal{N}(0, \mathbf{Q}) \\ \mathbf{z}_k &= \mathbf{H}\mathbf{x}_k + \mathbf{w}_k & \mathbf{w}_k &\sim \mathcal{N}(0, \mathbf{R}) \\ \mathbf{x}_0 &\sim \mathcal{N}(\hat{\mathbf{x}}_0, \mathbf{P}_0). \end{aligned} \tag{2.1}$$

The matrix $\mathbf{F}$ is the transition matrix, and the matrix $\mathbf{H}$ is the measurement matrix. $\mathbf{Q}$ and $\mathbf{R}$ are symmetric positive definite and describes the statistical properties of the process noise $\mathbf{v}_k$ and the measurement noise $\mathbf{w}_k$, respectively. The kinematic model will be further elaborated on in the next section, and the measurement

model will be discussed in relation to the sensors used in Section 2.4. All noises are assumed mutually independent.

The Kalman filter is

$$\begin{aligned}
\hat{\mathbf{x}}_{k|k-1} &= \mathbf{F}\hat{\mathbf{x}}_{k-1} && \text{The predicted state estimate} \\
\mathbf{P}_{k|k-1} &= \mathbf{F}\mathbf{P}_{k-1}\mathbf{F}^\top + \mathbf{Q} && \text{The predicted covariance} \\
\hat{\mathbf{z}}_{k|k-1} &= \mathbf{H}\hat{\mathbf{x}}_{k|k-1} && \text{The predicted measurement} \\
\boldsymbol{\nu}_k &= \mathbf{z}_k - \hat{\mathbf{z}}_{k|k-1} && \text{The innovation} \\
\mathbf{S}_k &= \mathbf{H}\mathbf{P}_{k|k-1}\mathbf{H}^\top + \mathbf{R} && \text{The innovation covariance} \\
\mathbf{W}_k &= \mathbf{P}_{k|k-1}\mathbf{H}^\top\mathbf{S}_k^{-1} && \text{The Kalman gain} \\
\hat{\mathbf{x}}_k &= \hat{\mathbf{x}}_{k|k-1} + \mathbf{W}_k\,\nu_k && \text{The posterior state estimate} \\
\mathbf{P}_k &= (\mathbf{I} - \mathbf{W}_k\mathbf{H})\,\mathbf{P}_{k|k-1} && \text{The posterior covariance.}
\end{aligned} \tag{2.2}$$

Note that the output density of an estimate of track i at timestep k would be represented by its expectation $\hat{\mathbf{x}}_k^i$ and its covariance $\mathbf{P}_k^i$. Thus, when later deriving track-to-track fusion formulas and track-to-track association formulas, we will work with the expectations and covariances of the tracks.

2.1.2 Kinematic Models

The kinematic model is used to describe how the state changes with time. The two most used models are the constant velocity (CV) and the coordinated turn (CT) models.

A kinematic model can be written in the form of

$$\mathbf{x}_{k|k-1} = \mathbf{f}(\mathbf{x}_{k-1}) + \mathbf{v}_k \qquad \mathbf{v}_k \sim \mathcal{N}(0, \mathbf{Q}), \tag{2.3}$$

where $\mathbf{f}$ is a function describing the change of $\mathbf{x}_{k-1}$, and $\mathbf{v}_k$ is zero-mean Gaussian white noise.

Constant Velocity

The CV model is used to model targets that move in an almost constant straight-line. The motion model is typically described in a continuous fashion and then discretized for the use in the discrete Kalman filter. Assuming that the state space is $\mathbf{x} = \begin{bmatrix} \text{position x-direction} \\ \text{position y-direction} \\ \text{velocity x-direction} \\ \text{velocity y-direction} \end{bmatrix}$, the $\mathbf{f}$ and $\mathbf{Q}$ of the discretized CV model is

$$\mathbf{f}(\mathbf{x}_{k-1}) = \begin{bmatrix} 1 & 0 & T & 0 \\ 0 & 1 & 0 & T \\ 0 & 0 & 1 & 0 \\ 0 & 0 & 0 & 1 \end{bmatrix} \mathbf{x}_{k-1}, \tag{2.4}$$

and

$$\mathbf{Q} = \begin{bmatrix} \frac{1}{3}T^3 & 0 & \frac{1}{2}T^2 & 0 \\ 0 & \frac{1}{3}T^3 & 0 & \frac{1}{2}T^2 \\ \frac{1}{2}T^2 & 0 & T & 0 \\ 0 & \frac{1}{2}T^2 & 0 & T \end{bmatrix} q_a^2, \tag{2.5}$$

where q_a is the acceleration process noise intensity. The value of q_a determines how much the target accelerates. For modeling targets moving with small changes in velocity and direction, q_a should be low. In chap. 4 of [32], it is shown that for a slow passenger ferry, $q_a = 0.05$ appears adequate, while for a high speed passenger ferry, $q_a = 0.5$ seems more adequate. In extreme scenarios, the acceleration can reach $3m/s^2$, where $q_a = 3$ can be used.

Coordinated Turn

The coordinated turn can be used to model turning targets. The assumption of the model is that it moves with an almost constant turn rate ω. Assuming the state space is $\mathbf{x} = \begin{bmatrix} \text{position x-direction} \\ \text{position y-direction} \\ \text{velocity x-direction} \\ \text{velocity y-direction} \\ \text{turn rate} \end{bmatrix}$, the $\mathbf{f}$ and $\mathbf{Q}$ of the CT model is

$$\mathbf{f}(\mathbf{x}_{k-1}) = \begin{bmatrix} 1 & 0 & \frac{\sin T\omega_{k-1}}{\omega_{k-1}} & \frac{-1+\cos T\omega_{k-1}}{\omega_{k-1}} & 0 \\ 0 & 1 & \frac{1-\cos T\omega_{k-1}}{\omega_{k-1}} & \frac{\sin T\omega_{k-1}}{\omega_{k-1}} & 0 \\ 0 & 0 & \cos T\omega_{k-1} & -\sin T\omega_{k-1} & 0 \\ 0 & 0 & \sin T\omega_{k-1} & \cos T\omega_{k-1} & 0 \\ 0 & 0 & 0 & 0 & 1 \end{bmatrix} \mathbf{x}_{k-1}, \tag{2.6}$$

and

$$\mathbf{Q} = \begin{bmatrix} \frac{T^3}{3}q_a^2 & 0 & \frac{T^2}{2}q_a^2 & 0 & 0 \\ 0 & \frac{T^3}{3}q_a^2 & 0 & \frac{T^2}{2}q_a^2 & 0 \\ \frac{T^2}{2}q_a^2 & 0 & Tq_a^2 & 0 & 0 \\ 0 & \frac{T^2}{2}q_a^2 & 0 & Tq_a^2 & 0 \\ 0 & 0 & 0 & 0 & Tq_\omega^2 \end{bmatrix}. \tag{2.7}$$

$\mathbf{f}(\mathbf{x}_{k-1})$ is non-linear as ω_{k-1} is both in the previous estimate $\mathbf{x}_{k-1}$ and in the transition. The extended Kalman filter (EKF) must be used, and we need the Jacobian of the mapping from $\mathbf{x}_{k-1}$ to $\mathbf{x}_k$. The Jacobian is

$$\mathbf{F} = \begin{bmatrix} 1 & 0 & \frac{1}{\omega}\sin T\omega & -\frac{1}{\omega}(1-\cos T\omega) & \mathbf{F}_{1,5} \\ 0 & 1 & \frac{1}{\omega}(1-\cos T\omega) & \frac{1}{\omega}\sin T\omega & \mathbf{F}_{2,5} \\ 0 & 0 & \cos T\omega & -\sin T\omega & \mathbf{F}_{3,5} \\ 0 & 0 & \sin T\omega & \cos T\omega & \mathbf{F}_{4,5} \\ 0 & 0 & 0 & 0 & \mathbf{F}_{5,5} \end{bmatrix}, \tag{2.8}$$

where

$$\mathbf{F}_{:,5} = \begin{bmatrix} \frac{1}{\omega^2}(\dot{y} - (T\omega\dot{y} + \dot{x})\sin T\omega + (T\omega\dot{x} - \dot{y})\cos T\omega) \\ \frac{1}{\omega^2}(-\dot{x} + (\omega T\dot{x} - \dot{y})\sin T\omega + (\omega T\dot{y} + \dot{x})\cos T\omega) \\ -T(\dot{x}\sin T\omega + \dot{y}\cos T\omega) \\ T(\dot{x}\cos T\omega - \dot{y}\sin T\omega) \\ 1 \end{bmatrix}. \tag{2.9}$$

2.2 Single- and Multi-Target Tracking

One of the main challenges of target tracking is data association, i.e. associating measurements with tracks. Data association is complicated due to several factors, such as several measurements originating from the same target, measurements that do not originate from targets, and that targets are not always detected so-called misdetections. The main divide between single- and multi-target tracking is that the former assumes a single target, and the latter includes the possibility of several targets. Single-target tracking can also be used to track multiple targets, but the data association algorithms will not take into account the possibility of multiple targets.

Another complicating factor of target tracking is track management, e.g. initializing tracks with the right covariance and deleting tracks when they are no longer visible or unlikely to follow a target.

In this section, we will look at some of the most used approaches to target tracking.

2.2.1 Nearest Neighbour Filter

The nearest neighbour filter (NNF) is a filter where a track is associated with the closest measurement to the predicted measurement. After associating a track and a measurement, the Bayes filter is applied to update the estimate of the track [34].

An extension to the NNF is the global nearest neighbour filter (GNNF), which searches for a joint association of the measurements based on optimising a cost function, e.g. maximising the likelihood or minimising the total distance. The GNNF is attractive due to its simplicity, but it is vulnerable to clutter and dense target scenarios. The GNFF is a non-probabilistic model, as it does not assume probabilistic models for clutter, false alarm rates or miss-detections [34].

2.2.2 Probabilistic Data Association Filter and its Relatives

Probabilistic Data Association Filter

The probabilistic data association filter (PDAF) was introduced by Bar-Shalom and Li in [35]. The PDAF is a probabilistic approach to determining the source of measurements. The approach calculates the probabilities for measurements originating from the target and the probability of a misdetection. The filter uses an

average of the considered measurements weighted according to their association probabilities.

Integrated Probabilistic Data Association Filter

An extension of the PDAF is the integrated probabilistic data association filter (IPDAF), which uses an existence based approach to handle track management [36]. A discrete-valued existence state is added, which estimates whether the target exists or not.

Joint Probabilistic Data Association Filter

The joint probabilistic data association filter (JPDA) is an extension of the PDAF, which allows for the data association to jointly process measurements for several tracks. It was first proposed in [37].

The JPDA calculates the association hypothesis for every track for every measurement, which is a combination of all possible associations between tracks and measurements. The probability of misdetections is also considered. In the case of two tracks, (t_1, t_2) and two measurements (m_1, m_2), a single association hypothesis would be $P(t_1 \leftarrow m_1) = P(t_1 \leftarrow m_1 \cap t_2 \leftarrow m_2) + P(t_1 \leftarrow m_1 \cap t_2 \leftarrow \emptyset)$. Next, the association hypothesis $P(t_1 \leftarrow m_2)$ and $P(t_1 \leftarrow \emptyset)$ would be calculated. Similarly to the PDAF, the association hypothesis will be weighted to determine the final association. Further, similar to the PDAF, the resulting distribution would be a multivariate Gaussian, which can be merged to produce an approximated single Gaussian.

Several approximations are used to avoid computational inefficiency. Firstly, only the m best association hypothesis is calculated, typically solved by using the Murty method [38]. Further, only measurements within a distance from the tracks are considered, a process known as gating. Another approximation used is to cluster tracks, such that only tracks and measurements within a cluster are jointly considered in the data association [34].

Joint Integrated Probabilistic Data Association Filter

A combination of the JPDAF and the IPDAF combines the track management of the IPDAF and the multi-target handling of the JPDAF and is known as the JIPDA [39].

2.2.3 Interacting Multiple Models

The process noise used to model a target differs widely for large, slowly moving ships compared to small, fast leisure vessels. An approach typically used is to have a bank of filters and use a weighted average when predicting, where the filter's performance determines the weight. Such an approach is known as the interacting multiple models (IMM) and was first introduced by Blom and Bar-Shalom in [40].

The IMM allows for using a set of filters, e.g. a low process noise CV, a high process noise CV, and a CT model, in combination. As maneuvering is arguably best modelled as an on-off phenomenon, such an approach seems intuitive.

2.3 Multi-Sensor Tracking

Multi-sensor tracking is the problem of estimating the state of objects when measurements from several sensors are available. There are two main approaches to multi-sensor tracking, the measurement-level approach and the track-level approach.

2.3.1 Homogeneous and Heterogeneous Sensors

In a multi-sensor setting, the sensors are either similar, homogeneous, or dissimilar, heterogeneous. When the sensors are homogeneous, all the methods in the previous chapter can be used without further complications. If they are heterogeneous, the methods might need some approximations to be applicable, depending on how the heterogeneous sensors are processed. The main approaches to heterogeneous sensors are

1. If possible: convert the measurements to the same measurement space.
2. Keep measurements in their original measurement space but use them to update the same state space.
3. Keep measurements in their original measurement space and use them to update different state spaces.

The three options can all be solved using the track level approach, while only the two first can be solved using the measurement level approach.

For fusion of AIS (Cartesian measurements) and radar (range-bearing measurements), all three options are possible. In this thesis, we will use the first approach, converting the range-bearing measurements to Cartesian. This will be further discussed in Section 2.4.

2.3.2 Measurement Level Approach

In the measurement-level approach, all the measurements from the sensors are sent to the same processor. There, the measurements are associated with tracks and used to update the estimates.

The methods described in Section 2.2 are all compatible with the measurement-level approach, which is an advantage, as one can quite easily use well-examined methods. In addition, other state-of-the-art methods, such as the Poisson multi-Bernoulli mixture, are also compatible with multiple sensors.

Another advantage of the measurement level approach is that one can cross-validate the measurements as they arrive.

Compared to the track-level approach, the measurement-level approach might have higher computation demands. For example, assume that we want to use a camera and a radar in a measurement-level approach. If one were to run a neural network on every camera image to find detections, it might require more computer power than running a single tracker on the camera images and fusing the estimates using a track-level approach. Further, transmitting the camera images to the central processor can be difficult due to communication constraints.

2.3.3 Track-Level Approach

In the track-level approach, each sensor is used in an individual tracker, and the estimates from each tracker are used to produce a fused estimate.

The track-level approach can be operated with a lower communication bandwidth compared to the measurement-level approach. As estimates from each sensor do not have to be communicated to the fusion processor for each updated estimate but rather be sent when the fusion processor demands it, the total communication bandwidth can be reduced. This is important for distributed surveillance systems, where the sensors are located at a distance from the fusion processor.

The track-level approach has a modularized architecture. This could simplify removing or upgrading sensors, as it does not require substantial change to the tracking algorithm.

One of the challenges with the track-level approach is that there is a correlation between the estimates due to the common process noise. These cross-covariances can be challenging to compute when asynchronous and time-delayed sensors are used. The cross-covariances is a returning theme of this thesis and is therefore discussed more in-depth in Section 3.2. Later, in Chapter 9, we will also see the effect of ignoring the cross-covariances when fusing.

2.4 Sensors

The following subsections on AIS and radar will introduce the reader to the sensors functionality, their robustness and define the parameters space. The subsections are mainly based on [41].

2.4.1 Radar

Radio detection and ranging (Radar) is a detection system that determines the range and bearing to objects.

Functionality

Radars function by transmitting radio waves and sensing the echo of the waves. By determining the time between transmission and echo, one can determine the

range of the object. The transmitter is a device that generates the radiated electromagnetic energy. The transmitter is located close to the antenna, often connected to it by a rotating joint, allowing the energy to travel between the typically static transmitter and the rotating antenna. The antenna is a device that radiates the energy produced by the transmitter and collects the returning echoes. The antenna is rotating, so that objects can be detected in all directions. When the radio waves travelling through air meets another material, especially for highly electrically conductive materials such as metal, it will reflect or scatter the waves. The reflection of the wave is also dependent on the geometry of the material. For example, corners with angles less than 90° will reflect the wave back to the sender, while tile flat areas will reflect less and, thus, be less visible.

Simplified, the bearing is determined by the direction the antenna is facing. Other factors, such as beamforming, are also used to determine the bearing but will not be further pursued in this thesis.

Parameter Space

There are several complicating factors when determining the parameter space of radars. First, there are fundamental considerations when configuring a radar for tracking of ASVs. E.g. the rotation speed of the antenna, the frequency of the radio wave, pulse length and pulse repetition frequency. Further, the post-processing of the radar blobs will play an important role in the accuracy and, thus, the size of the object detected. To keep the results of this thesis as general as possible, standard deviations between 1 meter and 200 meters will be examined. Finally, to detect maritime targets, radars can be set to rotation speeds of a couple of seconds and less.

Radar Model

Based on the functionality of the radar, we note that the radar measurements are range-bearing measurements. Range-bearing measurements have error in range and bearing, complicating the filtering process when the tracking coordinates are Cartesian. There are two main approaches to this. Either converting the measurements to the tracking coordinates or keeping the measurements in polar coordinates and using a non-linear measurement model. In the first case, a linear Kalman filter can be used, and in the latter, an extended Kalman filter must be used. In this thesis, the measurements will be transformed to Cartesian coordinates. The transformation used is given by

$$\mathbf{z}_k = \begin{bmatrix} r\cos\theta \\ r\sin\theta \end{bmatrix}, \tag{2.10}$$

which is known as the conventional polar to Cartesian conversion. The estimate of the converted measurement error covariance $\mathbf{R}_{conv}$ is found by linearization as

$$\mathbf{R}_{conv} = \mathbf{J}\mathbf{R}_p\mathbf{J}^T, \tag{2.11}$$

where $\mathbf{R}_p = \begin{bmatrix} \sigma_r^2 & 0 \\ 0 & \sigma_\theta^2 \end{bmatrix}$ and $\mathbf{J}$ is the Jacobian of the mapping from polar to Cartesian coordinates, given as

$$\mathbf{J} = \frac{\partial}{\partial} h^{-1}(\mathbf{z}_k) = \begin{bmatrix} cos\theta & -rsin\theta \\ sin\theta & rcos\theta \end{bmatrix}. \tag{2.12}$$

An analysis of the expected value of the conventional conversion can be found in [42]. The analysis shows that the conversion has a bias in the mean of the converted measurement and that the conversion is also not consistent. This is because an ellipse in polar coordinates becomes banana-shaped in Cartesian coordinates, which our linear approximation cannot successfully represent. Several approaches exist for bias compensation [43], but we will in this thesis assume that it is not necessary as the sensor resolution is assumed sufficiently fine.

In addition to the range-bearing noise, noises due to inaccurate time-stamping and clustering can be represented by a Cartesian element. The radar measurement model used in this thesis is therefore

$$\mathbf{Z}_k = \mathbf{H}_R \mathbf{x}_k + \mathbf{w}_k \qquad \mathbf{w}_k \sim \mathcal{N}(0, \mathbf{R}_R), \tag{2.13}$$

where $\mathbf{H}_R = \begin{bmatrix} 1 & 0 & 0 & 0 \\ 0 & 1 & 0 & 0 \end{bmatrix}$ and $\mathbf{R}_R$ is the radar measurement noise matrix given by

$$\mathbf{R}_r = \mathbf{R}_c + \mathbf{J}\mathbf{R}_p\mathbf{J}^T, \tag{2.14}$$

where $\mathbf{R}_c$ is the cartesian element and $\mathbf{R}_p$ is the polar component.

2.4.2 Automatic Identification System (AIS)

With the introduction of radar and automatic radar plotting aid (ARPA), the position of visible vessels was easily presented to users of such systems. However, identification of the visible vessels was not provided through these systems, which led to difficulty in establishing a dialogue with nearby vessels [41]. Also, vessels not in the line of sight were not shown on these systems, as the Radar could not spot them. The very-high-frequency (VHF) communication systems and the development of transponders enabled the establishment of AIS transceivers.

Functionality

AIS transmit information on two VHF frequencies, 161.975MHz and 162.025MHz. The range of AIS messages is determined by the range of VHF signals, which is typically 30-40 nautical miles (55-74 km) for antennas mounted on top of a large vessel, and 20 nautical miles (37 km) for a small craft [41].

To avoid situations where nearby vessels transmit simultaneously, the transmission systems limit the transponders to transmit for very short and precisely controlled time periods. The system used is time division multiple access (TDMA).

It functions by dividing the time into slots where only one message can be sent at a time. The GPS clocks determine the time. One second, called a frame, is divided into 2250 equal length slots. I.e., there are 4500 slots per second combined on the two frequencies. In each slot, approximately 256 bits can be sent, or 42 characters, if a 6-bit conversion system is used. The time slots are allocated to the transponder depending on the current AIS transmission mode.

Autonomous and continuous mode is the default mode, also known as self-organizing time division multiple access (SOTDMA). In this mode, the transponders decide which slots they will transmit information in. As the amount of information changes, depending on which information fields are included in the message, the number of slots required for a message will differ. The transponders will change the time slot if it detects that there are others transmitting in the same time slot. However, it will not always be successful in doing so, as situations, where the two conflicting transponders transmit to the same receivers but are too far away to transmit to each other, can occur. To avoid staying in such a situation, the transponders also periodically change the time slots they transmit in.

Assigned mode is a mode where a shore station will assign slots to individual transponders. In this way, one can minimize the number of transponders using the same time slots. However, this depends on everybody following the rules and only transmitting in their own time slots.

Polling mode allows transponders to "ask" for information from other transponders. This way, one can get information about a low update rate vessel, e.g. a moored vessel, which will typically send out a new message every three minutes.

AIS information

The information included in an AIS message differ. Firstly, static data and voyage related data is updated every 6 minutes, while dynamic data is updated depending on the vessel state. Secondly, some specific fields, such as a safety-related message, are optional. The fields are presented in Table 2.1. The update rates of dynamic data depending on the vessel state are shown in Table 2.2.

Parameter space

Now that we know how AIS is functioning and know what information one can expect to receive, we can take a closer look at the uncertainties behind these figures. Examining Table 2.1, we note that it is only relevant to look at the uncertainties behind the dynamic data. Firstly, we note that the ship position will come along with an accuracy indication, which can be used to approximate the covariance of the ship's position. It is not clear from what the author has read whether the position obtained by GPS is sent unprocessed or whether is it filtered by using, e.g. inertial measurement unit (IMU) measurements. [41] notes that it is the navigator's GNSS aerial position that should be included in the static message. This suggests that the GNSS position of the navigator's GNSS is sent with the message and not the GNSS internal to the AIS transponder. This further suggests that it depends

on whether the navigator's GNSS does some filtering based on dead-reckoning techniques or not, which will vary depending on the vessels GNSS system.

Assuming that an accuracy indication will always accompany the ship's position, we could use this to set the measurement noise of each new AIS message. The problem of such an approach would be the possible misreporting of accuracy, where, e.g., a vessel reports a smaller accuracy than the actual. This would lead to inconsistency, and specifically in the mentioned case, overconfidence. In the same sense, one can argue that using the same measurement noise for all AIS messages would also lead to inconsistency. A pragmatic approach could be to set a minimum measurement noise so that vessels that report better accuracy than the minimum would instead be treated as a measurement with the minimum measurement noise.

To determine the value of such a minimum measurement noise, we would have to take a look at the expected accuracy of GNSS measurements. GNSS measurements can typically be modelled as a measurement with a slowly varying bias. The biases are due to signal propagation errors, such as ionospheric delay and tropospheric delay. Other types of errors are due to clock related errors, both at the receiver and at the satellite. To further examine the error of GNSS measurements, one should examine the effect of these errors, which is outside of the scope of this thesis. We will assume that the GNSS measurements can be adequately approximated by a measurement with a standard deviation between 3 and 20 meters.

AIS Model

The ASI measurement model is simpler than the radar measurement model, as we can model the AIS measurement noise with a simple Cartesian component. The AIS measurement model is

$$\mathbf{Z}_k = \mathbf{H}_{AIS}\mathbf{x}_k + \mathbf{w}_k \qquad \mathbf{w}_k \sim \mathcal{N}(0, \mathbf{R}_{AIS}), \tag{2.15}$$

where $\mathbf{H}_{AIS} = \mathbf{H}_R = \begin{bmatrix} 1 & 0 & 0 & 0 \\ 0 & 1 & 0 & 0 \end{bmatrix}$ and $\mathbf{R}_{AIS}$ is the Cartesian component.

Type	information	Description
	MMSI	identification number
Static	IMO number	
	Callsign	Used when establishing contact on VHF
	Lenght and beam	
	Type of ship	
	Location of position fixing antenna	
Dynamic	Ship position	along with accuracy indication
	Time in UTC	
	Course over ground	
	Speed over ground	
	Heading	
	Navigational status	
	Rate of turn	When available
	Angle of heel	Optional and when available
	Pitch and roll	Optional and when available
Voyage related	Ship's draught	
	Hazardous cargo	if any
	Destination and ETA	
	Route-plan	Waypoints, optional
Other	Safety message	Short safety message, when required

Table 2.1: The table shows the information fields that could be sent in an AIS message. Information from [41].

Vessel state	Update rate
At anchor	3 minutes
Moving 0-14 knots	12 seconds
Moving 0-14 knots and changing course	4 seconds
Moving 14-23 knots	6 seconds
Moving 14-23 knots and changing course	2 seconds
Moving >23 knots	3 seconds
Moving >23 knots and changing course	2 seconds

Table 2.2: The table shows the update rate of dynamic information depending on the vessel state. Information from [41].

Chapter 3

Track-to-Track Fusion Survey

In this chapter, a brief overview of the existing methods for fusion of tracks will be presented. First, in Section 3.1, we will introduce the different fusion architectures. Then, in Section 3.2, we will discuss the effect of the common process noise, as it is central to the optimal fusion approaches.

3.1 Track-to-Track Fusion Architectures

There are several different architectures, or configurations, when processing information in a multi-sensor environment. Figure 3.1 presents some potential configurations. A similar figure is shown in [44]. Type II is the configuration that will be explored in this section. The figure shows possible fusion options, i.e. track-to-track fusion without memory (T2TFwoM), track-to-track fusion with memory (T2TFwM), and information matrix fusion (IMF). T2TFwoM is fusion when the fusion algorithm only uses the current estimates. T2TFwM uses information from previous fused results. Information matrix fusion (IMF) does not require calculating the cross-covariances of the errors of the tracks, which simplifies the implementation. Note that IMF fuses with memory, i.e. it uses track estimates from the previous fusion.

3.1.1 Feedback

Depending on how or whether information from the fusion is returned to the individual trackers, we divide it into three categories; no feedback, partial feedback and full feedback. Figure 3.2a, Figure 3.2b and Figure 3.2c shows the information flow of no feedback, partial feedback and full feedback for T2TFwoM, respectively. A similar figure is presented in [45]. Information on the fused estimate would be available for both the local trackers in the full feedback configuration. Only one of the local trackers would receive information on the fused estimate in the partial feedback configuration. Neither local tracker would receive information of the fused estimate in the no-feedback configuration.

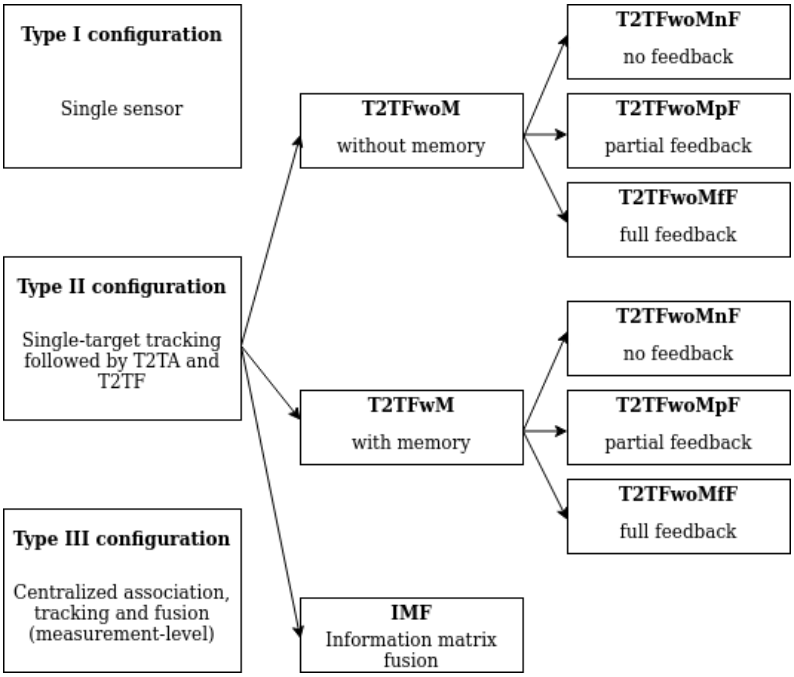

Figure 3.1: Configurations when processing information in a multi-sensor environment.

For T2TFwM, information about the fused estimates would be available at the next fusion iteration. A figure showing no feedback, partial feedback and full feedback for T2TFwM would be similar to that of Figure 3.2, but also include arrows indicating information flow between the fusion centres.

Surprisingly, information feedback has a negative impact on the accuracy of T2TFwoM [45]. It does, however, have a positive impact on the accuracy of T2TFwM.

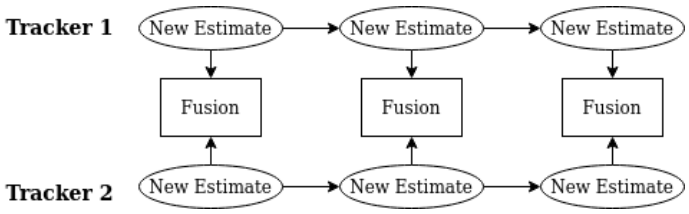

(a) T2TFwoM no feedback

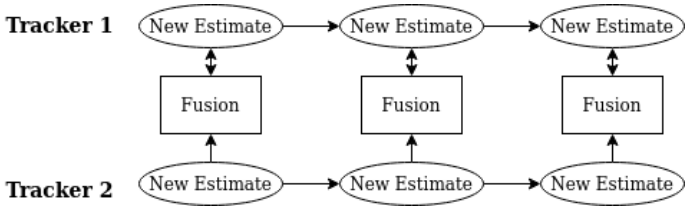

(b) T2TFwoM partial feedback

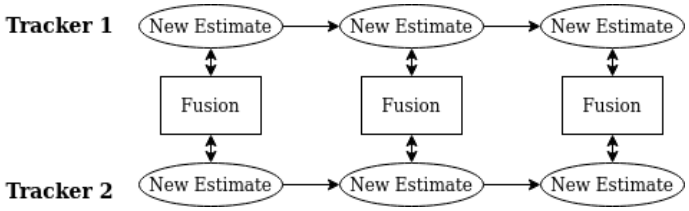

(c) T2TFwoM full feedback

Figure 3.2: The figure shows the information flow of T2TFwoM

3.2 The Effect of the Common Process Noise

If the two tracks originate from the same target, the tracks possess a common process noise. This can either be ignored (see Section 9.2) or handled (see Section 9.3). The effect of the common process noise depends on the ratio between the process and measurement noise. This is shown in [6], where Bar-Shalom uses the manoeuvring index to show the decrease of state covariance matrix elements after fusion. The manoeuvring index is given in [46] as

$$\lambda = \frac{\sigma_v T^2}{\sigma_w} \tag{3.1}$$

where σ_v is the process noise standard deviation, σ_w is the measurement noise standard deviation, and T is the sample interval. For manoeuvring indexes ranging from 0.1 to $\sqrt{5}$, Bar-Shalom shows that the covariance of the fused estimates fused using the fusion equation with cross-covariance (Equation (9.22)) decreases when the manoeuvring index increases. I.e. the effect of the common process noise is lower with a higher manoeuvring index. Bar-Shalom also states that the fused estimate is about 70 percent of the single-sensor uncertainty area over a wide range of process noise variances when the common process noise is accounted for. However, when it is not accounted for, the fused estimate uncertainty area is 50 percent of the single-sensor uncertainty area.

For maritime targets, we would expect σ_v to be somewhere between 0.05 and 0.5. In extreme scenarios, the acceleration can reach $3m/s^2$. As an example, assume $\sigma_v = 0.3g$, a measurement noise standard deviation $\sigma_w = 200m$, and a sample interval $T = 10s$. This yields $\lambda = 15$ (using $g = 10$), a substantially higher manoeuvring index than what Bar-Shalom considered. In this case, the conclusion of Bar-Shalom, that the fused estimate is about 70% of the single-sensor uncertainty area, might not apply. The effect of the common process noise would be smaller, and the fusion under the independence assumption might produce an equally good result as the fusion with cross-covariance. However, this example assumes that both trackers have a sample interval of 10s, which would not be the case with radar and AIS. Exact values depend on the choice of sensor. Typical values for radar is in the range $[0.5-5]$ seconds and in the range $[2-120]$ seconds for AIS. See Section 2.4 for more discussion on sensors. Also, when considering sensors with different sampling rates, the manoeuvring index can not be directly calculated using Equation (3.1). Based on this example, it is unclear whether fusion of independent tracks is usable or not when fusing radar and AIS data and that this should be explored.

Part II

Track-to-Track Association

Chapter 4

Two Methods for Track-to-Track Association

The track fusion problem can be split into fusion of state variables and association of tracks. The association of tracks, also known as track-to-track association (T2TA), is significant, as the fusing of state variables of different targets can yield a worse estimate than the estimates of the local trackers. T2TA is typically solved by formulating a hypothesis test, which can either be single-scan [5], or multi-scan [10]. Another divide goes between ignoring or including the cross-covariance due to the common process noise (see Section 3.2).

In particular practical settings, the covariance information used in the hypothesis tests is not available. Therefore, there is a need for solving the T2TA problem with only the mean state estimates in such cases. In [2], a method was used based on principles similar to those found in the M-of-N track initiation scheme [11], and the Recursive Random Sample and Consensus (RRANSAC) method for data association in multi-target tracking [14]. A variation of what used in [2] will be presented in this chapter and is by the author called the counting technique. This technique is also available in the Stone Soup library [15].

This chapter will first present and derive the theoretical formulas for associating two tracks, both for the probabilistic approach and the counting technique. Further, some implementation details will be discussed, such as generalizing the formulas to multiple targets.

4.1 Probabilistic Approaches

The probabilistic approaches typically try to formulate hypothesis tests for whether the origins of two tracks are similar or tries to calculate the probability that two tracks originate from the same target.

The first approach, specifying hypothesis tests, will be described and derived in the following subsection. The hypothesis tests can be done as a single-scan test, i.e., using only information from a single time step, or as a multi-scan test,

where information from several time steps is used. One might expect the multi-scan approach to yield superior results, but Tian and Bar-Shalom show that it is not always the case [45]. To see why the multi-scan test might yield inferior results to the single-scan test, one can examine the properties of the distribution of the multi-scan test. The multi-scan test is a non-central χ^2 test. The power of the test is decided by both the non-centrality parameter λ and the number of degrees of freedom k. The increase of the number of degrees of freedom k due to the inclusion of additional time frames has a negative effect on the power of the test, while using additional information has a positive effect on the power of the test, manifested through the non-centrality parameter λ. When the frames selected have a high correlation, the total effect can be negative. According to Tian and Bar-Shalom, this could be avoided by increasing the time difference between the selected time frames.

The second approach is similar to that in the Probabilistic Data Association Filter (PDAF). In the PDAF, one calculates the probability that each measurement originate from a certain track and use this in a weighted average of all relevant measurements (see Section 2.2.2). Such an approach is described in [47].

4.1.1 Single-Scan Hypothesis Test

Assumptions

When deriving the single-scan hypothesis test, the following is assumed.

- The tracker i estimates the position of a target at timestep k as a Gaussian distribution with expectation ${}^{i}\hat{\mathbf{x}}_k$and covariance ${}^{i}\mathbf{P}_k$, and tracker j estimates the position of a target, the same or a different target, at timestep k as a Gaussian distribution with expectation ${}^{j}\hat{\mathbf{x}}_k$and covariance ${}^{j}\mathbf{P}_k$.
- The true states of the targets are given by ${}^{m}\mathbf{x}_k$, m $\in [i, j]$.
- The state estimation errors

$$ {}^{m}\tilde{\mathbf{x}}_k = {}^{m}\mathbf{x}_k - {}^{m}\hat{\mathbf{x}}_k \qquad\qquad m \in [i, j], \tag{4.1} $$

  are independent. This assumption is referred to as the *Error Independence Assumption* and will only be used when deriving the hypothesis test of independent tracks.

A note should be made about *Error Independence Assumption*, as it is also used when deriving the fusion of independent tracks. As it is defined above, the state estimation errors are independent when the target tracked is the same, i.e. ${}^{i}\mathbf{x}_k = {}^{j}\mathbf{x}_k$, and when they are different, i.e. ${}^{i}\mathbf{x}_k \neq {}^{j}\mathbf{x}_k$. One could argue that the independence assumption should only include the case when the target tracked is the same, as it is trivial that the state estimation errors are independent when the targets tracked are different. However, this will clutter the derivations, as we do not know whether the two targets have the same true state or not when deriving the hypothesis test. When the assumption is used in deriving the fusion equations, we have already assumed that the estimates fused have the same target. In that case, we

only use that the state estimation errors of two estimates from the same target are independent.

Derivation of the Hypothesis Test of Independent and Dependent Tracks

To derive the single-scan hypothesis tests for associating two tracks, the hypothesis test of independent tracks and the hypothesis test of dependent tracks, we need to define two hypotheses, the same target hypothesis and the different target hypothesis. The same target hypothesis is that the difference of the true states of the two tracks is zero. The different target hypothesis is that the difference between the two tracks' true states is not zero. We denote the difference of the two estimates as

$$^{ji}\hat{\mathbf{\Delta}} = {}^{i}\hat{\mathbf{x}} - {}^{j}\hat{\mathbf{x}}, \tag{4.2}$$

and the difference of the true states as

$$^{ji}\mathbf{\Delta} = {}^{i}\mathbf{x} - {}^{j}\mathbf{x}. \tag{4.3}$$

The same target hypothesis then becomes

$$\mathbf{H_0} : {}^{ji}\mathbf{\Delta} = 0, \tag{4.4}$$

while the difference target hypothesis becomes

$$\mathbf{H_1} : {}^{ji}\mathbf{\Delta} \neq 0. \tag{4.5}$$

The covariance of the error in the difference between the state estimates becomes

$$\begin{aligned} {}^{ij}\mathbf{T} &= \mathbb{E}[{}^{ji}\tilde{\mathbf{\Delta}}\,{}^{ji}\tilde{\mathbf{\Delta}}^{T}] \\ &= \mathbb{E}[({}^{ji}\mathbf{\Delta} - {}^{ji}\hat{\mathbf{\Delta}})({}^{ji}\mathbf{\Delta} - {}^{ji}\hat{\mathbf{\Delta}})^{T}] \\ &= \mathbb{E}[({}^{i}\mathbf{x} - {}^{j}\mathbf{x} - {}^{i}\hat{\mathbf{x}} + {}^{j}\hat{\mathbf{x}})({}^{i}\mathbf{x} - {}^{j}\mathbf{x} - {}^{i}\hat{\mathbf{x}} + {}^{j}\hat{\mathbf{x}})^{T}] \\ &= \mathbb{E}[({}^{i}\tilde{\mathbf{x}} - {}^{j}\tilde{\mathbf{x}})({}^{i}\tilde{\mathbf{x}} - {}^{j}\tilde{\mathbf{x}})^{T}] \\ &= {}^{i}\mathbf{P} - {}^{ij}\mathbf{P} - {}^{ji}\mathbf{P} + {}^{j}\mathbf{P}. \end{aligned} \tag{4.6}$$

For independent tracks, using Assumption 1, we get that the cross-covariance of the two tracks are zero, i.e. ${}^{ji}\mathbf{P} = {}^{ij}\mathbf{P} = 0$, as the estimation errors are independent. For the hypothesis of independent tracks, the covariance of the error in difference between the state estimates becomes ${}^{ij}\mathbf{T} = {}^{i}\mathbf{P} + {}^{j}\mathbf{P}$, while for the hypothesis test of dependent tracks, it is as in Equation (4.6).

The cross-covariance assuming tracks from Kalman Filters is derived in Section 9.3.1.

Let $\mathbf{D}$ denote the normalised distance squared between the estimates, given as

$$\mathbf{D} = {}^{ji}\hat{\mathbf{\Delta}}^{T}[{}^{ij}\mathbf{T}]^{-1}\,{}^{ji}\hat{\mathbf{\Delta}}. \tag{4.7}$$

Assuming the estimation errors are Gaussian, we know $\mathbf{D}$ to be χ^2 distributed with the number of states estimated, n, as degrees of freedom. The test for association is then to check whether this is true, i.e.

$$\text{Accept } \mathbf{H_0} \text{ if:} \qquad \mathbf{D} \leq \mathbf{D}_\alpha, \tag{4.8}$$

where

$$\mathbf{D}_\alpha = \chi^2_n(1-\alpha), \tag{4.9}$$

where e.g. $\alpha = 0.05$.

Difference Between the Hypothesis Test of Independent Tracks and Dependent Tracks

The only difference between the hypothesis test of independent tracks and the hypothesis test of dependent tracks is the equation for calculating the covariance of the error in difference between the state estimates, ${}^{ij}\mathbf{T}$, Equation (4.6). We note that ${}^{ij}\mathbf{T}$ decreases when we include the cross-covariances, as ${}^{ij}\mathbf{P} = {}^{ji}\mathbf{P}^T > 0$ are positive definite. When ${}^{ij}\mathbf{T}$ decreases, it's inverse, $[{}^{ij}\mathbf{T}]^{-1}$, increases. By Equation (4.7), the normalised distance squared between the estimates, $\mathbf{D}$, increases. In other words, $\mathbf{D}_{dependent} > \mathbf{D}_{independent}$. By Equation (4.8) we then conclude that the hypothesis test of dependent tracks would require a smaller difference between the estimates to associated two tracks, than the hypothesis test of independent tracks.

In [17], La Scala and Farina examine the performance of the hypothesis test of independent and dependent tracks. They compare the expected true-positive rate (TPR) (rate of correctly associating two tracks originating from the same target) with the TPR found in experiments with one and two targets. They found that neither methods were superior in terms of matching theoretic TPR and experienced TPR.

Another approach to comparing the two methods could be to examine the TPR and the false-positive rate (FPR) using the Receiver operating characteristic (ROC). The ROC is a curve tracing out the TPR and FPR for a varying discrimination threshold.

Another important distinction between the hypothesis test of independent tracks and the hypothesis test of dependent tracks is that we need to calculate the cross-covariance for the latter. Calculating the cross-covariance can be tedious in most cases and impossible in other cases. When all information from the trackers are available, such as the previously used Kalman gain, process noises and measurement noises, one can recursively calculate the cross-covariance. If some information is missing, which may be the case when one uses a built-in tracking system of a radar, the cross-covariance can not be calculated.

If the covariances from the individual trackers are available, it is possible to estimate the cross-covariance. As discussed in Section 3.2, Bar-Shalom and Campo found that there seems to be an almost constant ratio between the covariances of fused estimates using the fusion of dependent tracks and the fused estimates using

the fusion of independent tracks [6]. Using that, Bar-Shalom shows in [11] that the cross-covariance can be approximated to ${}^{ij}\mathbf{P} = \rho({}^{i}\mathbf{P}{}^{j}\mathbf{P})^{\frac{1}{2}}$, where $\rho \approx 0.4$ when two states are estimated.

Effect of the α Parameter

The number α is the probability of type 1 error, i.e. when a true null hypothesis is rejected. In our case, it is the probability that we do not associate two tracks when they, in fact, were from the same target. When running multiple monte-carlo simulations with two Kalman filters tracking a single target, the author found that when the linear-Gaussian assumptions hold, the miss percentages will be equal to the α for the hypothesis test of dependent tracks, and smaller than α for the hypothesis test of independent tracks. As noted in Section 4.1.1, the hypothesis test of dependent tracks will require a smaller difference between the estimates to associate two tracks, compared to the hypothesis test of independent tracks. Therefore, the hypothesis test of independent tracks will associate more tracks than the hypothesis test of dependent tracks.

It is difficult to say what reasonable values of α is. As the method uses the covariance matrices of the estimates, the consistency of the trackers will greatly affect the results. It is unlikely that α will directly reflect the probability of a type 1 error in real-world scenarios, as trackers are often inconsistent. Therefore, different α values must be tested, and in a multi-target scenario, there will be a trade-off between miss associations and false associations. In Chapter 7, we shall see that in practice, the optimal α is larger than what the optimal theoretic α is.

4.2 Counting technique

The counting technique is a simple non-probabilistic method that only uses the mean position of estimates to determine whether to associate two tracks or not. It belongs to the category of multi-scan approaches, as it uses information from several timesteps.

The counting technique determines whether two tracks are associated by counting how many times in a row they are within a threshold away from each other. When two tracks are within *threshold* away from each other for ψ steps in a row, the tracks are considered associated. The tracks will remain associated until they are further away than *threshold* from each other for τ steps in a row.

In Figure 4.1 an example of the counting technique is presented. The parameters used are $\psi = 3$ and $\tau = 2$. Whether two estimates were within the *threshold*, considered a hit, or outside, considered a miss, is shown in the figure. A solid blue line between the two estimates signifies that the estimates were within *threshold* from each other, while a solid red line signifies that they were more than *threshold* from each other. The top row contains information on whether the tracks are associated at that time step or not. The information from a timestep is located directly

above the estimates at that time step, so it's easy to see at what estimates the association changes from true to false and from false to true.

In the example, we see that the association is true on the third timestep as the three first estimates are less than 0extitthreshold from each other. On the last time step, the association turns to false, as it then has been two time steps in a row where the estimates were further than *the threshold* from each other. Note that the tracks are associated on time step 4 and 6 even though the estimates are further than *the threshold* from each other.

Timestep	1	2	3	4	5	6	7
Associated?	False	False	True	True	True	True	False

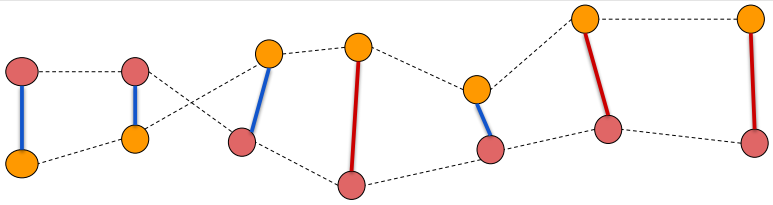

Figure 4.1: Caption

Effect of the Parameters

***Threshold*:** The *threshold* determines whether two estimates are close enough to be considered a hit, or the opposite, far enough away from each other to be considered a miss. The optimal *threshold* will vary with the estimation errors. We wish to select a *threshold* such that tracks with the same target will most of the time be within *the threshold* from each other while at the same time avoiding having tracks with other targets being within *threshold*. As the estimation error is tightly linked with the measurement and process noise, it is natural to assume that the optimal *threshold* will also be tightly linked with the measurement and process noise.

ψ and τ: ψ determines how many hits in a row is necessary to change the association of two tracks from false to true, while τ determines how many misses in a row is necessary to change the association from true to false. With a low ψ,

4.3 T2TA Strategy and Implementation

The association techniques described needs a couple of adjustments to fit our scenario of associating AIS and radar tracks. First off, the techniques presented check whether two tracks originate from the same target. As we look at multi-target

tracking, we need to generalize the techniques to multiple targets. Further, we need to figure out when to calculate new associations. The counting technique uses temporal information, so the time between each association needs to be constant.

4.3.1 Association Algorithm

To generalize the techniques to multiple targets, we use the following algorithm.

Algorithm 1: Associating multiple targets

```
associations ← [][];
for radar_track i in radar_tracks do
    for AIS_track j in AIS_tracks do
        associations[i][j] ←
         check_association(radar_track,AIS_track) ;
    end
end
reward_m ← calculate_reward_matrix(associations);
associations ← auction_method(reward_m);
```

A couple of things should be noted about the algorithm. First, the method is naive and not optimized. Instead of checking all combinations of AIS and radar tracks, one could first check whether two tracks' distance is below a certain threshold, similar to gating [47]. If the distance is below the threshold, one can calculate the association. The author did not find this necessary, as the number of associations to check never exceeded what the computer could handle in real-time. As the number of sensors used increases, the complexity would increase exponentially, and a gating approach must be used [18].

Note that it is the auction algorithm that determines the final associations. As we check all possible combinations of associations, it is possible that, e.g. several AIS tracks are associated with a single radar track. The reward matrix is populated such that the auction method maximizes the number of associations. If there are several combinations, it minimizes the total Euclidean distance between all associated pairs. The auction algorithm is described in [32].

The implementation of *check_association(...)* depends on the association technique used. This will be further elaborated on.

4.3.2 Timing

The counting technique uses temporal information in contrast to the hypothesis test. When temporal information is used, we need to ensure that the associations are checked at constant time intervals.

When it comes to determining the constant time interval, two aspects should be considered. First, the update rate of the sensors, and second, the desired information refresh rate of the tracking system. Refresh rate is in this setting referred

to as the refresh rate of estimates, which, e.g., the collision avoidance system determines. In this thesis, a radar update rate of 2 is assumed. The update rate of the AIS tracker is unknown and varies depending on the size and speed of the vessels transmitting the AIS message. Assuming that the collision avoidance system is fine with receiving updated estimates every 2 seconds, setting the constant time interval to 2 seconds would make sense. If the collision avoidance system requires updates every second, the option is to decrease the constant time interval to 1 second or predict the fused estimate every second.

In this thesis, we set the constant time interval to 1 second. The association techniques will then check for new associations every second. This means that associations will be checked with predicted values every second seconds when no updated estimates are available. One could argue that using predicted values to determine associations is a bit peculiar, as one uses the same information twice. However, the author did not see any clear caveats and found that predicting the fused estimates is not straightforward to do.

4.3.3 The Counting Technique

There are several possible approaches to implementing the counting technique. Exactly how it is implemented will affect the results. Therefore, some specific notes on the functionality of the implementation are discussed below.

As all combinations of tracks are checked for association, a single track may be associated to several tracks. This is, as described in the association algorithm, dealt with by the auction algorithm. As described in Section 4.2, when two tracks are associated, they are associated until they have had τ misses in a row. The output of the auction algorithm does not change the associated variable, it is only used to decide which associations are fed to the fuser. This small distinction is best explained with an example.

Assume a single AIS track is close to two radar tracks. Both radar tracks are close enough to be considered a hit for several steps. After some timesteps, both radar tracks are associated with the single AIS track according to the counting technique. When this is fed through the auction algorithm, the auction algorithm will decide that only one of the associations will be part of the final associations. The final associations will be fed to the fused, which will use the information to combine tracks. Even though only one of the tracks were associated with the AIS track in the final associations, the counting technique will view both tracks as associated to the AIS tracks. Such that next timestep, they are both still associated, and will remain associated until they are further than *threshold* for τ timesteps in a row.

This implementation detail is important, as it allows for a rapid change of associations if a track swap were to happen.

4.3.4 The Single-Scan Hypothesis Test

In this thesis, we will evaluate the performance of the hypothesis test of independent tracks, as described in Section 4.1.1. Based on the discussion in Section 4.1.1, it is not obvious that there would be any gain in using the hypothesis test of dependent tracks. In [13], a comparison between including the cross-covariance and not including the cross-covariance is examined. They use a bearing only sensor and a radar sensor. Their results suggest that there was no large gain in including the cross-covariance.

Therefore, considering the difficulty of calculating the cross-covariance, the hypothesis test of dependent tracks will not be examined.

The *check_association(...)* in the association algorithm is for the hypothesis test of independent tracks a check of Equation (4.8).

Chapter 5

Determining Ground Truth in Multi-Target Tracking

In multi-target tracking, determining the origin of tracks is challenging due to complications from wrong data association. Some of the easiest methods are single-scan, meaning that they determine the ground truth of a track by the information of a track at a single timestep. These methods all fall short due to either track loss or track swap. This chapter discusses why determining the ground truth in multi-target tracking is challenging, presents possible approaches and their shortcomings, and proposes a multi-scan approach to the problem.

5.1 Challenges of Determining Ground Truth

The challenges of determining ground truth in a multi-target scenario are largely due to wrong data association. A central component in any multi-target tracking system is the data association of measurements to tracks. The measurements associated with a single track can either be 1) from the target the track is tracking, 2) from another target, and 3) clutter, i.e., false alarms, such as measurements originating from birds and wakes or measurements appearing due to low sensor quality.

When measurements from another target are wrongly associated, it leads to a potential track swap. An example of a track swap is shown in Figure 5.2. Another potential problem with associating measurements from other targets is track coalescence, which is shown in Figure 5.3. Track coalescence can happen in trackers using soft association schemes, i.e. using a combination of measurements to update the estimates. The probabilistic data association filter (PDAF) use a soft association scheme, as described in Section 2.2.2. A multi-target version of the PDAF is the parallelized single-target PDAF, which is known to have this issue [32].

When clutter is wrongly associated, it leads to potential track loss, i.e. track divergence. Track loss is shown in Figure 5.1.

These three situations, track loss, track swap, and track coalescence, can either be temporary or permanent. When all measurements used in the update of a track originate from a single target, the question of ground truth is trivial. However, when two measurements in a row are clutter, and the track starts to diverge, what is the track's origin? And what if the track diverges and then, by chance, returns to its original target? What was the ground truth of the track during divergence? And what if two tracks swap targets? At what point are they no longer tracking their original target? The lack of answers to these questions makes determining the ground truth in multi-target tracking difficult.

Track loss can be somewhat handled in combination with the method of determining ground truth. Track loss can be defined as being far away from the ground truth, so we note that track loss can be consistently defined when we have the ground truth.

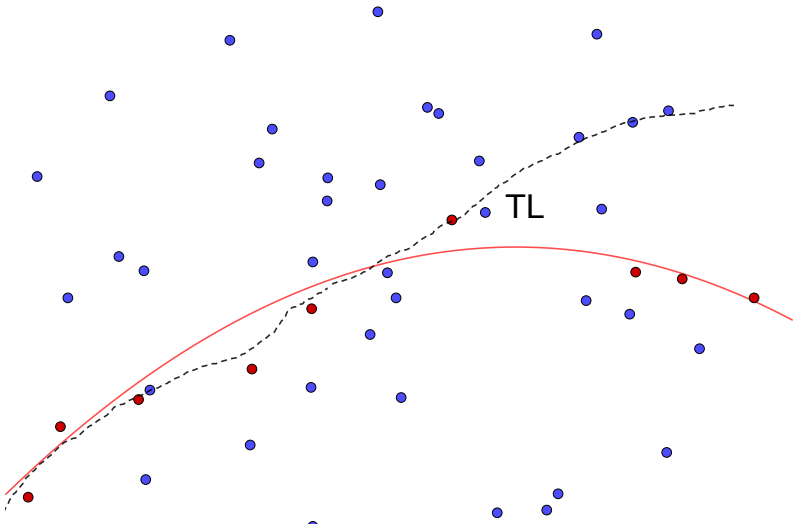

Figure 5.1: The figure shows an example of a track loss. The red dots represents measurements originating from the target, which moves along the red line. The blue dots are clutter. The point of which track loss happen is marked 'TL'.

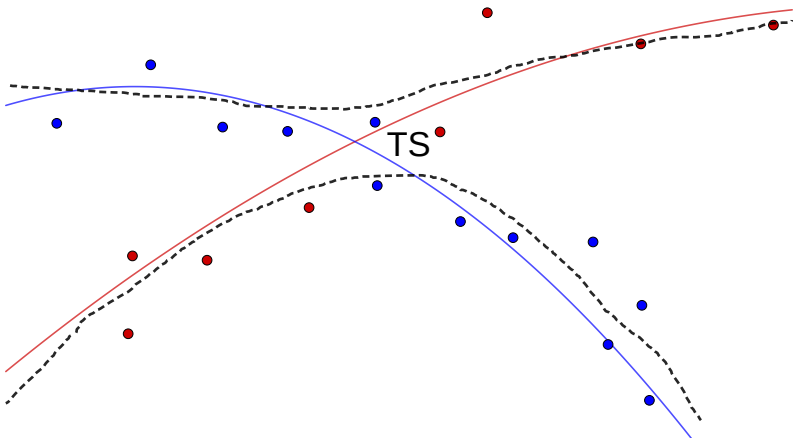

Figure 5.2: The figure shows an example of a track swap. The red dots represents measurements originating from the target with the red ground truth (the red solid line), and the blue dots represents measurements originating from the blue target. The two black dotted lines represents the two tracks. The point at which track swap happen is marked 'TS'.

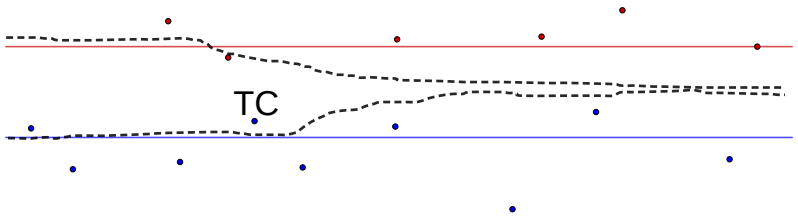

Figure 5.3: The figure shows an example of track coalescence. The red dots represents measurements originating from the target with the red ground truth (the red solid line), and the blue dots represents measurements originating from the blue target. The two black dotted lines represents the two tracks. The point at which track coalescence starts is marked 'TC'.

5.2 Handling Track Loss

Track loss handling can be used in combination with the method of determining ground truth. Assuming that the given ground truth is correct, we can calculate the deviation from ground truth and use this to determine whether the track is lost.

Different definitions of track loss have been used in the literature. In [48], a two-stage process is used. The method defines track loss as being further away than a constant c_1 from the target. If the estimate is further than c_2 from the target, it is considered indefinitely lost, but if it stays within c_2 and c_1 and then returns within c_1, it is considered recovered.

In this thesis, we will use a simple track loss definition. We define track loss as being further than c_1 from the ground truth. The track is no longer considered lost if the track is further than c_1 from the ground truth and then returns within c_1. The author views this approach as equally satisfying as the two-stage process and also simplifies implementation.

5.3 Discarded Methods of Determining Ground Truth

Several approaches to determining ground truth exist. In this section, we look at some of them and discuss how they would handle track loss and track swap. Track coalescence will be mostly ignored, as it is a problem most trackers can avoid with simple track management handling and will not be a problem for the trackers later used to evaluate the performance of T2TA approaches.

5.3.1 Method 1: Letting the first measurements determine the origin of the track

Method 1 lets the origin of a track be the origin of the first measurement originating from a target. When the initial measurement is clutter, it selects the origin of the first measurement originating from a target.

This method will produce sensible results, as long as the track does not undergo track swap, track loss or track coalescence. However, in highly target dense areas, track swap is inevitable. Especially at the start of a tracks life, where the position estimates are more uncertain than after some update steps.

In Figure 5.4a and Figure 5.4b, we see an example of method 1 not working as intended. In the first figure, we have plotted the estimates of the radar tracker and the AIS tracker along with colours signifying whether an association was made and it was correct (coloured green), whether an association was made and it was false (coloured black), or whether no association was made, but it should have been (coloured orange). By comparing the two figures, we can verify that the method does not produce sensible results. Quite a lot of the associations are considered as false associations, even though the associations looks correct according to Figure 5.4b. This is due to a track swap during the initial steps. By

further examining, one can see that the track swap occurs in pairs of two. These results suggest that method 1 is not usable in scenarios with a high target density.

Using this method in combination with the proposed track loss handling, one might expect to get decent results. The idea being that if a track swap happens, the track loss handling will view it as track loss. However, in the case of two targets moving close to each other, the track loss handling might not view it as a track loss, as they are too close to each other. Then the method will view the associations as false, and the results would be invalid.

5.3.2 Method 2: Letting the most recent measurement determine the origin of the track

Method 2 uses the origin of the measurement used in the most recent update as ground truth. If a measurement originates from clutter, the last measurement originating from a target determines the ground truth.

This method will work fine as long as no measurements from nearby tracks are associated to the track. In a multi-target setting, measurements from nearby targets will at some point be falsely associated to the track. Then this method will change the ground truth of the track.

If we had defined track swap as using a single measurement from another target in an update cycle, this method would be correct. However, as a filtering process is multi-scan by nature, this definition of track swap is not natural. The previous estimates affect the current estimates, and this should be reflected when determining the ground truth. As opposed to method 1, this method will change the ground truth when the track swaps but will, in the author's opinion, change ground truth also in situations where it should not.

5.3.3 Method 3: Letting the nearest target be the origin of a track

Method 3 lets the nearest target be the origin of a track. When two targets move close to each other, this method will match the targets and tracks by minimizing the total distance between each pair.

This method will go wrong when the tracks estimate is closer to a target than the target it is actually following. In cases such as two targets crossing each others path, this could happen.

This approach seems viable when we do not have information about the origin of the measurements, which we do when we use simulated scenarios.

Similar to method 2, an argument against such a method is that a single-scan method is not fair to the multi-scan nature of a filtering process. A multi-scan version of method 3 is surprisingly similar to the counting technique. Possible approaches of a multi-scan version could be 1) minimize the total distance between the track and target the last n timesteps, or 2) necessitate that the ground truth of a track must have been less than a threshold the last x timesteps, similar to the counting technique.

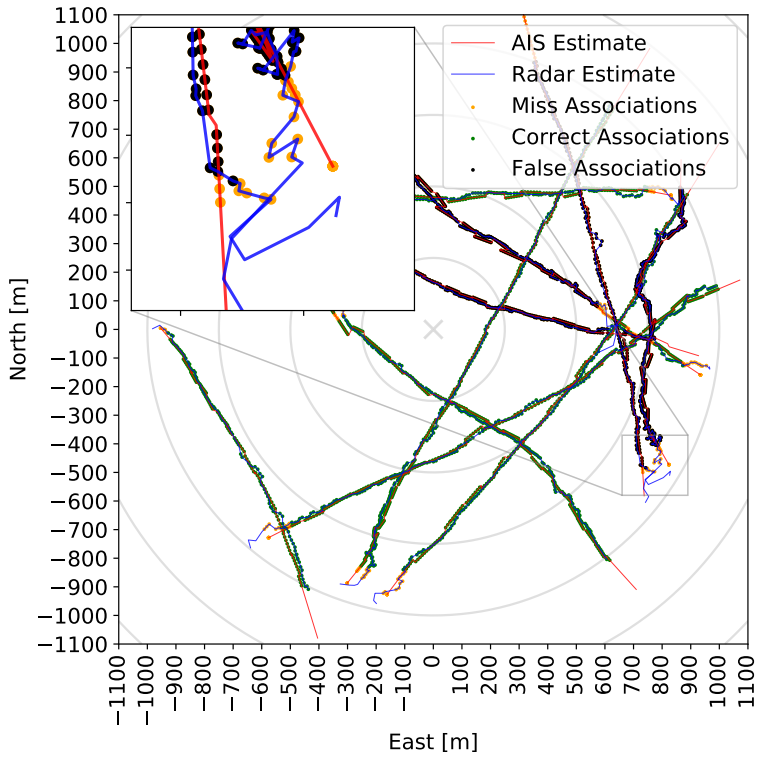

(a) caption

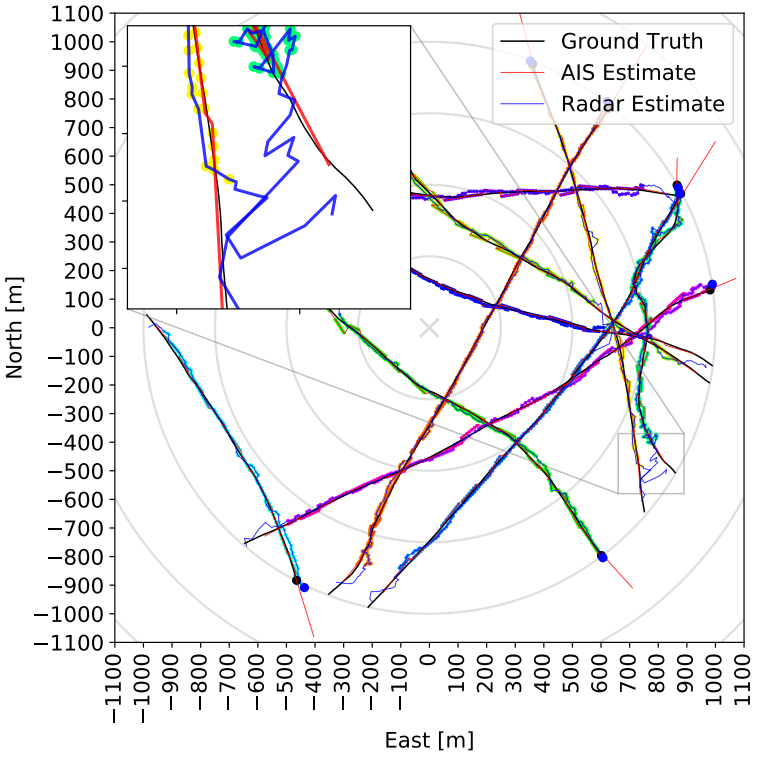

(b) Caption

Figure 5.4: Overall caption

5.4 Proposed Method of Determining Ground Truth

Our proposed method of determining ground truth is a sliding window approach, which uses the origins of the n last measurements used in the update of a track to determine its ground truth. The author has not seen this or any similar approaches in the literature.

5.4.1 Sliding Window Approach

Our method uses a sliding window approach to determine the origin of a track. The method works as follows; the measurement with the most probability mass used in the update of a state is saved to a list. When the ground truth of a track at a specific timestamp is calculated, each measurement in a window of n measurements votes for its origin as the ground truth of the track. Each measurement is equally important, so the origin which had the highest number of measurement originating from it is considered the ground truth of the track.

As opposed to method 1, method 2 can somewhat handle track swaps. The method will update the origin of the tracks when sufficiently of the last x measurements originates from the new track origin, although subjected to a delay, depending on the chosen size of x.

Determining the window size x When deciding on the sliding window size, x, one needs to examine the main challenges of determining the ground truth and how the window size affects these. The four main challenges, according to the author, are 1) track swap while the target is being initiated, 2) track swap at a later stage of the tracks life, 3) falsely associating a measurement from another target and clutter, and 4) track loss, listed in an arbitrary order. Some of these challenges are highly correlated, but the author finds it easiest to split them in this manner, as the window size affects them differently. Firstly, as seen in Figure 5.4, the tracks are highly susceptible to track swap while the track is being initiated. The tracks have a large uncertainty when first initiated, which leads to a large gate and track swaps likely in highly dense tracking scenarios. Luckily, the calculated ground truth will quickly reflect the track swap when using the sliding window approach, almost independent of the sliding window size. Track swap at a later stage is less likely to happen but also more difficult to adjust for. Assuming the window size is N, one can expect that it takes $N/2$ timesteps before the ground truth correctly reflects the track swap in a simplified scenario. The lower the window size, the quicker it will adjust to a track swap. However, a too low window size will yield the method less robust to false associations, either associating the track with clutter or with measurements origination from other targets. The last problem, track loss, is handled in other ways and will not be considered when determining the window size.

Now, disregarding track loss and track swap while the target is being initiated, we note that the final decision of the window size comes down to a trade-off

between robustness to false associations and clutter and quickly reflecting track swaps. The likelihood of track-swaps is highly dependent on the difficulty of the tracking scenario and is not quantifiable. Further, the number of false associations (but not track swaps) will also increase as the difficulty of the scenario increases. A difficult scenario is thought of as e.g. a high density of targets and low-resolution sensors, but not excluding other relevant factors. In this thesis, the main application of the ground truth is to evaluate the association techniques. To do so, we need to examine the results of the associations in different scenarios, ranging from easy scenarios, e.g. few targets and high sensor resolution, to challenging scenarios, e.g. high target density and low sensor resolution. With this in mind, we note that it is important that the ground truth is just to the whole range of difficulties, such that we reduce any potential bias in the results. For the most challenging scenarios, we expect track swaps to happen, but not frequently. The author would argue that a window size in the area of 7 to 15 timesteps would be applicable, as it would be somewhat robust to false associations (need at least 4 in the last 7 updates to change the GT) and would still be reasonably quick to adapt to track swaps (maximum 8 timesteps before the ground truth reflects the change).

In Figure 5.5, we see a similar figure as previously shown for method 1. In the top figure, the output of the ground truth evaluation is presented, where green dots signify correct associations, orange signifies miss associations, and black signifies false associations. For both figures, the estimates of the AIS tracker is shown as a solid red line, while the estimates of the radar tracker are shown as a solid blue line. The most interesting part of the figure is zoomed in. By examining the colours of the estimates, we see which are associated together, e.g., the light green estimates are associated to the same AIS track, while the cyan-coloured are associated to another AIS track. By inspection, one can conclude that all associations are correct, except one single association at the start. Further, we note that the radar tracker jumps between the two targets at the start, best visualized by looking at Figure 5.5b, before it stays on the top target. The method produces a couple of wrong associations but is relatively quick to handle early track swaps.

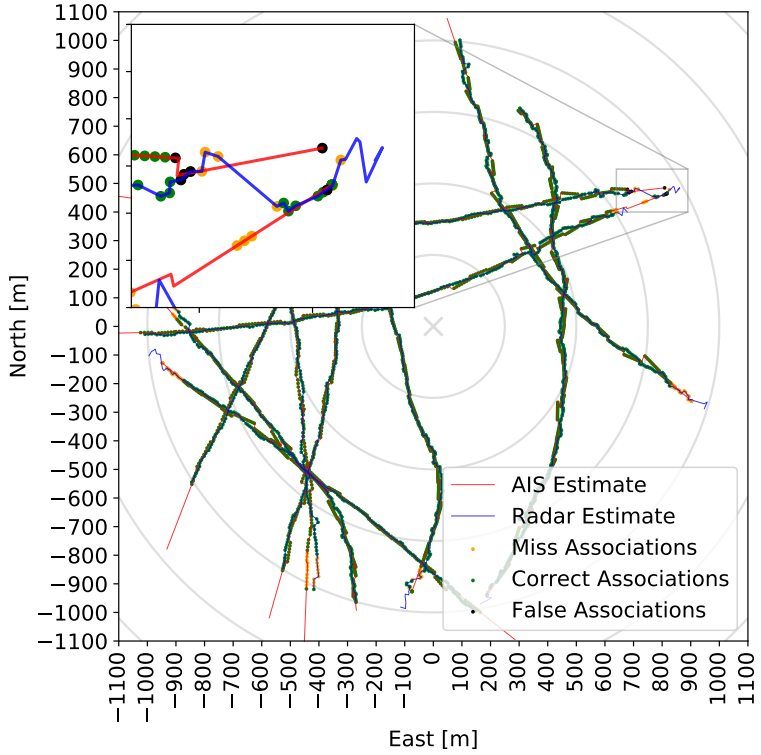

(a) caption

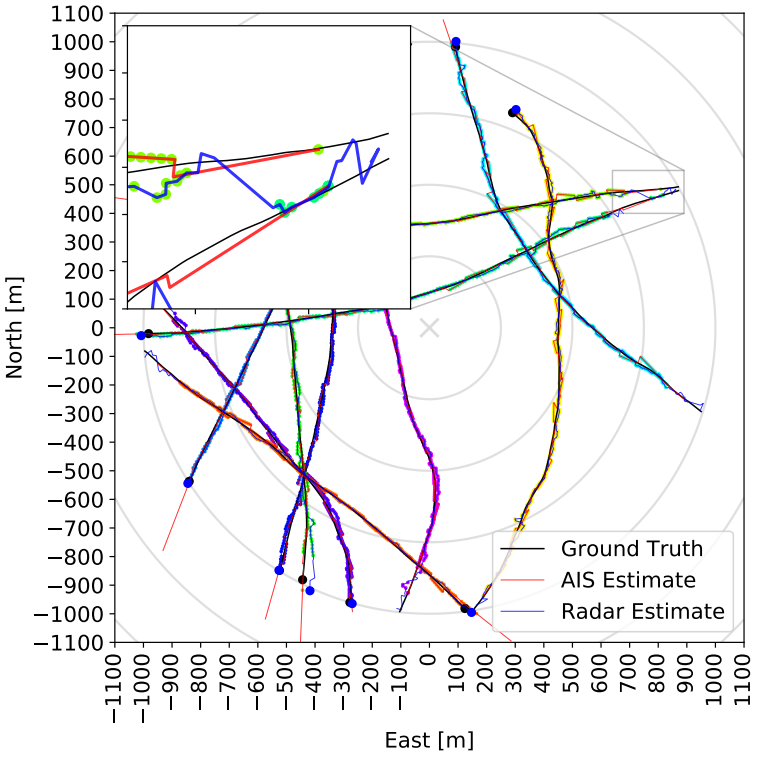

(b) Caption

Figure 5.5: Overall caption

Chapter 6

Experimental Setup

6.1 Simulation Setup

To simulate the multi-target scenarios, the simulator developed in A. G. Hem's thesis is used. The simulator is thoroughly described in his thesis, chapter 6 of [28]. In this section, we will describe the main characteristics along with the models used to simulate the targets and the measurements. The reader is referred to Hem's thesis for a more detailed description.

6.1.1 Target Generation

Targets are born at the edge of a circular surveillance area with a radius equal to the set maximum sensor range. A Poisson process is used to determine the birth of targets, and all targets are born within the first *max birth time* seconds. The targets initial velocity magnitude is randomly set within a preset maximum initial velocity parameter. The direction of the velocity is randomly set but with a maximum degree of 45 degrees between a line from the birth position to the origin.

The targets move according to the constant-velocity model described in Section 2.1.2. The targets evolve according to

$$\mathbf{x}_{k|k-1} = \mathbf{F}\mathbf{x}_{k-1} + \mathbf{v}_k \qquad \mathbf{v}_k \sim \mathcal{N}(0, \mathbf{Q}), \tag{6.1}$$

where $\mathbf{F}$ and $\mathbf{Q}$ are shown in Section 2.1.2, respectively.

The targets die when they move out of the surveillance area or when the scenario end time is reached, defined by the *scenario max time* parameter.

6.1.2 Sensor Simulation Models

Radar Measurements

The radar measurements are generated every two seconds in this thesis. The measurements are generated according to the radar measurement model, as described in Section 2.4.1. The model is

$$\mathbf{Z}_k = \mathbf{H}_R \mathbf{x}_k + \mathbf{w}_k \qquad \mathbf{w}_k \sim \mathcal{N}(0, \mathbf{R}_R). \tag{6.2}$$

The matrices $\mathbf{H}_R$ and $\mathbf{R}_R$ are shown in Section 2.4.1. Each target has a probability P_D of being detected, i.e., probability P_D of generating a measurement.

In addition to the measurements generated by the targets, additional clutter measurements are generated according to a Poisson process with measurements uniformly distributed on the surveillance area.

AIS Measurements

The AIS measurements are generated according to the velocity magnitude and the turn rate of the target, according to Table 2.2. The measurements are generated according to the AIS measurement model, as described in Section 2.4.2. The model is

$$\mathbf{Z}_k = \mathbf{H}_{AIS} \mathbf{x}_k + \mathbf{w}_k \qquad \mathbf{w}_k \sim \mathcal{N}(0, \mathbf{R}_{AIS}). \tag{6.3}$$

The matrices $\mathbf{H}_{AIS}$ and $\mathbf{R}_{AIS}$ are shown in Section 2.4.2. The probability of detection P_D for the AIS measurements is assumed to be 1, as we assume that all AIS messages are transmitted unaltered.

6.2 Radar and AIS Tracker

This part of the thesis concerns the association of tracks outputted from multi-target trackers. The two trackers will be shortly described in this section.

6.2.1 Radar Tracker

The radar tracker is a variation of the JIPDA (see Section 2.2.2) with IMM (see Section 2.2.3 and a visibility state, which we refer to as the VIMMJIPDA [27]. The visibility state is a discrete value that determines whether the target is observable or not. It uses three models: A low-noise constant velocity model, a high-noise constant velocity model and a coordinated turn model. The first two are handled by Kalman filters, while the third model is handled by an extended Kalman filter (EKF).

6.2.2 AIS Tracker

The AIS tracker is a Kalman filter-based tracker. The tracker assumes no clutter and that all MMSI numbers are unique. The track management is simple and exploits the assumptions.

Filtering: The tracker uses a Kalman filter and updates estimates as new AIS messages arrive. The process model is a CV model, as described in Section 2.1.2.

Track initiation: A new track is initiated for each MMSI number not among the active tracks.

Track termination: A track is terminated when it has received no new AIS messages in the last 20 seconds.

6.3 Performance Measures and Evaluation Methodology

There are several different approaches to evaluating T2TA techniques. A split goes between whether to assume the trackers are perfect or include aspects typically seen in multi-target tracking, such as false alarms, miss detections and slow initialization time. Almost all work seen by the author examines scenarios where the trackers whose tracks we wish to associate are perfectly consistent, e.g. [49, 50]. Some work includes assessing the effect of limited sensor resolution [17, 18]. Further, the scenarios examined concerns single-target tracking or two-target tracking, often moving in a parallel line, which seems to be a common theme for work on the fusion of radar and electronic support measures (ESM) [16], often referred to as the *standard test scenario*.

This thesis evaluates the T2TA techniques while including the challenges experienced in typical multi-target tracking, such as false alarms, false associations, miss detections, and delayed track initialization. Due to the fundamental difference in assumptions, the evaluation in this thesis cannot be benchmarked to any other work known to the author. However, this does not imply that other work is not relevant to this thesis.

The work of La Scala and Farina is especially relevant [17]. Their work analyses five different aspects of T2TA, of which four are relevant to us. They suggest evaluating the probability of associating tracks that originate from the same target, i.e. the true positive rate (TPR), the probability of associating tracks that originate from different targets, i.e. the false positive rate (FPR), the effect of limited sensor resolution, the method used to determine the threshold for the association test, and the effect of ignoring the cross-covariance. The last aspect will not be pursued, as we will only evaluate the hypothesis test of independent tracks and the counting technique.

In this section, we describe our proposed method of evaluating T2TA techniques used in multi-target tracking. Our proposed method differs from approaches in the literature. One of our contributions is introducing a new metric that, seemingly, has not been used before.

6.3.1 Metrics

To define our metrics, we first categorize the associations.

In this thesis, an association refers to an association between two tracks. An association can be characterized by whether the association was a correct association, wrong association, or a missed association.

True Positive is also referred to as a correct association. It is an association between two tracks that originate from the same target.

True Negative is not associating two tracks that do not originate from the same target. It is the correct lack of an association.

False Positive is also referred to as a wrong association. It is associating two tracks that do not originate from the same target.

False Negative is also referred to as a missed association. It is not associating two tracks that originate from the same target.

$\boldsymbol{P_{TP}}$ is the percentage of associations of tracks that originate from the same target that is associated. It can also be thought of as the probability of associating two tracks that originate from the same target. It is referred to as true-positive rate (TPR). It is calculated as $\boldsymbol{P_{TP}} = \frac{\#\textit{True Positive}}{\#\textit{True Positive}+\#\textit{False Negative}}$.

$\boldsymbol{P_{FP}}$ is the percentage of associations of tracks that do not originate from the same target that is associated. Or the probability of associating two tracks that did not originate from the same target. Referred to as false-positive rate (FPR). It is calculated as $\boldsymbol{P_{FP}} = \frac{\#\textit{False Positive}}{\#\textit{False Positive}+\#\textit{True Negative}}$.

Initialization time is the amount of time it takes a method to associate two tracks, starting from when the tracks were viewed as originating from the same target. One can also view it as counting the missed associations (false negatives) until the first correct association of two tracks. These initially missed associations are not counted when calculating the FPR.

The initialization time of a T2TA technique is a novel metric to evaluate the performance of a T2TA technique. The counting technique needs a couple of timesteps, depending on the ψ parameter, to initialize the first association. Therefore, this should be examined to evaluate the performance of the method. It is important to note that the initialization time is only calculated the first time a new target appears. I.e., after the first correct association, all missed associations will be counted in the FPR.

6.3.2 Proposed Method to Evaluate Association Techniques

Our proposed method to evaluate the T2TA techniques is to evaluate the FPR, TPR and initialization time for different tracking conditions. The conditions examined are chosen such that the analysis covers the conditions an ASV could experience.

The main tool for assessing the performance is the Receiver Operating Characteristic (ROC) curve. Hard association of tracks in track-to-track fusion is fundamentally a detection problem, i.e. a binary decision problem, and can therefore be assessed by detection theoretic concepts. The performance of a detector is typically assessed by the ROC. The ROC is a monotonous curve that traces out the true-positive rate (TPR) as a function of the false-positive rate (FPR). Typically, the ROC curve is plotted for varying discrimination thresholds [51].

Surprisingly, it does not seem like the ROC curve have been used in the literature on T2TA evaluation. Typically, TPR and FPR are shown for each scan number,

which is reasonable to examine when the scenario evaluated becomes more difficult for a higher scan number as the targets move away from the sensors.

As suggested in [17], the T2TA methods must be assessed in various conditions. One method might perform better in *normal* conditions, while another more robust method might perform better in more *difficult* conditions. In this thesis, we will examine the methods in four different conditions.

The conditions will be present along with the results in Chapter 7.

Chapter 7

Track-to-Track Association Results

In this chapter, we compare the performance of the hypothesis test (HT) and the counting technique (CT) according to the method described in Section 6.3. The simulated data are generated according to the simulation scheme described in Section 6.1. As described in Chapter 5, it is challenging to determine the ground truth of tracks from multi-target tracking system with false alarms, wrong associations and delayed initialization time. For all results presented, we use our proposed sliding window approach, Section 5.4, along with the proposed track loss handling, Section 5.2.

The main result of this chapter is the comparison of the CT and the HT in terms of false-positive rate (FPR), true-positive rate (TPR), and initialization time. The metrics are described in Section 6.3.1. The parameters of the T2TA techniques are examined in Section 7.2 before the performance is evaluated in varying conditions in Section 7.3. First, the conditions examined are presented.

7.1 Scenario Descriptions

To test the association techniques in varying conditions, four different sets of simulation parameters were chosen. For all sets of parameters, the same tracking parameters and association technique parameters were used. The four conditions are labelled 1) easy, 2) normal, 3) difficult and 4) very difficult. In combination with the condition parameters, the targets were generated according to the simulation parameters in Table 14.2, and the ais and radar tracker used the tracker parameters in Table 14.1. The sliding window length n was set to 10, while the track loss constant was $c_1 = 100$ meters.

Easy Conditions The easy conditions parameters are shown in Table 7.3. A total of 5 targets will spawn at random between timestep 0 and 200. A low process noise intensity q_a and high detection probabilities lead to both the radar tracker and the

Parameter	Symbol/Units	Value
Radar sample interval	T [s]	2
CV 1 process noise	$q_{a,1}$ [m/s^2]	0.1
CV 2 process noise	$q_{a,2}$ [m/s^2]	1.5
Turn rate process noise	q_ω [1/s^2]	0.02
Cartesian range std. radar	σ_{c_R} [m]	6.6
Cartesian range std. AIS	σ_{c_A} [m]	3
Polar range std.	σ_r [m]	5
Polar bearing std.	σ_θ [deg]	1
Detection probability	P_D [–]	0.92
Survival probability	P_S [–]	0.99
Visibility transition probabilities	w [–]	$\begin{bmatrix} 0.9 & 0.1 \\ 0.52 & 0.48 \end{bmatrix}$
Gate size	g [–]	3
Track fusion hypothesis significance level	[–]	0.01
Clutter intensity	λ [1/m^2]	2×10^{-7}
Initial new target intensity	b [1/s^2]	1×10^{-8}
Initial velocity std.	σ_{init} [m/s]	15
Initial mode probabilities	μ^0 [–]	$[0.8, 0.1, 0.1]^\top$
Mode transition probabilities	π^{ss} [–]	$[0.99, 0.99, 0.99]$
Existence confirmation threshold	[–]	0.999

Table 7.1: Tracker parameters.

Parameter	Symbol/Units	Value
Radar sample interval	T [s]	2
Cartesian range std. radar	σ_{c_R} [m]	6.6
Cartesian range std. AIS	σ_{c_A} [m]	3
Polar range std.	σ_r [m]	3
Polar bearing std.	σ_θ [deg]	1
Clutter intensity	λ [1/m^2]	2×10^{-7}
Max initial velocity	V_{init} [m/s]	10

Table 7.2: Simulated data parameters.

sensor range	#targets	max birth time	q_a	P_D^{radar}	P_D^{AIS}
1000	5	200	0.1	0.92	0.999

Table 7.3: The parameters used to generate the scenarios labeled easy.

sensor range	#targets	max birth time	q_a	P_D^{radar}	P_D^{AIS}
1000	10	5	0.3	0.92	0.999

Table 7.4: The parameters used to generate the scenarios labeled normal.

AIS tracker performing well, and the low target density yields a low likelihood of targets interfering with each other. The conditions are similar to what one could expect at the open sea.

Normal Conditions The normal conditions parameters are shown in Table 7.4. A total of 10 targets will spawn at random between timestep 0 and 5. Both the radar tracker and the AIS tracker have reasonable performance, and the false track ratio is quite small. The short period of time where track spawns yields a higher chance of targets tracks interfering with each other compared to the easy conditions. The conditions are similar to what one could expect to experience in heavily trafficked waters.

Difficult Conditions The difficult conditions parameters are shown in Table 7.5. A total of 10 targets will spawn at random between timestep 0 and 5. The tracks spawn area is substantially smaller than for the easy and normal conditions due to the sensor range being 600 meters compared to 1000 meters. The trackers start to struggle, and track swaps and track loss is likely to be seen once or twice per monte-carlo simulation. A very high chance of targets tracks interfering with each other. Such conditions could be experienced when the shore obstruct the sensors view in a heavily trafficked area.

Very Difficult Conditions The very difficult conditions are shown in Table 7.6. The only difference between the very difficult conditions and the difficult conditions is the radars detection probability. A substantially smaller radar detection probability further reduces the capability of the radar to track targets. Radar track loss and track swap are more likely than in the difficult conditions. The conditions can be experienced in close-to-shore heavily trafficked areas with degraded radar measurements.

sensor range	#targets	max birth time	q_a	P_D^{radar}	P_D^{AIS}
600	10	5	0.3	0.92	0.999

Table 7.5: The parameters used to generate the scenarios labeled difficult.

sensor range	#targets	max birth time	q_a	P_D^{radar}	P_D^{AIS}
600	10	5	0.3	0.6	0.999

Table 7.6: The parameters used to generate the scenarios labeled very difficult.

7.2 Parameter Examination

7.2.1 Counting Technique

In Figure 7.2a, the TPR and the FPR are plotted for varying association parameters. In Figure 7.2b, the initialization time and the FPR are plotted for varying association parameters. The results are from the *normal* conditions, as described in Section 7.1.

Both the hypothesis test (HT) and the counting technique (CT) are shown in the figures. For the CT, the letter ψ refers to the number of hits in a row that is needed to associate two tracks, and τ refers to how many misses in a row is needed to end an association as described in Section 4.2. The *distance_threshold* is not included in the figure to avoid clutter. The *distance_threshold*'s used are similar for all combinations of τ and ψ and is 10-20-30-40 meters. The top-left point of each τ-ψ combination in Figure 7.2b is 10 meter, the next is 20 meters, the third 30 meters and the bottom right is 40 meters. Note that the FPR axis is similar in both figures.

An increase of τ and ψ leads to a higher TPR and a lower FPR, when the *distance_threshold* is constant. An increase of τ and ψ also leads to a higher initialization time. As a larger ψ would require more *hits* in a row, the initialization time would also increase. A smaller *distance_threshold* makes it harder for two estimates to be considered a hit. We see that a smaller *distance_threshold* cause a lower TPR and a higher initialization time, while decreasing the FPR.

7.2.2 Hypothesis Test

Examining the same figures as in the previous section, Figure 7.2.

The α values considered are $[0.01, 0.1, 0.3, 0.5, 0.7, 0.9, 0.99]$. In Figure 7.2a, the bottom left point is 0.01, the next is 0.1, etc. In theory, α is the probability of not associating two tracks originating from the same target. The definition of miss percentages (Section 6.3.1) coincides with that definition. However, this does not hold when we examine multiple targets.

A higher α leads to a higher initialization time, and a lower FPR, while in-

creasing the TPR. The results are as expected, as a higher α makes it harder for two estimates to be associated.

7.3 Performance Evaluation

For all four conditions, the same association technique parameters are used. For the hypothesis test (HT), the alphas used are [0.99, 0.9, 0.7, 0.5, 0.3, 0.1, 0.01]. For the counting technique (CT), the *distance_threshold*s used are [40 m, 30 m, 20 m, 10 m]. The ψ and τ used are listed in the figures.

The results consist of figures showing the initialization time, the true-positive rate (TPR), and the false-positive rate (FPR) for the association parameters discussed. The performance characteristics of the CT and the HT simulated using the easy conditions parameters can be seen in Figure 7.1. The results using the normal conditions, difficult conditions and very difficult conditions can be found in Figure 7.2, Figure 7.3, and Figure 7.4, respectively.

Examining the results of the *easy* conditions, Figure 7.1, note that the CT have 0 FPR for all values examined. The HT is close to zero, with about 0.00009 FPR for most parameters. Further, we note that both methods have parameter choices that yield perfect TPR equal to 1. The HT has zero initialization time, meaning it associates two tracks the first time two tracks are considered originating from the same target for several parameter choices. The CT has some initialization time, depending on the choice of parameters.

In Figure 7.2, we see the results of the *normal* conditions. Compared to the easy conditions, the normal conditions yield a shape more commonly seen in ROC curves. A higher ψ-τ combination leads to a better performance in terms of TPR and FPR, but at the cost of a higher initialization time. For ψ-τ equal 5 and 4, we note that the shortest initialization time is 10, which in most applications would be considered quite high. The CT performs better in terms of FPR, while the HT performs better in terms of initialization time.

The results of the *difficult* conditions, in Figure 7.3, seems at first very similar to the results of the *normal* conditions. The relative performance of the CT and HT seems similar. Both methods are slightly shifted down in terms of TPR and up in terms of FPR. The HT performs slightly worse in terms of the initialization time.

In the *very difficult* conditions, Figure 7.4, the situation is quite different from the previous plots. With the other conditions in mind, the HT performs better in terms of FPR and TPR compared to the CT. There is also a greater difference in initialization time between the HT and the CT relative to the other conditions. Both methods are shifted to a considerable higher FPR, while the TPR is slightly smaller for all parameter choices.

In all conditions, the HT is considerably quicker to initialize the first association. This comes as no surprise, as the HT is a single-scan approach, and the CT is a multi-scan approach.

The initialization time of the CT is higher than what the author would have expected. Considering the easy conditions in Figure 7.1, the author would have

expected the initialization time to be slightly higher than ψ. In most cases, ψ sets a lower limit of the initialization time, as the minimum amount of timesteps to associate two tracks would be ψ. However, it is also possible that the initialization time is lower than ψ. The CT can consider two tracks a hit, two tracks being within *distance_threshold* of each other, even when the ground truth says they are of different targets. In the case of a track swap, this might happen, which is especially likely to happen when two targets enter sensors view approximately in the same area. One might expect that there is a non-linear relationship between ψ and the initialization time. As ψ increases, the chance of two tracks not being associated due to a single miss, two tracks being too far away from each other to be considered a hit, increases. The relationship is not evident from the results but can help explain why the initialization time of $\psi = 2$ is about 2 seconds, while $\psi = 6$ is about 10 seconds. By this explanation, one would expect scenarios with more difficult conditions to yield even higher initialization times as the rate of misses increases, but this is not seen in the results. Another approach to the same line of thought is that a lower TPR would yield a higher deviation from ψ. The reasoning is similar to previously. A lower TPR must mean that there is a higher rate of misses. A higher rate of misses means an increase of misses stopping two tracks from being considered associated, which increases the initialization time. By this approach, one would not view whether the conditions are more or less difficult, but rather how the TPR changes.

The *very difficult* conditions differ from the other conditions in that the radar tracker is severely reduced due to its low detection probability. The performance of the HT seems to be better relative to the CT in those conditions. It might be due to the fundamental difference in the two methods, in that the HT considers the covariance when determining whether to associate two tracks. It is possible that the information from the covariances becomes more important when the estimates are degraded.

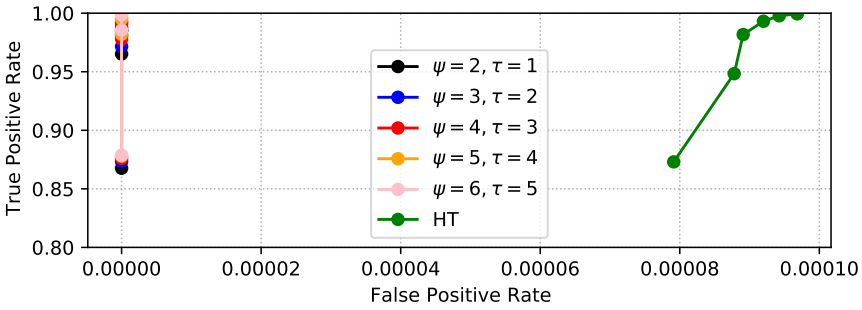

(a) True-positive rate and false-positive rate.

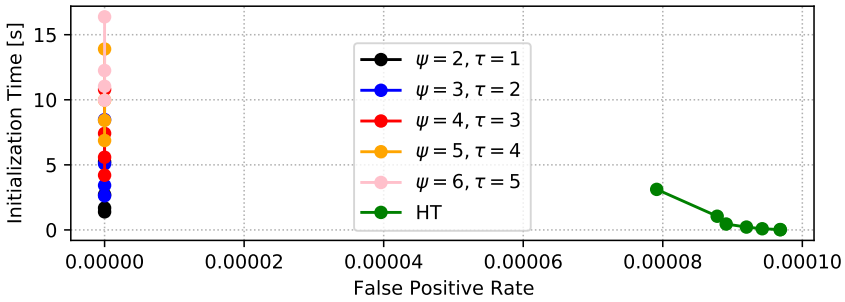

(b) Association initiation performance.

Figure 7.1: Performance characteristic for easy conditions.

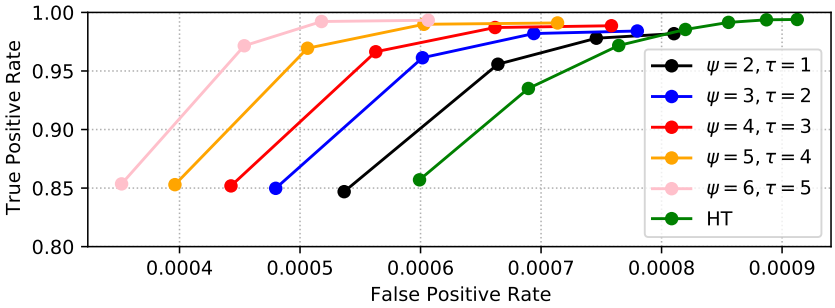

(a) True-positive rate and false-positive rate.

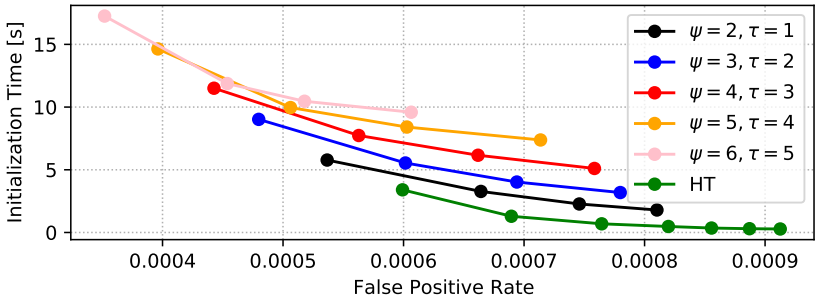

(b) Association initiation performance.

Figure 7.2: Performance characteristic for normal conditions.

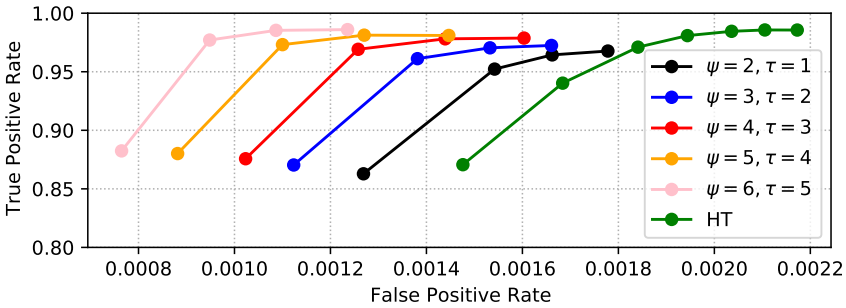

(a) True-positive rate and false-positive rate.

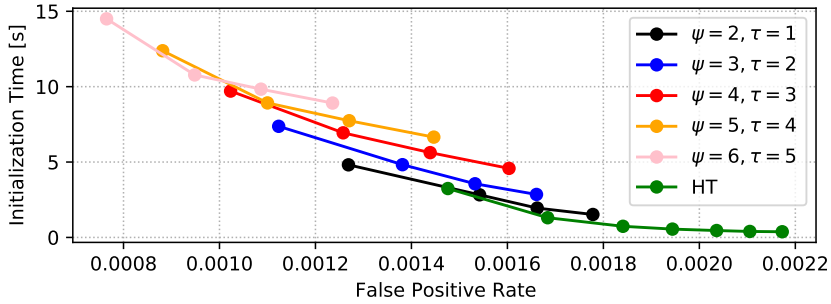

(b) Association initiation performance.

Figure 7.3: Performance characteristic for difficult conditions.

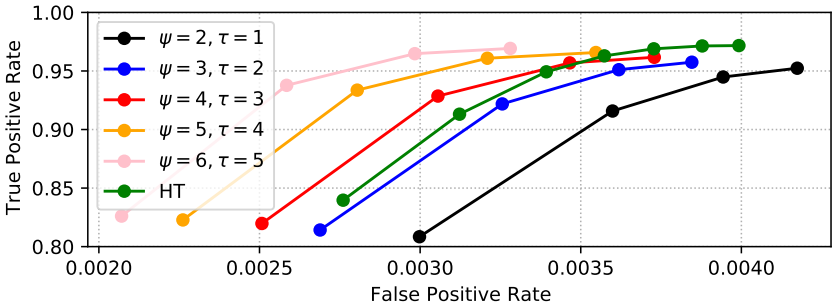

(a) True-positive rate and false-positive rate.

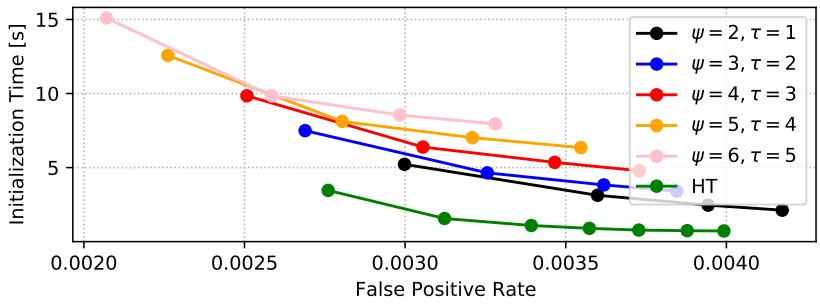

(b) Association initiation performance.

Figure 7.4: Performance characteristic for very difficult conditions.

Chapter 8

Track-to-Track Association Discussion

8.1 Ground Truth Evaluation

The ground truth of each track was evaluated using the proposed sliding window approach. Our approach differs from other known approaches in that it is a sliding-window approach. We avoid short-term changes of ground truth by using temporal information due to false alarms or falsely associating measurements from nearby tracks. However, this can also have a negative effect, as the method, depending on the chosen window size n, can be slow at reflecting a track swap.

The window size n was set to 10 in this thesis. The reasoning behind this number was discussed in Chapter 5. In short, the number was deemed to yield a method robust to associations from nearby clutter and measurements from other targets while still being able to reflect a track swap quickly. Another option could be to calculate the rate of track swaps, would then need to be able to calculate when a track swap happens, along with the rate of false associations in the radar tracker, would also need a method to calculate that, which could be used to determine whether track swaps or clutter and false associations is the main concern. There is a very big *but* to this approach, as it would require a clearer definition of track swaps to distinguish the two situations.

The sliding window approach has some similarities to the counting technique. This might yield a small bias in favour of the counting technique. However, as the sliding-window approach seems to be a reasonable approach to determining ground truth, it might also argue that the counting technique seems to be a reasonable approach to T2TA.

With the proposed approach, several tracks may be associated to the same target. This is not necessarily wrong but could, in certain situations, lead to unnatural results. The T2TA implementation of the CT and the HT makes sure that only two tracks can be associated together. This makes it impossible for the T2TA to be correct when three tracks are deemed to originate from the same target.

It is possible to use the auction algorithm to deal with situations where too

many tracks have the same ground truth. This was not further examined by the author and is left as further work.

8.2 Performance of the Counting Technique and the Hypothesis Test

There are two fundamental differences between the CT and the HT. Firstly, the CT does not use information about the covariance of the estimates when associating tracks. Having more information when making a decision is arguably better, as long as the information is correct. If the information is wrong, it might lead to a wrong decision. The effect of trackers with severely degraded consistency was not examined in this thesis. This is interesting to analyze, as the performance of the CT and HT may differ more than when associating tracks from consistent trackers. The second fundamental difference between the CT and the HT is that the CT use temporal information. The additional information from previous timesteps should, arguably, make the method more robust to temporary track swaps.

The CT performed well in terms of FPR and TPR compared to the HT. However, in terms of initialization time, it was substantially worse. Ideally, the CT would perform as robust as it does with an initialization time comparable with the hypothesis test. There may exist a combination of two methods that allow for a quicker initialization time. A possibility is to combine two CT's, where the first has a large ψ, τ and threshold, and the other has a lower ψ, τ, and threshold. It is unclear how one would determine when the two-combined CT associates two tracks. Still, a possibility is always to associate two tracks if one of the methods associates the tracks. This would initially lead to a higher FPR, but this could be reduced by tuning.

When it comes to tuning, the HT arguably has an advantage over the CT, as it only requires one parameter to set. However, based on the results in this thesis, it seems like the ψ and τ must be set depending on the requirements of the initialization time. It is also possible that the threshold could be set based on the process noise or expected RMSE, but this was not investigated. Further, the choice of alpha might depend on the consistency of the local trackers, which is not necessarily known in advance. The effect of the inconsistency of local trackers on the choice of α was not examined in this thesis. La Scala and Farina examined the methods of determining the α but did not examine inconsistency issues possible to experience in multi-target tracking systems [17].

8.2.1 Applicability

Based on the results, it seems like the CT is superior to the HT in terms of FPR and TPR for most conditions while being inferior in terms of initialization time. This leads to the question of whether the two methods should be used in different situations.

The choice of whether to opt for the CT or the HT comes down to the use case. If the lower initialization time is not deemed a big issue, the CT is arguably a good choice. For example, this might be the case at open sea, where long-distance radars track large and slowly moving vessels. On the other hand, in close to shore tracking with short-range radars and faster vessels, the HT might be a better option. The AIS measurement rate should also be considered, as a slow AIS measurement rate will likely make the initialization time higher.

In any case, the results show that the CT is a viable choice when no covariance information is available. However, when using the CT, the slow initialization time should be kept in mind.

Part III

Track-to-Track Fusion

Chapter 9

Three Methods for Track-to-Track Fusion

In the following sections, we will derive two methods for synchronous track-to-track fusion and present the formulas for asynchronous track-to-track fusion. Both the derived methods belong to the T2TF without memory and no feedback (T2TFwoMnF) category, as presented in Chapter 3. First, assumptions for the synchronous methods are presented in Section 9.1. The first method, presented in Section 9.2, assumes that the error of the state estimates is independent. The second method, presented in Section 9.3, accounts for the common process noise, which was previously discussed in Section 3.2. This method is known as the optimal T2TFwoMnF. In Section 9.4, we will present an asynchronous track-to-track fusion method. Lastly, in Section 9.5, we will discuss the usage of the Kalman Filter to fuse measurements from two sensors.

Most of the work on T2TF is from the author's pre-thesis [52]. It is included for its completeness and because later discussion is based on the results.

The following is based on chapter eight of the book Multitarget-multisensor tracking: principles and techniques [11].

9.1 Assumptions

The following is assumed when deriving the fusion formulas.

- The two trackers, i and j, estimates the position of target 1 at timestep k as a Gaussian distribution with expectation ${}^{m}\hat{\mathbf{x}}_k^1$ and covariance ${}^{m}\mathbf{P}_k^1$, $m \in [i, j]$. The trackers are Kalman filters, and use the formulas in Section 2.1.1.
- The two trackers, i and j, are synchronised, i.e. their estimates at timestep k are updated with measurements obtained simultaneously.
- The measurement model and process model used in tracker i and j are identical, i.e. the transition matrix $\mathbf{F}$ and measurement matrix $\mathbf{H}$ are identical for the two trackers. Further, the matrices $\mathbf{Q}$ and $\mathbf{R}$, which governs the statistical properties of the process noise and the measurement noise, are as-

sumed identical for both trackers.
- The true state of target 1 is given by $\mathbf{x}_k^1$.
- The associations are assumed perfect and given, i.e. we assume that the estimate from tracker i and tracker j originate from the same target.

Further, the error independence assumption is used when deriving the fusion of independent tracks.

Assumption 1 *Error independence assumption*
The state estimation errors

$$ {}^m\tilde{\mathbf{x}}_k = {}^m\mathbf{x}_k - {}^m\hat{\mathbf{x}}_k, m \in [i, j] \tag{9.1} $$

where ${}^i\mathbf{x}_k = {}^j\mathbf{x}_k = \boldsymbol{x}_k$ *is the true state, are independent.*

At timestep k, we are given the estimates from tracker i and j of track 1 as ${}^i\hat{\mathbf{x}}_k^1$ and ${}^j\hat{\mathbf{x}}_k^1$ along with the respective covariances ${}^i\mathbf{P}_k^1$ and ${}^j\mathbf{P}_k^1$. As association is assumed perfect and we are only looking at the single-target scenario here, we will disregard the track number notation. Further, the timestep notation will only be used when deriving the cross-covariance in Section 9.3.1. Unless specified otherwise, all information used is from timestep k. We are then left with ${}^i\hat{\mathbf{x}}$ and ${}^j\hat{\mathbf{x}}$ along with the respective covariances ${}^i\mathbf{P}$ and ${}^j\mathbf{P}$.

9.2 Track-to-Track Fusion of Independent Tracks

In this section, we derive the fusion of two tracks under the error independence assumption, Assumption 1.

Let the information from tracker i and j be denoted as ${}^i\mathbf{D}$ and ${}^j\mathbf{D}$, respectively. The goal of the fusion is to find $p(\mathbf{x}|{}^i\mathbf{D}, {}^j\mathbf{D})$. Using the linear estimation equation we can fuse prior information $\bar{\mathbf{x}}$ with a measurement $\mathbf{z}$ according to

$$ \hat{\mathbf{x}} = \bar{\mathbf{x}} + \mathbf{P}_{xz}\mathbf{P}_{zz}^{-1}(\mathbf{z} - \bar{\mathbf{z}}). \tag{9.2} $$

Note that we can write ${}^m\hat{\mathbf{x}}$ as

$$ {}^m\hat{\mathbf{x}} = \mathbf{x} - {}^m\tilde{\mathbf{x}}, m \in [i, j], \tag{9.3} $$

where ${}^m\tilde{\mathbf{x}}$ is the error of the estimate ${}^m\hat{\mathbf{x}}$, which is zero-mean and has covariance ${}^m\mathbf{P}$. We specify the terms in Equation (9.2) as

$$ \hat{\mathbf{x}} \to \mathbb{E}[\mathbf{x}|{}^i\mathbf{D}, {}^j\mathbf{D}] \tag{9.4} $$

$$ \bar{\mathbf{x}} \to {}^i\hat{\mathbf{x}} = \mathbb{E}[\mathbf{x}|{}^i\mathbf{D}] \tag{9.5} $$

$$ \mathbf{z} \to {}^j\hat{\mathbf{x}} \tag{9.6} $$

$$ \bar{\mathbf{z}} \to \mathbb{E}[{}^j\hat{\mathbf{x}}|{}^i\mathbf{D}] = {}^i\hat{\mathbf{x}}. \tag{9.7} $$

By these terms, the covariances in Equation (9.2) becomes

$$\begin{aligned}\mathbf{P}_{xz} &= \mathbb{E}[(\mathbf{x}-\bar{\mathbf{x}})(\mathbf{z}-\bar{\mathbf{z}})^T] \\ &= \mathbb{E}[(\mathbf{x}-{}^i\hat{\mathbf{x}})({}^j\hat{\mathbf{x}}-{}^i\hat{\mathbf{x}})^T] \\ &= \mathbb{E}[({}^i\tilde{\mathbf{x}}(\mathbf{x}-{}^j\tilde{\mathbf{x}})-((\mathbf{x}-{}^i\tilde{\mathbf{x}}))^T] \\ &= \mathbb{E}[{}^i\tilde{\mathbf{x}}({}^i\tilde{\mathbf{x}}-{}^j\tilde{\mathbf{x}})^T] \\ &= \mathbb{E}[{}^i\tilde{\mathbf{x}}{}^i\tilde{\mathbf{x}}^T] \\ &= {}^i\mathbf{P},\end{aligned} \tag{9.8}$$

where the last step is by the error independence assumption, and

$$\begin{aligned}\mathbf{P}_{zz} &= \mathbb{E}[(\mathbf{z}-\bar{\mathbf{z}})(\mathbf{z}-\bar{\mathbf{z}})^T] \\ &= \mathbb{E}[({}^j\hat{\mathbf{x}}-{}^i\hat{\mathbf{x}})({}^j\hat{\mathbf{x}}-{}^i\hat{\mathbf{x}})^T] \\ &= \mathbb{E}[((\mathbf{x}-{}^j\tilde{\mathbf{x}})-(\mathbf{x}-{}^i\tilde{\mathbf{x}}))((\mathbf{x}-{}^j\tilde{\mathbf{x}})-(\mathbf{x}-{}^i\tilde{\mathbf{x}}))^T] \\ &= \mathbb{E}[({}^i\tilde{\mathbf{x}}-{}^j\tilde{\mathbf{x}})({}^i\tilde{\mathbf{x}}-{}^j\tilde{\mathbf{x}})^T] \\ &= {}^i\mathbf{P}+{}^j\mathbf{P}.\end{aligned} \tag{9.9}$$

With these covariances, the fused $\hat{\mathbf{x}}$ becomes

$$\hat{\mathbf{x}} = {}^i\hat{\mathbf{x}} + {}^i\mathbf{P}({}^i\mathbf{P}+{}^j\mathbf{P})^{-1}({}^j\hat{\mathbf{x}}-{}^i\hat{\mathbf{x}}), \tag{9.10}$$

or, rewritten to symmetric form

$$\hat{\mathbf{x}} = {}^j\mathbf{P}({}^i\mathbf{P}+{}^j\mathbf{P})^{-1}{}^i\hat{\mathbf{x}} + {}^i\mathbf{P}({}^i\mathbf{P}+{}^j\mathbf{P})^{-1}{}^j\hat{\mathbf{x}}. \tag{9.11}$$

To find the covariance of the fused estimate, we use the covariance update equation

$$\mathbf{P}_{xx|z} = \mathbf{P}_{xx} - \mathbf{P}_{xz}\mathbf{P}_{zz}^{-1}\mathbf{P}_{zx}, \tag{9.12}$$

which becomes

$$\mathbf{P} = {}^i\mathbf{P} - {}^i\mathbf{P}({}^i\mathbf{P}+{}^j\mathbf{P})^{-1}{}^i\mathbf{P}, \tag{9.13}$$

or, in symmetric form

$$\mathbf{P} = {}^i\mathbf{P}({}^i\mathbf{P}+{}^j\mathbf{P})^{-1}{}^j\mathbf{P}. \tag{9.14}$$

Note that when the two trackers have equal covariance matrices ($P^i = P^j$), the covariance of the fused estimate becomes $P = \frac{1}{2}P^m$, $m \subset [i, j]$. Also, note that we could have swapped the terms in Equation (9.4), i.e. which estimate is considered prior and which is considered a measurement, and we would have arrived at the same fusion formulas.

9.3 Track-to-Track Fusion of Dependent Tracks

As discussed in Section 3.2, if the tracks originate from the same target, the estimates are dependent due to the common process noise. In this section, we will derive the fusion when the dependence is accounted for. To do so, we first need to find an expression for the cross-covariance of the estimation errors.

9.3.1 The cross-covariance of the estimation errors

To account for the dependence due to the common process noise, we need to calculate the cross-covariance of the estimation errors. I.e., we need an expression for

$$ {}^{ij}\mathbf{P}_k \triangleq \mathbb{E}[{}^{i}\tilde{\mathbf{x}}_k {}^{j}\tilde{\mathbf{x}}_k^T]. \tag{9.15} $$

We first find the estimation error of the estimate from tracker m at timestep k, ${}^{m}\tilde{\mathbf{x}}_k$, expressed by the estimation error of the estimate from tracker m at timestep $k-1$, ${}^{m}\tilde{\mathbf{x}}_{k-1}$, using the Kalman filter equations described in Section 2.1.1.

$$ \begin{aligned} {}^{m}\tilde{\mathbf{x}}_k &= {}^{m}\mathbf{x}_k - {}^{m}\hat{\mathbf{x}}_k \\ &= \mathbf{F}^{m}\mathbf{x}_{k-1} + \mathbf{v}_{k-1} - (\mathbf{F}^{m}\hat{\mathbf{x}}_{k-1} + {}^{m}\mathbf{W}_k[\mathbf{z}_k - {}^{m}\hat{\mathbf{z}}_{k|k-1}]) \\ &= \mathbf{F}^{m}\mathbf{x}_{k-1} + \mathbf{v}_{k-1} - \mathbf{F}^{m}\hat{\mathbf{x}}_{k-1} - {}^{m}\mathbf{W}_k[\mathbf{H}(\mathbf{F}^{m}\mathbf{x}_{k-1} + \mathbf{v}_{k-1}) \\ &\qquad + {}^{m}\mathbf{w}_k - \mathbf{H}\mathbf{F}^{m}\hat{\mathbf{x}}_{k-1}] \\ &= \mathbf{F}^{m}\tilde{\mathbf{x}}_{k-1} - {}^{m}\mathbf{W}_k\mathbf{H}\mathbf{F}^{m}\tilde{\mathbf{x}}_{k-1} + \mathbf{v}_{k-1} - {}^{m}\mathbf{W}_k\mathbf{H}\mathbf{v}_{k-1} - {}^{m}\mathbf{W}_k {}^{m}\mathbf{w}_k \\ &= [\mathbf{I} - {}^{m}\mathbf{W}_k\mathbf{H}]\mathbf{F}^{m}\tilde{\mathbf{x}}_{k-1} + [\mathbf{I} - {}^{m}\mathbf{W}_k\mathbf{H}]\mathbf{v}_{k-1} - {}^{m}\mathbf{W}_k {}^{m}\mathbf{w}_k, \end{aligned} \tag{9.16} $$

where ${}^{m}\mathbf{W}_k$ is the Kalman gain for tracker m, $\mathbf{v}_k$ is the process noise, identical for both trackers, and ${}^{m}\mathbf{w}_k$ is the measurements noise for tracker m. By inserting $m = i$ and multiplying it with the transposed of $m = j$, and calculating the expectation of that, we get the cross-covariance recursion

$$ \begin{aligned} {}^{ij}\mathbf{P}_k &= \mathbb{E}[{}^{i}\tilde{\mathbf{x}}_k {}^{j}\tilde{\mathbf{x}}_k^T] \\ &= [\mathbf{I} - {}^{i}\mathbf{W}_k\mathbf{H}][\mathbf{F}^{ij}\mathbf{P}_{k-1}\mathbf{F}^T + \mathbf{Q}][\mathbf{I} - {}^{j}\mathbf{W}_k\mathbf{H}]^T. \end{aligned} \tag{9.17} $$

Note that ${}^{ij}\mathbf{P} = {}^{ji}\mathbf{P}^T = {}^{ji}\mathbf{P}$. Also note that ${}^{ij}\mathbf{P} \neq 0$ for all timesteps but the first.

Using Equation (9.17) one can for each timestep calculate the cross-covariance given the previous timesteps cross-covariance. The initial error is assumed to be uncorrelated,

$$ {}^{ij}\mathbf{P}_0 = 0, \tag{9.18} $$

which, assuming that the initial estimate is only based on the initial measurements, is a reasonable assumption.

9.3.2 Fusion of Dependent Tracks

As under the independence assumption, the linear equation Equation (9.2) is used to fuse the results. We specify the terms of Equation (9.2) as in Equation (9.4). The covariances become

$$ \begin{aligned} \mathbf{P}_{xz} &= \mathbb{E}[(\mathbf{x} - \bar{\mathbf{x}})(\mathbf{z} - \bar{\mathbf{z}})^T] \\ &= \mathbb{E}[(\mathbf{x} - {}^{i}\hat{\mathbf{x}})({}^{j}\hat{\mathbf{x}} - {}^{i}\hat{\mathbf{x}})^T] \\ &= \mathbb{E}[({}^{i}\tilde{\mathbf{x}}(\mathbf{x} - {}^{j}\tilde{\mathbf{x}}) - ((\mathbf{x} - {}^{i}\tilde{\mathbf{x}}))^T] \\ &= \mathbb{E}[{}^{i}\tilde{\mathbf{x}}({}^{i}\tilde{\mathbf{x}} - {}^{j}\tilde{\mathbf{x}})^T] \\ &= {}^{i}\mathbf{P} - {}^{ij}\mathbf{P}, \end{aligned} \tag{9.19} $$

and

$$\begin{aligned}\mathbf{P}_{xz} &= \mathbb{E}[(\mathbf{z}-\bar{\mathbf{z}})(\mathbf{z}-\bar{\mathbf{z}})^T] \\ &= \mathbb{E}[({}^j\hat{\mathbf{x}}-{}^i\hat{\mathbf{x}})({}^j\hat{\mathbf{x}}-{}^i\hat{\mathbf{x}})^T] \\ &= \mathbb{E}[((\mathbf{x}-{}^j\tilde{\mathbf{x}})-(\mathbf{x}-{}^i\tilde{\mathbf{x}}))((\mathbf{x}-{}^j\tilde{\mathbf{x}})-(\mathbf{x}-{}^i\tilde{\mathbf{x}}))^T] \\ &= \mathbb{E}[({}^i\tilde{\mathbf{x}}-{}^j\tilde{\mathbf{x}})({}^i\tilde{\mathbf{x}}-{}^j\tilde{\mathbf{x}})^T] \\ &= {}^i\mathbf{P}-{}^{ij}\mathbf{P}-{}^{ji}\mathbf{P}+{}^j\mathbf{P}.\end{aligned} \tag{9.20}$$

Inserting the covariances in Equation (9.2), the fusion of dependent tracks becomes

$$\hat{\mathbf{x}} = {}^i\hat{\mathbf{x}} + [{}^i\mathbf{P}-{}^{ij}\mathbf{P}][{}^i\mathbf{P}+{}^j\mathbf{P}-{}^{ij}\mathbf{P}-{}^{ji}\mathbf{P}]^{-1}[{}^j\hat{\mathbf{x}}-{}^i\hat{\mathbf{x}}]. \tag{9.21}$$

Using the covariance update equation Equation (9.12), the associated covariance becomes

$$\mathbf{P} = {}^i\mathbf{P}-[{}^i\mathbf{P}-{}^{ij}\mathbf{P}][{}^i\mathbf{P}+{}^j\mathbf{P}-{}^{ij}\mathbf{P}-{}^{ji}\mathbf{P}]^{-1}[{}^i\mathbf{P}-{}^{ji}\mathbf{P}]. \tag{9.22}$$

9.3.3 Notes on the Assumptions

Some of the assumptions described in Section 9.1 needs to be relaxed to be compatible with the fusion of radar and AIS measurements.

First, we note that the fusion formulas assume i.i.d. measurement noises. I.e., the matrix $\mathbf{R}$, that govern the statistical properties of the measurement noise, is assumed to be equal for both the sensors. Based on the discussion in Section 2.4, we note that this will not be the case for real radar and AIS data. However, the effect of ignoring this assumption is not evident based on the formulas, and this will be further examined with Monte-Carlo simulations in Section 11.2.

A crucial assumption for the formulas derived is that the sensors are synchronous. A potential pragmatic approach to fusion with asynchronous sensors is to fuse predicted estimates when there are no new measurements. When considering fusion of independent tracks, the implementation would be straightforward. However, it is not straightforward that the results produced would be any good, as the assumption of independent tracks would still not hold. When applying this pragmatic approach to fusion of dependent tracks, the problem of calculating the cross-covariance becomes apparent. Therefore, the formulas derived cannot be directly used for asynchronous sensors. However, with some small adjustments, they become the optimal approach of the type asynchronous T2TFwoMpF. This will be elaborated on in the next section.

9.4 Asynchronous Track-to-Track Fusion

In this section, we will present the asynchronous T2TFwoMpF (AT2TFwoMpF) formulas. AT2TFwoMpF is a special version of T2TFwoMpF. According to Tian and Bar-Shalom, AT2TFwoMpF can be achieved by fusing the updated estimate and

the predicted estimate, along with an appropriate cross-covariance [9]. Therefore, to describe AT2TFwoMpF, we first need to present the formulas for T2TFwoMpF.

According to Tian and Bar-Shalom, the optimal T2TFwoMpF will be equal to the formulas derived for T2TFwoMnF in Section 9.3, but with an additional step [53]. When the fusion is performed, the fused result is returned to one of the trackers. I.e., one of the trackers will be equal the fused result. This configuration is presented in Section 3.1. Assume that we have fused the estimates from tracker i and j at timestep k (${}^{i}\hat{\mathbf{x}}_k$, ${}^{j}\hat{\mathbf{x}}_k$, ${}^{i}\mathbf{P}_k$, and ${}^{j}\mathbf{P}_k$) according to the formulas in Section 9.3. We then update the estimate of tracker i according to

$$\begin{aligned} {}^{i}\hat{\mathbf{x}}_k &= \hat{\mathbf{x}}_k \\ {}^{i}\mathbf{P}_k &= \mathbf{P}_k, \end{aligned} \tag{9.23}$$

where $\hat{\mathbf{x}}_k$ and $\mathbf{P}_k$ is the fused estimate. This feedback to tracker i adds a correlation of the two estimates, so the cross-covariance has to be updated according to

$${}^{ij}\mathbf{P}_k^* = [\mathbf{I} - {}^{ij}\mathbf{K}_k]{}^{ij}\mathbf{P}_k + {}^{ij}\mathbf{K}_k{}^{j}\mathbf{P}_k, \tag{9.24}$$

where

$${}^{ij}\mathbf{K}_k = [{}^{i}\mathbf{P}_k - {}^{ij}\mathbf{P}_k][{}^{i}\mathbf{P}_k + {}^{j}\mathbf{P}_k - {}^{ij}\mathbf{P}_k - {}^{ji}\mathbf{P}_k]^{-1}. \tag{9.25}$$

To use these formulas for asynchronous sensors, we can, according to [9], fuse each time a new measurement arrives, and use the predicted estimate when no updated estimate is available. For the predicted estimate, the Kalman gain will be set to zero. The fusion scheme of the AT2TFwoMpF is shown in Section 10.2.

9.5 Kalman Filter Fusion

Fusion using the Kalman Filter can be used as a base for the comparison of fusion algorithms. We know that when the assumptions of the Kalman Filter hold (linear Gaussian measurement model, linear Gaussian process model, and the Markov-assumptions), fusion using the Kalman Filter will produce consistent results. Note that this is not track-level fusion, which is the main topic of this thesis, but measurement level fusion, i.e. we fuse measurements and not tracks. As per previous assumptions, we assume that the association is perfect and given, in this case, the measurement to track association.

The formulas of the Kalman filter can be found in Section 2.1.1. In the case of multiple sensors, synchronous or asynchronous, the Kalman Filter still produces consistent results. When the measurements arrive with different timestamps, a normal predict and update cycle will be performed for each measurement. When the measurements are received at the same timestep, an extra update step is performed. Assuming that the estimate after updating with measurement ${}^{i}\mathbf{z}$ is ${}^{i}\hat{\mathbf{x}}$ along with the updated covariance ${}^{i}\mathbf{P}$. Then the posterior mean after updating with measurement ${}^{j}\mathbf{z}$ becomes

$$\hat{\mathbf{x}} = {}^{i}\hat{\mathbf{x}} + {}^{i}\mathbf{W}({}^{j}\mathbf{z} - \mathbf{H}{}^{i}\hat{\mathbf{x}}), \tag{9.26}$$

and the posterior covariance becomes

$$\mathbf{P} = (\mathbf{I} - {}^{j}\mathbf{W}\mathbf{H})^{i}\mathbf{P}. \tag{9.27}$$

We see that the second update step is equal to the first update step, using the updated posterior instead of the predicted posterior.

Chapter 10

Track-to-Track Fusion Method

To test and analyze the fusion algorithms, a framework written in Python was created. The code can be found on Github [52]. The framework is using modules from Stone Soup [15] for basic filtering and generating scenarios.

In Section 10.2, the fusion scheme for tracking using synchronous and asynchronous sensors will be related to the equations derived and presented in Chapter 9.

10.1 Experimental Setup

10.1.1 Target Generation

The single target is born around the origin at the start of the scenario. The kinematic model used in the experiments is the constant-velocity model. The model is described in Section 2.1.2 and is given by

$$\mathbf{x}_{k|k-1} = \mathbf{F}\mathbf{x}_{k-1} + \mathbf{v}_k \qquad \mathbf{v}_k \sim \mathcal{N}(0, \mathbf{Q}). \tag{10.1}$$

10.1.2 Measurement Models

In this part of the thesis, the measurement model of the two local trackers is similar. As discussed in Section 2.4, the measurement model of the AIS and radar sensors should be dissimilar due to their functionality. For simplicity of the experiments and to analyze the performance of the methods when the assumptions hold, a Cartesian measurement model with white Gaussian noise is used. The model is similar to that of Section 2.4.2, and is given by

$$\mathbf{Z}_k = \mathbf{H}\mathbf{x}_k + \mathbf{w}_k \qquad \mathbf{w}_k \sim \mathcal{N}(0, \mathbf{R}), \tag{10.2}$$

The measurement noise matrix $\mathbf{R}$ can be different for the two trackers and will be specified in the different scenarios. The validity of using such a measurement model to simulate a radar is discussed in Chapter 12.

In the previous part, where we examined T2TA, and in the next part, where we will examine the complete tracker, the measurement models suggested in Section 2.4 is used.

10.1.3 Scenarios

To test the fusion algorithms, a set of scenarios were simulated. All associations are perfect and given. The implementation can be found on Github [52].

Scenario 1: Synchronous Sensors

In scenario 1, the AIS and radar measurements are simulated with the same sampling rate. The fusion under the error independence assumption, Section 9.2, and the fusion accounting for the common process noise, Section 9.3, assumes that the sensors have the same sampling rate and that the measurement noises are identical. Further, no clutter or misdetection was included in the scenario. Different sets of noises were used when generating the scenario, and these are specified along with the results. An example of the generated scenario with noise parameters $\sigma_{AIS} = 10$, $\sigma_{radar} = 5$, and $\sigma_{process} = 1$ can be seen in Figure 10.1a.

Scenario 2: Asynchronous Sensors

In scenario 2, the sampling rates of the sensors are different. Typical sampling rates, such as $[1, 5]$ for the radar and $[10, 120]$ for the AIS receiver, are examined. The noise parameters used are presented along with the results. An example of the generated scenario with noise parameters $\sigma_{AIS} = 10$, $\sigma_{radar} = 5$, and $\sigma_{process} = 1$ is shown in Figure 10.1b. The AIS measurement rate is 5 and the radar measurement rate is 1.

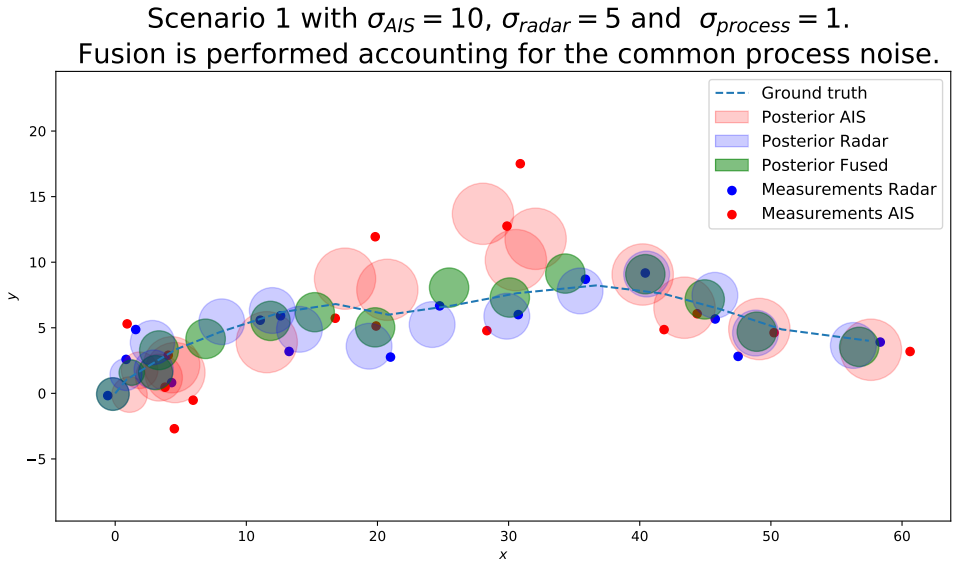

(a) Example of scenario 1. The fused posterior is produced by fusion of dependent tracks.

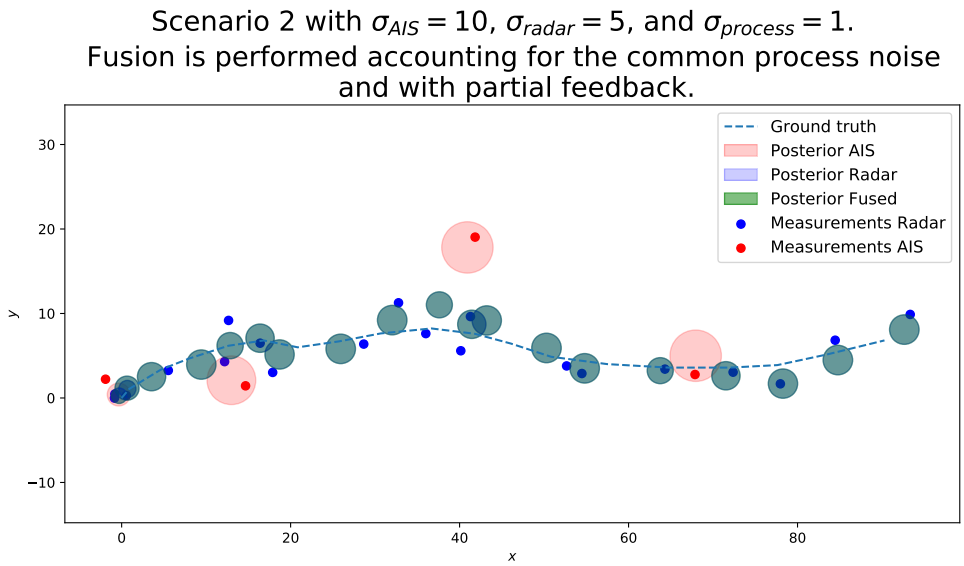

(b) Example of scenario 2. The AIS measurement rate is 5, and the radar measurement rate is 1. The fused posterior is produced by asynchronous T2TFwoMpF. I.e., the radar trackers estimate is the same as the fused estimate.

Figure 10.1: Example of scenario 1 and scenario 2. The dotted blue lines are the ground truth. The small solid circles represents measurements, and the larger circles represents the estimates and their uncertainties. Note that the measurement standard deviation is not represented, and that the size of the solid circles is arbitrary.

10.2 Fusion Scheme

Two Kalman filters are used to produce estimates which are fused. If one of the Kalman filters does not have an updated estimate, as will be the case of asynchronous sensors, the Kalman filter will output a predicted estimate. The fusion algorithms will produce a new estimate at each timestep. A simulated timestep is representing a second, so a new estimate is produced each second.

10.2.1 Synchronous Sensors

For the synchronous sensors tracking scenario, the T2TFwoMnF fusion scheme is used, as presented in Section 3.1. In Figure 10.2, the fusion scheme for synchronous sensors is showed. Note that no information is returned from the fuser to the Radar and AIS trackers.

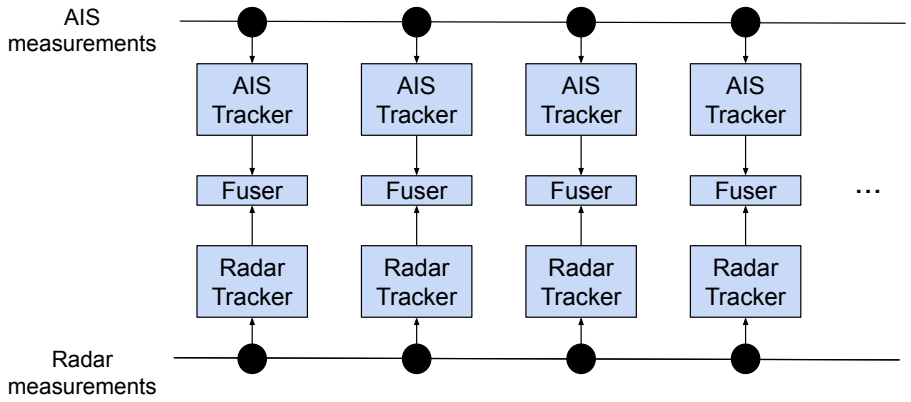

Figure 10.2: The figure shows the fusion scheme of synchronous AIS and Radar measurements. The filled circles represents a new measurement. The black arrows indicate information flow.

Fusion of independent tracks

For each updated estimate received from the individual trackers, a fused mean and covariance is calculated using Equation (9.11) and Equation (9.14), which are implemented in the *Data fuser* module. The fused result is returned, and no information is saved in the tracker.

Fusion of dependent tracks

For the fusion of dependent tracks, we need to keep an updated cross-covariance of the estimation errors. For the first timestep, the cross-covariance is assumed

zero, which is reasonable assuming that the initial mean and covariance is based on the measurements. When updated estimates are available, the cross-covariance of the estimates are calculated. This requires the previous cross-covariance, which is stored in the tracker. The update of the cross-covariance is given by Equation (9.17), and is implemented in the *Data fuser* module. Then, the estimates are fused according to Equation (9.21) and Equation (9.22), and the cross-covariance is stored for the next timestep.

Kalman filter fusion

The Kalman filter fusion implementation is identical for synchronous and asynchronous sensors. The measurements are simply used to update the estimate using Equation (9.26) and Equation (9.27).

10.2.2 Asynchronous Sensors

For asynchronous sensors, the AT2TFwoMpF scheme presented in Section 3.1 is used. In Figure 10.3, the fusion scheme for synchronous sensors is showed. Note that the fused estimate is returned to the Radar tracker. The Radar tracker then uses the fused estimate as its estimate.

By inspecting Figure 10.3, we note that we have three situations; 1) we receive two updated estimates, 2) we receive one updated estimate and one predicted estimate, 3) we receive 2 predicted estimates. These three situations are handled differently and will be addressed independently below.

1) Two updated estimates: For two updated estimates, we will first update the cross-covariance according to Equation (9.17). Then we will produce a fused estimate as for fusion of dependent tracks, i.e., using Equation (9.21) and Equation (9.22). As the fused result will be returned to the Radar tracker, this will change the cross-covariance of the individual trackers estimate errors, so the cross-covariance has to be updated according to Equation (9.23). Then the fused estimate is returned to the Radar tracker, and the cross-covariance is stored for the next timestep.

2) One updated estimate and one predicted estimate: In this situation, we update the cross-covariance according to Equation (9.17), and use a zero Kalman gain for the updated estimate. The rest is performed as described for situation 1).

3) Two predicted estimates: For two predicted estimates, the fused estimate will be the estimate of the Radar tracker. Notice that the predicted estimate of the Radar tracker is simply the prediction of the previous timesteps fusion. Therefore, the cross-covariance is left as is and is not updated in this situation.

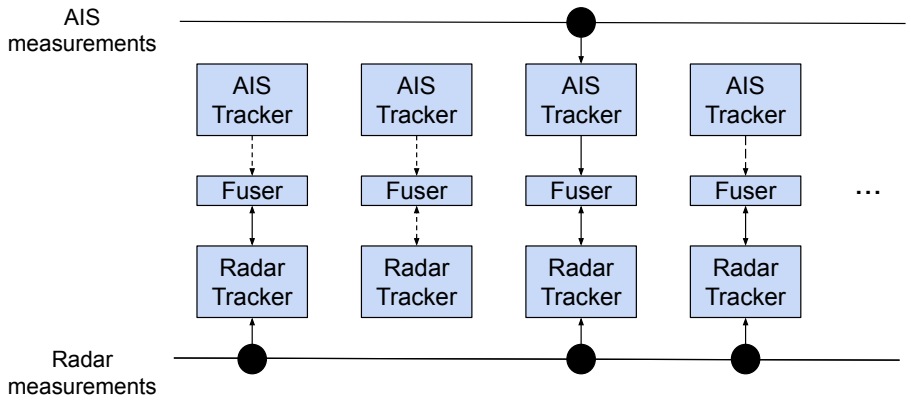

Figure 10.3: The figure shows the fusion scheme of synchronous AIS and Radar measurements. The filled circles represents a new measurement. The black arrows indicate information flow. The dashed black arrow indicates that a predicted estimate is sent.

Chapter 11

Track-to-Track Fusion Results

To test and analyze the results of the fusion algorithms, different scenarios were simulated. In this chapter, we will present some results on the fusion algorithms described in Chapter 9 and Chapter 10. First, in Section 11.1, we will show that the algorithms produce consistent results when the assumptions (see Section 9.1 and Section 9.3.3) holds. We wish to examine whether the track level approach performs worse than the optimal measurement level approach and see how inconsistent the fusion of independent tracks is. This will be presented for both synchronous and asynchronous sensors. In Section 11.2, noise parameters and sampling rates are chosen according to what we found out about radar and AIS data in Section 2.4.

11.1 Fusion of Tracks with Identical Measurement Noise Matrix

In this section, we evaluate and compare the T2TF of dependent tracks, T2TF of independent tracks and the optimal measurement-level approach, exemplified by a simple Kalman filter, when the assumptions in Section 9.1 hold. We analyze whether an increase of the AIS measurement rate increases the consistency of the T2TF of independent track, and validate the implementations of the fusion schemes. The results are used as a baseline for later analysis of T2TF when the measurement models use dissimilar noise matrices.

11.1.1 Synchronous sensors

The average normalised estimation error squared (ANEES) after performing 100 Monte-Carlo (MC) simulations to scenario 1 with 200 timesteps by fusion of independent tracks, fusion of dependent tracks and Kalman filter fusion can be seen in Table 11.2, Table 11.3 and Table 11.4, respectively. The root-mean-squared-error (RMSE) is given in Table 11.5, Table 11.6, and Table 11.7, respectively. The measurement noise standard deviation is identical for both sensors. Note that ANEES

is averaged over all timesteps and all simulations.

In Figure 11.1, we can see the development of the ANEES. The figure shows how the ANEES changes for each additional Monte-Carlo Simulation.

	$\sigma_{meas} = 1$	$\sigma_{meas} = 5$	$\sigma_{meas} = 20$
$\sigma_{process} = 0.05$	0.05	0.01	0.0025
$\sigma_{process} = 0.5$	0.5	0.1	0.025
$\sigma_{process} = 3$	3	0.6	0.15

Table 11.1: The manoeuvring index for the parameter settings used.

	$\sigma_{meas} = 1$	$\sigma_{meas} = 5$	$\sigma_{meas} = 20$
$\sigma_{process} = 0.05$	5.82	5.88	5.91
$\sigma_{process} = 0.5$	5.73	5.79	5.85
$\sigma_{process} = 3$	5.68	5.73	5.78

Table 11.2: The ANEES of fusion of independent tracks after performing 100 Monte-Carlo simulations. The 95% confidence interval is 3.95 and 4.05.

	$\sigma_{meas} = 1$	$\sigma_{meas} = 5$	$\sigma_{meas} = 20$
$\sigma_{process} = 0.05$	3.97	3.98	3.98
$\sigma_{process} = 0.5$	3.97	3.97	3.98
$\sigma_{process} = 3$	3.98	3.97	3.97

Table 11.3: The ANEES of fusion of dependent tracks after performing 100 Monte-Carlo simulations. The 95% confidence interval is 3.95 and 4.05.

	$\sigma_{meas} = 1$	$\sigma_{meas} = 5$	$\sigma_{meas} = 20$
$\sigma_{process} = 0.05$	3.96	3.96	3.96
$\sigma_{process} = 0.5$	3.98	3.97	3.96
$\sigma_{process} = 3$	3.99	3.98	3.97

Table 11.4: The ANEES of fusion using the Kalman filter after performing 100 Monte-Carlo simulations. The 95% confidence interval is 3.95 and 4.05.

	$\sigma_{radar} = 1$	$\sigma_{radar} = 5$	$\sigma_{radar} = 20$
$\sigma_{process} = 0.05$	0.88	1.57	2.65
$\sigma_{process} = 0.5$	1.36	2.22	3.57
$\sigma_{process} = 3$	2.15	3.17	4.77

Table 11.5: The RMSE of fusion of independent tracks after performing 100 Monte-Carlo simulations.

	$\sigma_{radar} = 1$	$\sigma_{radar} = 5$	$\sigma_{radar} = 20$
$\sigma_{process} = 0.05$	0.88	1.57	2.65
$\sigma_{process} = 0.5$	1.36	2.22	3.57
$\sigma_{process} = 3$	2.15	3.17	4.77

Table 11.6: The RMSE of fusion of dependent tracks after performing 100 Monte-Carlo simulations.

	$\sigma_{radar} = 1$	$\sigma_{radar} = 5$	$\sigma_{radar} = 20$
$\sigma_{process} = 0.05$	0.86	1.53	2.58
$\sigma_{process} = 0.5$	1.33	2.17	3.48
$\sigma_{process} = 3$	2.11	3.11	4.66

Table 11.7: The RMSE of fusion using the Kalman filter after performing 100 Monte-Carlo simulations.

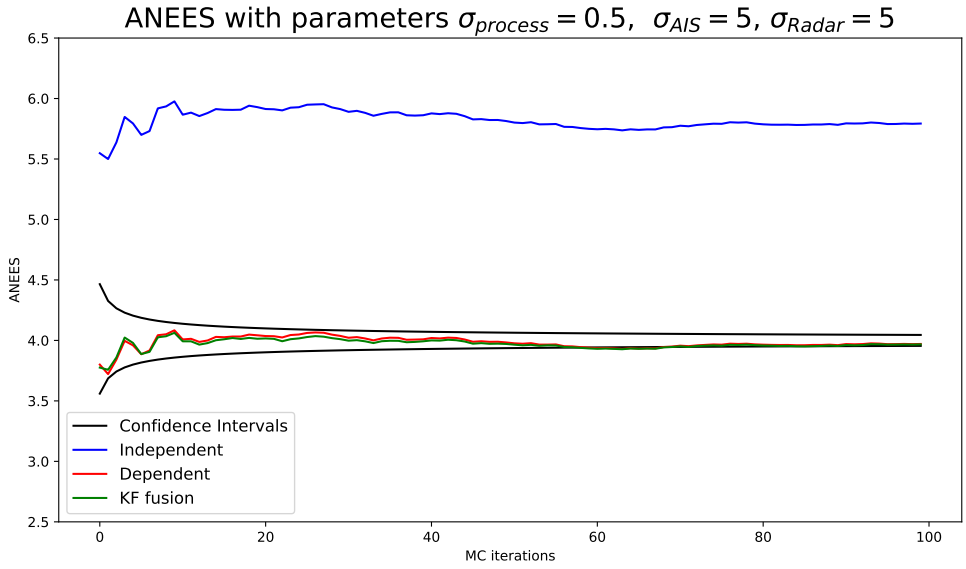

Figure 11.1: The figure shows the evolvement of the ANEES of each fusion algorithm plotted for each new Monte-Carlo simulation.

By inspecting Figure 11.1, we note that the ANEES is barely changing after the addition of new Monte-Carlo simulations. Therefore, we assume, for the simulation presented in the figure, that the calculated ANEES and RMSE are approximately equal to what they would be after infinitely many Monte-Carlo simulations. A similar evolvement of the ANEES was found for the other noise settings as well.

By examining the RMSE in Table 11.5 and Table 11.6 we note that the RMSE of fusion of independent tracks and fusion of dependent tracks is identical. This seems a bit strange at first, considering that the fusion formulas are different (see Equation (9.21) and Equation (9.11)). Still, considering that the sensors are

identical, it would be stranger if the results were different. If the RMSE was different, it would suggest that dependent fusion added some information about one of the estimates, which led it to trust it more. This is, however, not the case. Further, we note that the RMSE of Kalman filter fusion (see Table 11.7), is lower than the T2TF techniques. As noted previously, T2TF is known to be theoretically inferior to Kalman filter fusion [54]. As Chang et al. noticed, the derivation of T2TF makes an assumption that is not met, which leads to the results being optimal in the maximum likelihood (ML) sense and not in the mean squared error (MSE) sense [7]. The Kalman Filter is, however, optimal both in the ML sense and the MSE sense [33]. This might be why the RMSE of Kalman filter fusion is superior to T2TF for all noise settings.

There seems to be a constant offset between fusion of dependent tracks and Kalman filter fusion in Figure 11.1. One might ask oneself whether there is a small error, and they are, in fact, supposed to be equal. However, as noted, the fusion of dependent tracks is optimal in maximum likelihood (ML) sense and not in mean squared error (MSE) sense, while the Kalman filter is optimal in both the ML and MSE sense. From that, one can induce that they are not equal. The similar changes in ANEES can be seen as a correlation of what Monte-Carlo simulations the algorithms find difficult and easy.

By examining the ANEES of fusion of dependent tracks and Kalman filter fusion in Table 11.2 and Table 11.3, we note that all values are within their confidence intervals. I.e., they produce consistent results for the values examined.

By inspecting the ANEES of fusion of independent tracks in Table 11.2, we note that all the values are above the 95% confidence interval $[3.935, 4.065]$. This means that the filter is overconfident, i.e. that the covariance matrix underrepresents the error of the estimate. This is as expected, as fusion of independent tracks assumes no common process noise.

When comparing the ANEES with the manoeuvring indexes shown in Table 11.1, we see that a higher manoeuvring index leads to lower ANEES values, i.e., more consistent results. This is similar to the conclusion of Bar-Shalom in [6], where he concludes that a higher manoeuvring index reduces the effect of the common process noise. Bar-Shalom shows this relationship for manoeuvring indexes between 0.1 and $\sqrt{5}$. Our results show that this relationship also holds for manoeuvring indexes between 0.0025 and 3.

In conclusion, fusion of dependent tracks and Kalman filter fusion produced consistent results for all noise levels examined. Kalman filter fusion produced superior results in terms of RMSE. This could be due to the T2TF techniques being optimal in ML sense and not in MSE sense, while the Kalman filter is optimal in both ML sense and MSE sense.

11.1.2 Asynchronous sensors

In Figure 11.2 we can see the ANEES of the three methods plotted for varying AIS measurement rate. The process and measurement noises are constant, and set to

$_{process} = 0.5$ $_{AIS} = \sigma_{Radar} = 5$. The number of AIS messages per MC simulation is 40. For an AIS measurement rate of 15, the number of radar measurements is $40 * 15 = 600$. Therefore, the number of NEES values included in calculating ANEES increases with a higher AIS measurement rate, and the confidence interval becomes smaller. 40 MC simulations were performed at each AIS measurement rate.

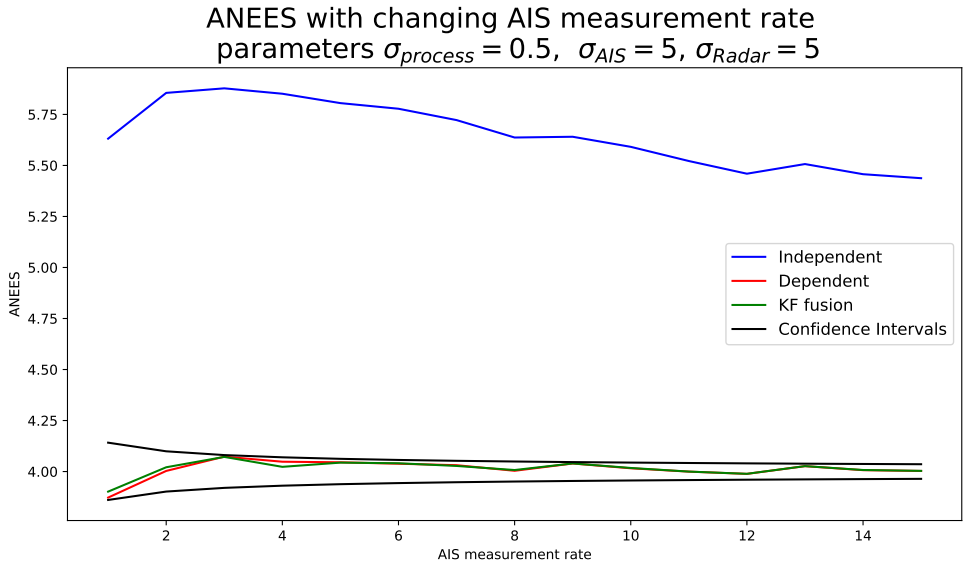

Figure 11.2: The figure shows the ANEES for changing AIS measurement rate.

By inspecting Figure 11.2, we note that fusion of dependent tracks and Kalman filter fusion produce consistent results for the AIS measurement rates examined.

The ANEES of independent fusion seems to attenuate for higher AIS measurement rates. Considering that a higher measurement rate would yield a larger manoeuvring index (see Equation (3.1)), and per the conclusion of Bar-Shalom - that higher manoeuvring index reduces the effect of the common process noise - this is reasonable [6]. However, for the values examined here, fusion of independent tracks is not consistent, as expected.

11.2 Fusion of Tracks with Dissimilar Measurement Noise Matrices

This section examines the results of AT2TFwoMpF, fusion of independent tracks, and Kalman filter fusion for noise levels typical when tracking vessels at sea using radar and AIS. Based on the discussion in Section 2.4, we examine the following noise standard deviations and measurement rates; $\sigma_{radar} \in [5, 200]$, $\sigma_{AIS} \in [10]$, $\sigma_{process} \in [0.05, 3]$, AIS measurement rate $\in [2, 12]$ seconds, and radar measurement rate $\in [1]$ seconds. To reduce the complexity, we have assumed that the AIS

measurement noise standard deviation can be approximated to 10. We have also assumed that the radar measurement rate can be set to 1.

The ANEES and RMSE after performing 150 MC simulations to scenario 2 with AIS measurement rate equal 6 seconds with 300 timesteps by T2TF of dependent tracks, T2TF of independent tracks, and Kalman filter fusion can be found in Table 11.9, Table 11.10, Table 11.8, Table 11.12, Table 11.13, and Table 11.11. The ANEES for T2TF of dependent tracks, T2TF of independent tracks, and Kalman filter fusion with $\sigma_{radar} = 15$, $\sigma_{AIS} = 10$, $\sigma_{process} = 0.3$ for varying AIS measurement rate from 2 to 11 can be seen in Figure 11.3.

	$\sigma_{radar} = 5$	$\sigma_{radar} = 30$	$\sigma_{radar} = 200$
$\sigma_{process} = 0.05$	4.01	4.01	4.01
$\sigma_{process} = 0.5$	4.01	4.01	4.01
$\sigma_{process} = 3$	4.01	4.01	4.01

Table 11.8: The ANEES of fusion using the Kalman filter after performing 150 Monte-Carlo simulations with AIS measurement rate equal to 6, and $\sigma_{AIS} = 10$. The 95% confidence interval is 3.99 and 4.01.

	$\sigma_{radar} = 5$	$\sigma_{radar} = 30$	$\sigma_{radar} = 200$
$\sigma_{process} = 0.05$	4.01	4.0	4.01
$\sigma_{process} = 0.5$	4.01	4.01	4.02
$\sigma_{process} = 3$	4.01	4.01	4.02

Table 11.9: The ANEES of fusion of dependent tracks after performing 150 Monte-Carlo simulations with AIS measurement rate equal to 6, and $\sigma_{AIS} = 10$. The 95% confidence interval is 3.99 and 4.01.

	$\sigma_{radar} = 5$	$\sigma_{radar} = 30$	$\sigma_{radar} = 200$
$\sigma_{process} = 0.05$	5.66	5.96	5.95
$\sigma_{process} = 0.5$	5.61	5.93	5.99
$\sigma_{process} = 3$	5.4	5.41	5.17

Table 11.10: The ANEES of fusion of independent tracks after performing 150 Monte-Carlo simulations with AIS measurement rate equal to 6, and $\sigma_{AIS} = 10$. The 95% confidence interval is 3.99 and 4.01.

Examining the ANEES for fusion of dependent tracks, fusion of independent tracks, and Kalman filter fusion in Table 11.9, Table 11.10, and Table 11.8, we note that the fusion of dependent tracks and the Kalman filter fusion produces almost consistent results for AIS measurement rate equal to 6. However, the fusion of dependent tracks is slightly above the confidence intervals for certain parameters. The slight overconfident results might be due to the difference in the measurement standard deviations. Consistent results were shown in the previous section for AT2TF with identical measurement noise standard deviation.

	$\sigma_{radar} = 5$	$\sigma_{radar} = 30$	$\sigma_{radar} = 200$
$\sigma_{process} = 0.05$	1.94	3.44	4.94
$\sigma_{process} = 0.5$	2.69	4.68	7.2
$\sigma_{process} = 3$	3.73	6.21	10.31

Table 11.11: The RMSE of fusion using the Kalman filter after performing 150 Monte-Carlo simulations. $\sigma_{AIS} = 10$ and AIS measurement rate equal to 6.

	$\sigma_{radar} = 5$	$\sigma_{radar} = 30$	$\sigma_{radar} = 200$
$\sigma_{process} = 0.05$	1.96	3.49	5.04
$\sigma_{process} = 0.5$	2.69	4.72	7.29
$\sigma_{process} = 3$	3.73	6.24	10.37

Table 11.12: The RMSE of fusion of dependent tracks after performing 150 Monte-Carlo simulations. $\sigma_{AIS} = 10$ and AIS measurement rate equal to 6.

	$\sigma_{radar} = 5$	$\sigma_{radar} = 30$	$\sigma_{radar} = 200$
$\sigma_{process} = 0.05$	1.99	3.52	5.06
$\sigma_{process} = 0.5$	2.76	4.8	7.38
$\sigma_{process} = 3$	3.88	6.43	10.69

Table 11.13: The RMSE of fusion of independent tracks after performing 150 Monte-Carlo simulations. $\sigma_{AIS} = 10$ and AIS measurement rate equal to 6.

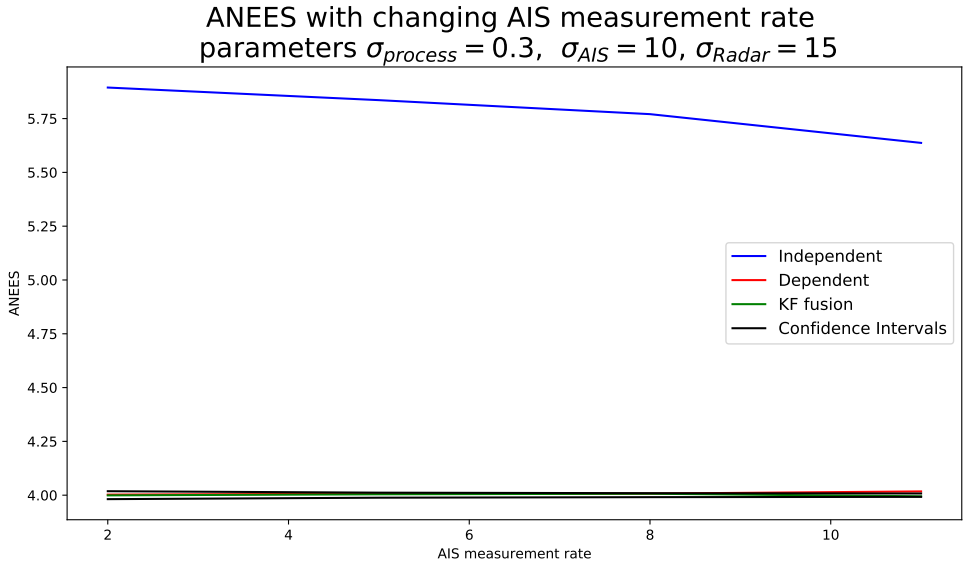

Figure 11.3: The figure shows ANEES plotted for different AIS measurement rates.

For all parameter, the RMSE of the Kalman filter fusion is lower than the fusion of dependent tracks. Further, for all parameters, the RMSE of the fusion of dependent tracks is lower than the fusion of independent tracks. Different from the previous section, the RMSE of fusion of dependent tracks is no longer similar to the RMSE of the fusion of independent tracks. This is due to the partial feedback, which we see have a positive effect on the RMSE.

In Figure 11.3, we see that the Kalman filter fusion produce consistent results for the examined parameters. The fusion of dependent tracks produces consistent results for all AIS measurements rates except 11, where the approach is a bit over-confident. The fusion of independent is over-confident, in a degree similar to what was seen with identical measurement matrices. The inconsistency of the fusion of independent tracks decreases with an increased AIS rate, confirming Bar-Shalom's note that the inconsistency decreases with increasing manoeuvrability index.

Chapter 12

Track-to-Track Fusion Discussion

12.1 Validity of Using a Cartesian Measurement Model for Simulating Radar Measurements

An important detail to keep in mind when discussing the results of the fusion of tracks with AIS and radar noises is the radar measurement model. Different from the radar measurement model used in Part II and Part IV, the simulations in this chapter use a radar measurement model with cartesian measurement noise. As described in Section 2.4, the measurement model of a radar should represent the noises one would expect to see in the sensor, which for a radar is noise in range and noise in bearing in addition to Cartesian noise due to clustering and time-stamping inaccuracies. Using such a measurement model would yield results that would contain more information about the usage of the T2TF approaches for AIS-radar fusion. Based on the discussion in Section 2.4, one could hypothesize whether the change of model would lead to an inconsistency of the fused estimates, as we know the conventional conversion from polar to cartesian to underestimate the covariance of the measurements. This is because an ellipse in polar coordinates becoming banana-shaped in cartesian coordinates, which we cannot fully represent with a Gaussian distribution in Cartesian coordinates. However, the author would argue that even though there is room for improvement, as there always is, the results can still be used to evaluate whether the fusion of independent tracks can be used or whether an approximation should be used when the cross-covariance is unknown.

12.2 Target Generation

In the simulations shown, a Constant-Velocity (CV) model is used to generate the targets. A wide range of process noises is used, to examine the fusion of slower vessels, such as container ships and ferries and fast vessels, such as leisure vessels and water scooters. A Coordinated-Turn (CT) model, as described in Section 2.1.2, could have been used for simulating turning targets. As targets with high process

noises were simulated, one could argue that it should also cover targets with high turn rates. However, implementing a CT model as the process model would require using the extended Kalman filter (EKF). The inclusion of the CT models leads to linearizations that do not necessarily produce consistent results. As discussed in [55], the CT EKF ANEES is up to twice as large as it should be for the values they examined. The CV model was even more inconsistent. These results suggest that it would be interesting to look at the consistency of T2TF when the targets move according to a CT model. The derivations of the cross-covariance assume a linear process model, and as the CT model is non-linear, the derived cross-covariance would only be an approximation.

12.3 Feedback versus No Feedback

There is a fundamental difference between feedback of fused estimates and no feedback. In our AIS-radar scenario, it is most relevant to discuss feedback to the radar tracker, as it has a higher measurement frequency. Feedback to the radar tracker can either have a positive effect or a negative effect. If the track-to-track association (T2TA) was correct and the AIS tracker had a consistent estimate, the feedback would increase the accuracy of the radar trackers estimate. If the T2TA was wrong, or the AIS tracker was overconfident, the feedback would lead to either a worse estimate or at least a less consistent estimate. In most cases, the feedback would be positive. If not, there would be no reason to use the AIS tracker in the first place. Regardless of the quality of the individual trackers, the point is that feedback of fused estimates might have a negative effect and might make the radar tracker more likely to diverge. With no feedback, one does not risk a negative-feedback loop, where the result of a couple of false radar measurements leads to a wrong T2T association which further leads to a worsen estimate.

Implementing the T2TFwoMpF in practice can be challenging in the best case or near undoable in the worst case. First, the cross-covariance must be calculated. In our simple Kalman filter simulations, the cross-covariance was calculated using the linear formulas of the Kalman filter. When multiple models are used, such as for the Interacting Multiple Models (IMM) [56], the calculation of the cross-covariance becomes complex. Furthermore, when data association is not solved by hard association as assumed in our calculations, the calculations become further cluttered. In practice, one can hope for a decent estimate or opt for an approximation as in e.g. [57]. Further, partial feedback must be implemented in the radar tracker. Depending on the selected radar tracker, this might be easy or impossible if an off the shelf radar tracker is used, where source code is not available.

Part IV

Track-to-Track Association and Fusion

Chapter 13

Track-to-Track Association and Fusion Method

We have examined track-to-track association (T2TA) and track-to-track fusion (T2TF) independently of each other in the previous two parts. For T2TF, we assumed perfect associations, and for T2TA, we only analyzed the associations. This chapter discusses why we opt for the T2TF of independent tracks in combination with the hypothesis test (HT) for our final tracking system. We also describe our experimental setup for analyzing the complete tracker.

13.1 Choosing a T2TA and T2TF Method

In the previous parts, we have evaluated several approaches to T2TA and T2TF. Within T2TA, we have looked at the counting technique (CT) and the hypothesis test of independent tracks (HT). Within T2TF, we have looked at the fusion of independent tracks and track-to-track fusion without memory partial feedback (T2TFwoMpF). All combinations of T2TF and T2TA is possible.

The combination of the counting technique and the T2TFwoMpF is interesting. One can assume the AIS tracks will not swap targets, as it could only happen if two vessels with the same MMSI number is in the same area or if a vessel actively changed the MMSI number to a nearby vessels MMSI number. Either case is improbable. By assuming that the AIS tracks will not swap tracks, the feedback of the fused estimates can aid the radar tracker in not swapping tracks. When we use the counting technique, the tracks will remain associated until they have been further away than *threshold* from each other for τ timesteps in a row. If the radar tracker starts to diverge or swap tracks, being associated with the AIS tracker might guide it back on track.

A problem of the T2TFwoMpF is the need to calculate the cross-covariance. The author would argue that calculating the exact cross-covariance of the output of the VIMMJIPDA radar tracks and the AIS tracks would be too cumbersome, so an approximation to the cross-covariance must be taken. The T2TFwoMpF is

not further examined, as the author found that the inconsistency of the fusion of independent tracks is not too severe. Further, the partial feedback ruins the modularity that this thesis seeks to obtain.

The author found that both the CT and the HT would be a viable approach to the T2TA problem. However, the author chose to use the HT as it had a lower initialization time while still performing well in terms of false-positive rate and true-positive rate.

The complete tracker is combined such that when there are no fused estimates available, the estimates from the radar tracker is used.

13.2 Experimental Setup

The experimental setup is identical to that used in Section 6.1.

In addition to the Average Normalized Estimation Error Squared (ANEES) and root-mean-squared-error (RMSE), an OSPA-like metrics for tracks will be used. The metric is called OSPA^2 and was presented in [58].

Chapter 14

Track-to-Track Association and Fusion Results

In this chapter, the whole tracking system will be evaluated. First, we will examine the average normalized estimation error squared (ANEES) along with the root-mean-squared-error (RMSE) in a consistency analysis. The results will be compared to the measurement-to-track (M2T) approach, in this thesis exemplified with the AIS-radar VIMMJIPDA described in Hem's Thesis [28]. Our track-to-track approach (T2T) will also be compared with M2T using the OSPA$^{(2)}$ metric to examine which feature of the trackers are superior to the other.

The results presented are from 100 monte-carlo simulations using the tracker parameters in Table 14.1 and scenario parameters in Table 14.2.

Parameter	Symbol/Units	Value
Radar sample interval	T [s]	2
CV 1 process noise	$q_{a,1}$ [m/s^2]	0.1
CV 2 process noise	$q_{a,2}$ [m/s^2]	1.5
Turn rate process noise	q_ω [1/s^2]	0.02
Cartesian range std. radar	σ_{c_R} [m]	6.6
Cartesian range std. AIS	σ_{c_A} [m]	3
Polar range std.	σ_r [m]	5
Polar bearing std.	σ_θ [deg]	1
Detection probability	P_D [–]	0.92
Survival probability	P_S [–]	0.99
Visibility transition probabilities	w [–]	$\begin{bmatrix} 0.9 & 0.1 \\ 0.52 & 0.48 \end{bmatrix}$
Gate size	g [–]	3
Track fusion hypothesis significance level	[–]	0.01
Clutter intensity	λ [1/m^2]	2×10^{-7}
Initial new target intensity	b [1/s^2]	1×10^{-8}
Initial velocity std.	σ_{init} [m/s]	15
Initial mode probabilities	μ^0 [–]	$[0.8, 0.1, 0.1]^\top$
Mode transition probabilities	π^{ss} [–]	$[0.99, 0.99, 0.99]$
Existence confirmation threshold	[–]	0.999

Table 14.1: Tracker parameters.

Parameter	Symbol/Units	Value
Radar sample interval	T [s]	2
CV process noise	q_a [m/s^2]	0.3
Cartesian range std. radar	σ_{c_R} [m]	6.6
Cartesian range std. AIS	σ_{c_A} [m]	3
Polar range std.	σ_r [m]	3
Polar bearing std.	σ_θ [deg]	1
Clutter intensity	λ [1/m^2]	2×10^{-7}
Detection probability radar	P_D^{radar}	0.92
Detection probability AIS	P_D^{AIS}	1
Max initial velocity	V_{init} [m/s]	10
Birth time max	[s]	50
Scenario length	[s]	400
Number of target		5

Table 14.2: Simulated data parameters.

14.1 Consistency Analysis

In Table 14.3, the ANEES and RMSE for the two approaches are shown. The 95% confidence interval is 3.95 and 4.05.

The ANEES of the M2T approach is within the confidence interval, while the ANEES of the T2T approach is below the confidence interval. This shows that the T2T approach is under-confident. It suggests that, on average, the covariances of the estimates of the T2T approach is too large. However, the under-confidence is small and is not necessarily a reason for concern. As we do not feedback the fused estimates, the under-confidence of the fused estimates do not have a negative effect on the local trackers. Therefore, the author would argue that the RMSE is of more concern.

Examining the RMSE, we note that the T2T approach has a smaller RMSE than the M2T approach. There is almost a 20% decrease in RMSE using the T2T approach. This large decrease in RMSE is surprising, as the M2T is theoretically superior to the T2T approach.

ANEES T2T	ANEES M2T	RMSE T2T	RMSE M2T
3.50	3.95	4.71	5.65

Table 14.3: The RMSE and ANEES of the T2T and M2T approach.

14.2 Comparison of the M2T and the T2T Approach

To compare the M2T and T2T approaches, OSPA$^{(2)}$ for varying parameters are examined. By varying the window size n, the cutoff threshold c and the norm order p, we can evaluate the trackers' properties and compare their positional errors, their cardinality errors and the magnitude of outliers. A similar analysis between the radar VIMMIJPDA and the AIS-radar VIMMJIPDA is shown in [28].

OSPA$^{(2)}$ for varying window size n with $c = 100$ and $p = 2$ are shown in Figure 14.1. The T2T approach produces lower OSPA$^{(2)}$ values for all n. With $n = 1$, the OSPA$^{(2)}$ metric will not penalize any track swap, while with $n = 20$, track swaps will be penalized over 20 timesteps. The difference in OSPA$^{(2)}$ values increases with an increasing n. The slight increase in difference might suggest an increase of track swaps in the M2T approach. It might also be due to the slightly lower positional errors of the T2T approach, as shown by the RMSE in Table 14.3. The author finds the positional error explanation to be more plausible, but more examination is needed to conclude on the cause.

In Figure 14.2, OSPA$^{(2)}$ for varying cutoff threshold, $p = 2$, and $n = 10$ is shown. A low cutoff threshold will penalize cardinality errors less than what a high cutoff threshold will. With the cutoff threshold set to 100, any tracks more than 100 meters from their ground truth will be considered a cardinality error. The OSPA$^{(2)}$ values are almost identical for the T2T and the M2T approach, with the M2T approach slightly beating the T2T approach when the cutoff threshold is above 240.

Figure 14.3 shows the OSPA$^{(2)}$ for varying norm order p, $n = 10$, and $c = 100$. A higher norm will penalize outliers more than a lower norm. We see that the difference between T2T and M2T is similar to that when varying the cutoff threshold c. The results might show that the T2T approach has greater outliers than the M2T approach. With $p = 2$, we get the euclidean norm. The results show that the positional errors are smaller for the T2T approach but have a larger variation, i.e., larger outliers. The difference is small and might change with other scenario parameters.

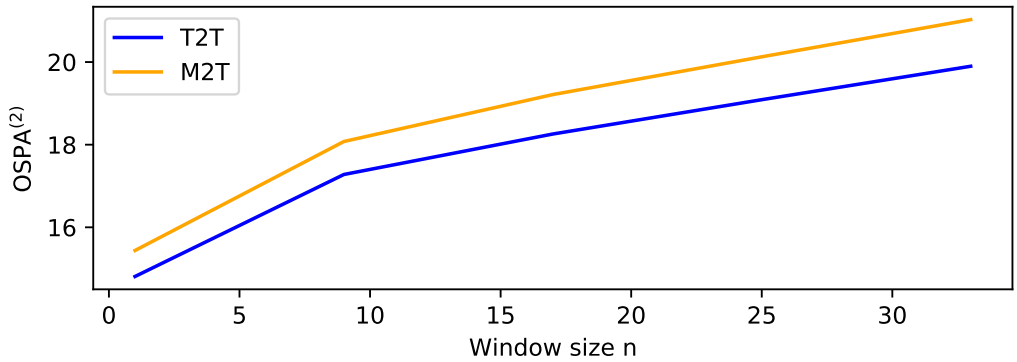

Figure 14.1: OSPA$^{(2)}$ for varying window size n with $c = 100$ and $p = 2$.

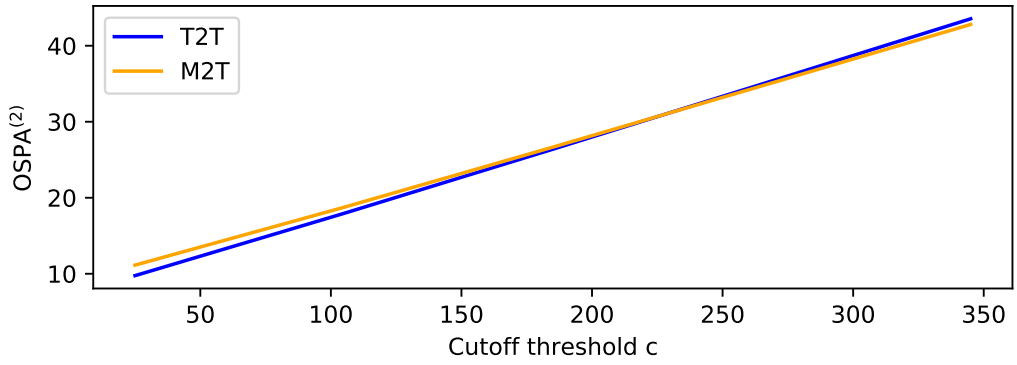

Figure 14.2: OSPA$^{(2)}$ for varying cutoff threshold c with $n = 10$ and $p = 2$.

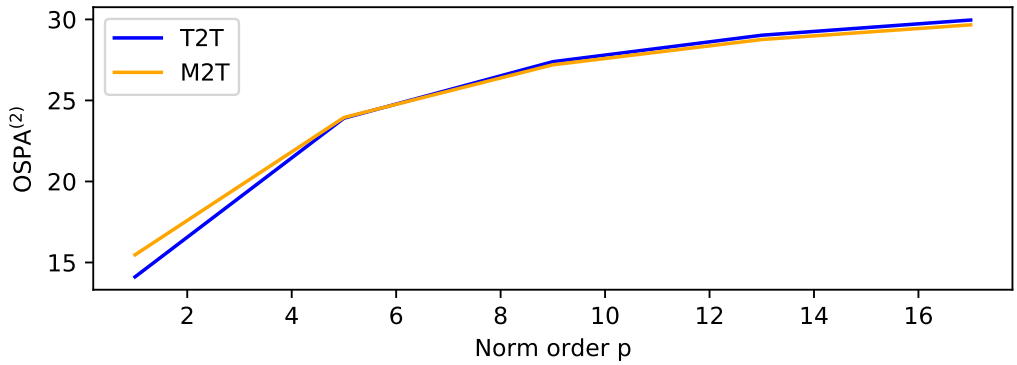

Figure 14.3: OSPA$^{(2)}$ for varying norm order p with $c = 100$ and $n = 10$.

Chapter 15

Track-to-Track Association and Fusion Discussion

15.1 Track-to-Track versus Measurement-to-Track

The results showed that the track-to-track (T2T) approach was superior to the measurement-to-track (M2T) approach in terms of root-mean-squared-error (RMSE) and also scored a lower OSPA$^{(2)}$ for most parameter choices. In terms of average normalized estimation error squared (ANEES), the M2T approach was consistent, while the T2T approach was slightly under-confident.

Using the sub-optimal track-to-track fusion of independent track, one would, in a single-target tracking scenario with perfect associations, get an over-confident estimate. This is discussed in Section 3.2, and shown in the results in Chapter 9. The results of the complete system show that the T2T approach was under-confident. The author thinks that this can be explained by considering how the hypothesis test works. As shown in Section 4.1, the hypothesis test determines whether two tracks originate from the same target by comparing their state estimates along with their covariances. Assuming two tracks with fixed positional estimates. Then, it is more likely that the two tracks are associated if the covariances are large than if they were small. The larger the covariances, the larger the positional difference between the tracks can be and still be associated. Further, if the two tracks are under-confident, they would have a large covariance and are more likely to be associated. If the two tracks are over-confident, they would have smaller covariances and, thus, would be less likely to be associated. This leads the author to think that under-confident estimates from the local trackers are more likely to be associated than over-confident estimates. This could explain why the complete tracker is under-confident, even though it uses an over-confident fusion approach.

This could be examined in future work by checking whether the associated tracks are more often under-confident than over-confident, given that the tracker is, on average is consistent.

Surprisingly, the T2T approach yielded better results than the M2T approach, as it is using a sub-optimal fusion and association approach. Further, even if the

cross-covariance had been included, the T2T approach is known to be theoretically inferior to the M2T approach [54]. The analysis of the OSPA$^{(2)}$ values showed no clear superiority in terms of cardinality errors or smaller outliers, and the gain seems to be mostly in terms of smaller positional error. Exactly why the T2T approach yielded superior results is beyond the scope of this thesis, but the author would propose two hypotheses that could be further examined;

1) The AIS-Radar VIMMJIPDA has some undesirable behaviour. Due to its consistency, the author does not think that there is a fault in the filtering, but rather that there might be a sub-optimal track management scheme. A first step could be to check whether there is a sub-optimal initialization scheme. This could be done by only calculating OSPA$^{(2)}$ values after all tracks have been alive for some timesteps. Then, by comparing the results to OSPA$^{(2)}$ values when the initialization steps are included, one could see whether there was a clear difference.

2) The T2T approach is superior to the M2T approach for fusion of AIS and radar. In theory, the T2T approach is inferior to the M2T approach [54]. As all the theory's assumptions are not always met, a theoretically sub-optimal method may end up being better in practice. Coraluppi et al. note that in certain conditions, T2T approaches outperform M2T approaches [59].

Regardless of why the T2T approach yielded better results than the M2T approach, the results suggest that the tracking system developed is a viable solution to fusion of AIS messages and radar measurements.

Chapter 16

Conclusion

16.1 Conclusion

This thesis has developed a complete multi-target tracking (MTT) system which fuses radar measurements and AIS messages. The radar tracker used is the VIMMJIPDA tracker of [27]. The MTT solves the problem of track-to-track association (T2TA) and track-to-track fusion (T2TF) using the hypothesis test of independent tracks and the fusion of independent tracks.

To decide on a solution to the T2TA problem, two methods were compared by means of simulations using a complete MTT system. The simulations included MTT challenges not found in the literature on the evaluation of T2TA, such as late track initialization, track loss, and track swap. These challenges lead to a non-trivial problem of determining the ground truth of the tracks, which is solved by a proposed sliding window approach. The results showed that the counting technique was superior to the hypothesis test in terms of false-positive rate and true-positive rate while being inferior in terms of initialization time. The results suggest that the counting technique is a viable approach to T2TA when the covariance information is not available and can also be a better choice if the higher initialization time is of less concern.

The developed MTT system was compared to the measurement level AIS-radar VIMMJIPDA of [28]. The results showed that the T2T approach was superior in terms of positional error and OSPA^2 while being slightly under-confident. Thus, the results suggest that the T2T approach to the fusion of AIS and radar is viable.

16.2 Recommendation for Further Work

This work has covered a range of topics, including T2TA, evaluation of T2TA, T2TF, and comparing the track level approach and the measurement level approach. To cover all the topics, one has to, at some point, decide that it is time to move on. However, there are several things that the author would have liked to have further examined if there had been more time. Some of them are discussed below.

This work has presented a full T2T approach that performs better than a similar M2T approach. The M2T approach is known to be theoretically superior to the T2T approach, so further work can try to understand why the T2T approach yielded better results in the fusion of Radar and AIS. The author suggested two hypotheses in the discussion of Chapter 12 which could be further investigated. The first hypothesis is that there is some undesirable behaviour of the implemented AIS-Radar VIMMJIPDA, e.g. the initialization scheme. The second hypothesis is that the T2T approach is superior for fusion of AIS and radar in practice. Coraluppi et al. note that in some conditions, the T2T approach performs better [59].

One of the main contributions of this work was to compare the counting technique (CT) and the hypothesis test of independent tracks (HT). Further performance evaluation can include using the coordinated turn model and examining specific cases that can be challenging in a T2T approach.

Comparing the CT and the HT when the local trackers produce inconsistent results is interesting. As the HT use covariance information, one would think that the results are quite affected by inconsistent local trackers. Challenging conditions were examined in this thesis. However, no consistency of the local trackers was presented, and we cannot directly assume that the local trackers became more inconsistent with increased difficulty. Therefore, no analysis on the effect of inconsistency on the T2TA approaches was presented. Previous work on the effect of inconsistent trackers on the HT does not include typical MTT problems such as misdetection, missed detections, false alarms and delayed initialization [17].

The prospect that most excites the author is the possibility of combining two counting techniques. Such a combination was proposed in Chapter 8. The goal of such a combination would be to reduce the initialization time while keeping the high TPR and low FPR. A possible solution would be to use two CTs in combination, where two tracks are considered associated if either of the two CTs associated them. The author would have started by examining the performance of using a CT with a small *threshold* and e.g. parameters $\psi = 2$ and $\tau = 1$ in combination with a CT with a large *threshold* and e.g. parameters $\psi = 4$ and $\tau = 3$.

In Chapter 10, a combination of the T2TFwoMpF and the CT was proposed. The author finds the combination especially interesting, as it might aid the radar tracker in reducing the likelihood of losing track or swapping tracks. The premise is that one can assume that the AIS tracker is immune to track swaps and track loss. Then, as the CT keeps associating tracks that are further than *threshold* from each other for τ timesteps, it is possible that the feedback of the fused estimate to the radar tracker helps the radar tracker avoid track swap and track loss.

Bibliography

[1] M. Aeberhard and N. Kaempchen, 'High-level sensor data fusion architecture for vehicle surround environment perception,' *Proc. 8th Int. Workshop Intell. Transp*, 2011.

[2] K. Cisek, E. Brekke, M. Jahangir and T. A. Johansen, 'Track-to-track data fusion for Unmanned Traffic Management System,' in *2019 IEEE Aerospace Conference*, Big Sky, MT, USA: IEEE, Mar. 2019, pp. 1–9, ISBN: 978-1-5386-6854-2. DOI: 10.1109/AERO.2019.8741727. [Online]. Available: https://ieeexplore.ieee.org/document/8741727/.

[3] C. Chong, 'Hierarchical estimation,' *Proc. MIT/ONR Workshop on C3*, pp. 205–220, 1979.

[4] J. Speyer, 'Computation and transmission requirements for a decentralized linear-quadratic-Gaussian control problem,' en, *IEEE Transactions on Automatic Control*, vol. 24, no. 2, pp. 266–269, Apr. 1979, ISSN: 0018-9286. DOI: 10.1109/TAC.1979.1101973. [Online]. Available: http://ieeexplore.ieee.org/document/1101973/.

[5] Y. Bar-Shalom, 'On the track-to-track correlation problem,' en, *IEEE Transactions on Automatic Control*, vol. 26, no. 2, pp. 571–572, Apr. 1981, ISSN: 0018-9286. DOI: 10.1109/TAC.1981.1102635. [Online]. Available: http://ieeexplore.ieee.org/document/1102635/.

[6] Y. Bar-Shalom and L. Campo, 'The Effect of the Common Process Noise on the Two-Sensor Fused-Track Covariance,' *IEEE Transactions on Aerospace and Electronic Systems*, vol. AES-22, no. 6, pp. 803–805, Nov. 1986, ISSN: 0018-9251. DOI: 10.1109/TAES.1986.310815. [Online]. Available: http://ieeexplore.ieee.org/document/4104300/.

[7] K. Chang, R. Saha and Y. Bar-Shalom, 'On optimal track-to-track fusion,' *IEEE Transactions on Aerospace and Electronic Systems*, vol. 33, no. 4, pp. 1271–1276, Oct. 1997, ISSN: 0018-9251. DOI: 10.1109/7.625124. [Online]. Available: http://ieeexplore.ieee.org/document/625124/.

[8] K. Chang, Tian Zhi and R. Saha, 'Performance evaluation of track fusion with information matrix filter,' en, *IEEE Transactions on Aerospace and Electronic Systems*, vol. 38, no. 2, pp. 455–466, Apr. 2002, ISSN: 0018-9251.

DOI: 10.1109/TAES.2002.1008979. [Online]. Available: http://ieeexplore.ieee.org/document/1008979/.

[9] X. Tian and Y. Bar-Shalom, 'On algorithms for asynchronous Track-to-Track Fusion,' in *2010 13th International Conference on Information Fusion*, Edinburgh: IEEE, Jul. 2010, pp. 1–8, ISBN: 978-0-9824438-1-1. DOI: 10.1109/ICIF.2010.5711956. [Online]. Available: http://ieeexplore.ieee.org/document/5711956/.

[10] X. Tian and Y. Bar-Shalom, 'Sliding window test vs. single time test for Track-to-Track Association,' in *2008 11th International Conference on Information Fusion*, 2008.

[11] Y. Bar-Shalom and X.-R. Li, *Multitarget-multisensor tracking: principles and techniques*, eng, 3rd printing. Storrs, Conn: YBS, 1995, ISBN: 978-0-9648312-0-9.

[12] R. Saha, 'Track-to-track fusion with dissimilar sensors,' *IEEE Transactions on Aerospace and Electronic Systems*, vol. 32, no. 3, pp. 1021–1029, Jul. 1996, ISSN: 0018-9251. DOI: 10.1109/7.532261. [Online]. Available: http://ieeexplore.ieee.org/document/532261/.

[13] B. La Scala and A. Farina, 'Effects of cross-covariance and resolution on track association,' in *Proceedings of the Third International Conference on Information Fusion*, Paris, France: IEEE, 2000, WED1/10–WED1/16 vol.2, ISBN: 978-2-7257-0000-7. DOI: 10.1109/IFIC.2000.859854. [Online]. Available: http://ieeexplore.ieee.org/document/859854/.

[14] P. C. Niedfeldt, K. Ingersoll and R. W. Beard, 'Comparison and Analysis of Recursive-RANSAC for Multiple Target Tracking,' *IEEE Transactions on Aerospace and Electronic Systems*, vol. 53, no. 1, pp. 461–476, Feb. 2017, ISSN: 0018-9251. DOI: 10.1109/TAES.2017.2650818. [Online]. Available: http://ieeexplore.ieee.org/document/7812590/.

[15] D. C. Last, P. . Thomas, S. Hiscocks, J. Barr, D. Kirkland, M. Rashid, S. B. Li and L. Vladimirov, 'Stone Soup: Announcement of beta release of an open-source framework for tracking and state estimation,' in *Signal Processing, Sensor/Information Fusion, and Target Recognition XXVIII*, L. L. Grewe, E. P. Blasch and I. Kadar, Eds., Baltimore, United States: SPIE, May 2019, p. 6, ISBN: 978-1-5106-2701-7 978-1-5106-2702-4. DOI: 10.1117/12.2518514. [Online]. Available: https://www.spiedigitallibrary.org/conference-proceedings-of-spie/11018/2518514/Stone-Soup%E2%80%93announcement-of-beta-release-of-an-open/10.1117/12.2518514.full.

[16] H. Chen and Y. Bar-Shalom, 'Track association and fusion with heterogeneous local trackers,' in *2007 46th IEEE Conference on Decision and Control*, New Orleans, LA, USA: IEEE, 2007, pp. 2675–2680, ISBN: 978-1-4244-1497-0. DOI: 10.1109/CDC.2007.4434638. [Online]. Available: http://ieeexplore.ieee.org/document/4434638/.

[17] B. F. La Scala and A. Farina, 'Choosing a track association method,' en, *Information Fusion*, vol. 3, no. 2, pp. 119–133, Jun. 2002, ISSN: 15662535. DOI: 10.1016/S1566-2535(02)00050-7. [Online]. Available: https://linkinghub.elsevier.com/retrieve/pii/S1566253502000507.

[18] L. Kaplan, Y. Bar-Shalom and W. Blair, 'Assignment costs for multiple sensor track-to-track association,' *IEEE Transactions on Aerospace and Electronic Systems*, vol. 44, no. 2, pp. 655–677, Apr. 2008, ISSN: 0018-9251. DOI: 10.1109/TAES.2008.4560213. [Online]. Available: http://ieeexplore.ieee.org/document/4560213/.

[19] Y. Bar-Shalom and Huimin Chen, 'Multisensor track-to-track association for tracks with dependent errors,' in *2004 43rd IEEE Conference on Decision and Control (CDC) (IEEE Cat. No.04CH37601)*, Nassau, Bahamas: IEEE, 2004, 2674–2679 Vol.3, ISBN: 978-0-7803-8682-2. DOI: 10.1109/CDC.2004.1428864. [Online]. Available: http://ieeexplore.ieee.org/document/1428864/.

[20] D. Gaglione, P. Braca and G. Soldi, 'Belief Propagation Based AIS/Radar Data Fusion for Multi - Target Tracking,' in *2018 21st International Conference on Information Fusion (FUSION)*, Cambridge: IEEE, Jul. 2018, pp. 2143–2150, ISBN: 978-0-9964527-6-2. DOI: 10.23919/ICIF.2018.8455217. [Online]. Available: https://ieeexplore.ieee.org/document/8455217/.

[21] E. Liland, 'AIS Aided Multi Hypothesis Tracker - Multi-Frame Multi-Target Tracking Using Radar and the Automatic Identification System,' M.S. thesis, Norwegian University of Science and Technology, 2017. [Online]. Available: http://folk.ntnu.no/edmundfo/msc2020-2021/.

[22] B. Habtemariam, R. Tharmarasa, M. McDonald and T. Kirubarajan, 'Measurement level AIS/radar fusion,' en, *Signal Processing*, vol. 106, pp. 348–357, Jan. 2015, ISSN: 01651684. DOI: 10.1016/j.sigpro.2014.07.029. [Online]. Available: https://linkinghub.elsevier.com/retrieve/pii/S0165168414003636.

[23] B. K. Habtemariam, R. Tharmarasa, E. Meger and T. Kirubarajan, 'Measurement level AIS/radar fusion for maritime surveillance,' in *SPIE Defense, Security, and Sensing*, Baltimore, Maryland, May 2012, pp. 83930I–83930I–8. DOI: 10.1117/12.920156. [Online]. Available: http://proceedings.spiedigitallibrary.org/proceeding.aspx?articleid=1354715.

[24] C. Carthel, S. Coraluppi and P. Grignan, 'Multisensor tracking and fusion for maritime surveillance,' in *2007 10th International Conference on Information Fusion*, Quebec City, QC, Canada: IEEE, Jul. 2007, pp. 1–6, ISBN: 978-0-662-45804-3. DOI: 10.1109/ICIF.2007.4408025. [Online]. Available: http://ieeexplore.ieee.org/document/4408025/.

[25] Suo Jidong and Liu Xiaoming, 'Fusion of radar and AIS data,' in *Proceedings 7th International Conference on Signal Processing, 2004. Proceedings. ICSP '04. 2004.*, vol. 3, Beijing, China: IEEE, 2004, pp. 2604–2607, ISBN: 978-0-7803-8406-4. DOI: 10.1109/ICOSP.2004.1442315. [Online]. Available: http://ieeexplore.ieee.org/document/1442315/.

[26] D. Danu, A. Sinha, T. Kirubarajan, M. Farooq and D. Brookes, 'Fusion of over-the-horizon radar and automatic identification systems for overall maritime picture,' in *2007 10th International Conference on Information Fusion*, Quebec City, QC, Canada: IEEE, Jul. 2007, pp. 1–8, ISBN: 978-0-662-45804-3. DOI: 10.1109/ICIF.2007.4408147. [Online]. Available: http://ieeexplore.ieee.org/document/4408147/.

[27] E. F. Brekke, A. G. Hem and L.-C. N. Tokle, 'The VIMMJIPDA: Hybrid state formulation and verification on maritime radar benchmark data,' in *Global Oceans 2020: Singapore – U.S. Gulf Coast*, Biloxi, MS, USA: IEEE, Oct. 2020, pp. 1–5, ISBN: 978-1-72815-446-6. DOI: 10.1109/IEEECONF38699.2020.9389007. [Online]. Available: https://ieeexplore.ieee.org/document/9389007/.

[28] A. G. Hem, 'Maritime multi-target tracking with radar and asynchronous transponder measurements,' M.S. thesis, Norwegian University of Science and Technology, 2021. [Online]. Available: http://folk.ntnu.no/edmundfo/msc2020-2021/.

[29] W. Kazimierski and A. Stateczny, 'Fusion of data from AIS and tracking radar for the needs of ECDIS,' in *2013 Signal Processing Symposium (SPS)*, Serock, Poland: IEEE, Jun. 2013, pp. 1–6, ISBN: 978-1-4673-6319-8. DOI: 10.1109/SPS.2013.6623592. [Online]. Available: http://ieeexplore.ieee.org/document/6623592/.

[30] S. Matzka and R. Altendorfer, 'A comparison of track-to-track fusion algorithms for automotive sensor fusion,' in *2008 IEEE International Conference on Multisensor Fusion and Integration for Intelligent Systems*, Seoul: IEEE, Aug. 2008, pp. 189–194, ISBN: 978-1-4244-2143-5. DOI: 10.1109/MFI.2008.4648063. [Online]. Available: http://ieeexplore.ieee.org/document/4648063/.

[31] J. Å. Sagild, A. G. Hem and E. F. Brekke, 'Counting Technique versus Single-Time Test for Track-to-Track Association,' in *24th International Conference on Information Fusion*, 2021.

[32] E. Brekke, *Fundamentals of Sensor Fusion*. 2019.

[33] R. G. Brown and P. Y. Hwang, *Introduction to random signals and applied Kalman filtering: with MATLAB exercises*. John Wiley & Sons New York, NY, USA, 2012, vol. 4.

[34] B.-n. Vo, M. Mallick, Y. Bar-shalom, S. Coraluppi, R. Osborne III, R. Mahler and B.-t. Vo, 'Multitarget tracking,' *Wiley Encyclopedia of Electrical and Electronics Engineering*, pp. 1–15, 1999, Publisher: Wiley Online Library.

[35] Y. Bar-Shalom and E. Tse, 'Tracking in a cluttered environment with probabilistic data association,' en, *Automatica*, vol. 11, no. 5, pp. 451–460, Sep. 1975, ISSN: 00051098. DOI: 10.1016/0005-1098(75)90021-7. [Online]. Available: https://linkinghub.elsevier.com/retrieve/pii/0005109875900217.

[36] D. Musicki, R. Evans and S. Stankovic, 'Integrated probabilistic data association,' *IEEE Transactions on Automatic Control*, vol. 39, no. 6, pp. 1237–1241, Jun. 1994, ISSN: 00189286. DOI: 10.1109/9.293185. [Online]. Available: http://ieeexplore.ieee.org/document/293185/.

[37] T. Fortmann, Y. Bar-Shalom and M. Scheffe, 'Multi-target tracking using joint probabilistic data association,' in *1980 19th IEEE Conference on Decision and Control including the Symposium on Adaptive Processes*, Albuquerque, NM, USA: IEEE, Dec. 1980, pp. 807–812. DOI: 10.1109/CDC.1980.271915. [Online]. Available: http://ieeexplore.ieee.org/document/4046781/.

[38] R. Fitzgerald, 'Track Biases and Coalescence with Probabilistic Data Association,' *IEEE Transactions on Aerospace and Electronic Systems*, vol. AES-21, no. 6, pp. 822–825, Nov. 1985, ISSN: 0018-9251. DOI: 10.1109/TAES.1985.310670. [Online]. Available: http://ieeexplore.ieee.org/document/4104154/.

[39] D. Musicki and R. Evans, 'Joint integrated probabilistic data association: JIPDA,' en, *IEEE Transactions on Aerospace and Electronic Systems*, vol. 40, no. 3, pp. 1093–1099, Jul. 2004, ISSN: 0018-9251. DOI: 10.1109/TAES.2004.1337482. [Online]. Available: http://ieeexplore.ieee.org/document/1337482/.

[40] H. Blom and Y. Bar-Shalom, 'The interacting multiple model algorithm for systems with Markovian switching coefficients,' *IEEE Transactions on Automatic Control*, vol. 33, no. 8, pp. 780–783, Aug. 1988, ISSN: 00189286. DOI: 10.1109/9.1299. [Online]. Available: http://ieeexplore.ieee.org/document/1299/.

[41] A. G. Bole, A. Wall and A. Norris, *Radar and ARPA manual: radar, AIS and target tracking for marine radar users*, 3rd edition. Oxford: Butterworth-Heinemann, 2014, ISBN: 978-0-08-097752-2.

[42] Y. Bar-Shalom, X. R. Li and T. Kirubarajan, *Estimation with applications to tracking and navigation: theory algorithms and software*. John Wiley & Sons, 2004.

[43] S. V. Boronaro, 'Converted measurement trackers for systems with nonlinear measurement functions,' Doctoral Dissertations, University of Connecticut Graduate School, 2015. [Online]. Available: https://opencommons.uconn.edu/dissertations/957/?utm_source=opencommons.uconn.edu%2Fdissertations%2F957&utm_medium=PDF&utm_campaign=PDFCoverPages.

[44] X. Tian, T. Yuan and Y. Bar-Shalom, 'Track-to-Track Fusion in Linear and Nonlinear Systems,' en, in *Advances in Estimation, Navigation, and Spacecraft Control*, D. Choukroun, Y. Oshman, J. Thienel and M. Idan, Eds., Berlin, Heidelberg: Springer Berlin Heidelberg, 2015, pp. 21–41, ISBN: 978-3-662-44784-0 978-3-662-44785-7. DOI: 10.1007/978-3-662-44785-7_2. [Online]. Available: http://link.springer.com/10.1007/978-3-662-44785-7_2.

[45] X. Tian and Y. Bar-Shalom, 'Track-to-Track Fusion Configurations and Association in a Sliding Window.,' *J. Adv. Inf. Fusion*, vol. 4, no. 2, pp. 146–164, 2009, Publisher: Citeseer.

[46] T. Kirubarajan and Y. Bar-Shalom, 'Kalman filter vs. IMM estimator: When do we need the latter?,' O. E. Drummond, Ed., ser. ignal and Data Processing of Small Targets, vol. 4048, Orlando, FL: International Society for Optics and Photonics, Jul. 2000, pp. 576–582. DOI: 10.1117/12.392013. [Online]. Available: http://proceedings.spiedigitallibrary.org/proceeding.aspx?articleid=905832.

[47] T. Zajic, 'Probabilistic track-to-track association,' I. Kadar, Ed., Baltimore, Maryland, United States, May 2015, 94740B. DOI: 10.1117/12.2177206. [Online]. Available: http://proceedings.spiedigitallibrary.org/proceeding.aspx?doi=10.1117/12.2177206.

[48] E. Brekke, O. Hallingstad and J. Glattetre, 'Improved Target Tracking in the Presence of Wakes,' *IEEE Transactions on Aerospace and Electronic Systems*, vol. 48, no. 2, pp. 1005–1017, 2012, ISSN: 0018-9251. DOI: 10.1109/TAES.2012.6178045. [Online]. Available: http://ieeexplore.ieee.org/document/6178045/.

[49] S. Mori, W. Barker, Chee-Yee Chong and Kuo-Chu Chang, 'Track association and track fusion with nondeterministic target dynamics,' *IEEE Transactions on Aerospace and Electronic Systems*, vol. 38, no. 2, pp. 659–668, Apr. 2002, ISSN: 0018-9251. DOI: 10.1109/TAES.2002.1008994. [Online]. Available: http://ieeexplore.ieee.org/document/1008994/.

[50] A. Farina and R. Miglioli, 'Association of active and passive tracks for airborne sensors,' en, *Signal Processing*, vol. 69, no. 3, pp. 209–217, Sep. 1998, ISSN: 01651684. DOI: 10.1016/S0165-1684(98)00103-0. [Online]. Available: https://linkinghub.elsevier.com/retrieve/pii/S0165168498001030.

[51] V. Bewick, L. Cheek and J. Ball, 'Statistics review 13: Receiver operating characteristic curves,' *Critical Care*, vol. 8, no. 6, p. 508, 2004, ISSN: 13648535. DOI: 10.1186/cc3000. [Online]. Available: http://ccforum.biomedcentral.com/articles/10.1186/cc3000.

[52] J. Å. Sagild, 'Track-to-Track Radar-AIS fusion,' Norwegian, The Norwegian University of Science and Technology, Pre-project thesis, Dec. 2020.

[53] X. Tian and Y. Bar-Shalom, 'Exact algorithms for four track-to-track fusion configurations: All you wanted to know but were afraid to ask,' 2009 12th International Conference on Information Fusion, 2009, pp. 537–544.

[54] H. Chen and T. Kirubarajan, 'Performance limits of track-to-track fusion versus centralized estimation: Theory and application,' en, *IEEE Transactions on Aerospace and Electronic Systems*, vol. 39, no. 2, pp. 386–400, Apr. 2003, ISSN: 0018-9251. DOI: 10.1109/TAES.2003.1207252. [Online]. Available: http://ieeexplore.ieee.org/document/1207252/.

[55] A. L. Flaten and E. F. Brekke, 'Rao-blackwellized particle filter for turn rate estimation,' in *2017 IEEE Aerospace Conference*, Big Sky, MT, USA: IEEE, Mar. 2017, pp. 1–7, ISBN: 978-1-5090-1613-6. DOI: 10.1109/AERO.2017.7943746. [Online]. Available: http://ieeexplore.ieee.org/document/7943746/.

[56] E. Mazor, A. Averbuch, Y. Bar-Shalom and J. Dayan, 'Interacting multiple model methods in target tracking: A survey,' *IEEE Transactions on Aerospace and Electronic Systems*, vol. 34, no. 1, pp. 103–123, Jan. 1998, ISSN: 00189251. DOI: 10.1109/7.640267. [Online]. Available: http://ieeexplore.ieee.org/document/640267/.

[57] X. Tian and Y. Bar-Shalom, 'Sequential track-to-track fusion algorithm: Exact solution and approximate implementation,' O. E. Drummond, Ed., Orlando, FL, Apr. 2008, p. 696 910. DOI: 10.1117/12.775570. [Online]. Available: http://proceedings.spiedigitallibrary.org/proceeding.aspx?doi=10.1117/12.775570.

[58] M. Beard, B. T. Vo and B.-N. Vo, 'A Solution for Large-Scale Multi-Object Tracking,' *IEEE Transactions on Signal Processing*, vol. 68, pp. 2754–2769, 2020, ISSN: 1053-587X, 1941-0476. DOI: 10.1109/TSP.2020.2986136. [Online]. Available: https://ieeexplore.ieee.org/document/9063553/.

[59] S. Coraluppi, M. Guerriero, P. Willett and C. Carthel, 'Fuse-before-track in large sensor networks.,' *J. Adv. Inf. Fusion*, vol. 5, no. 1, pp. 18–31, 2010, Publisher: Citeseer.

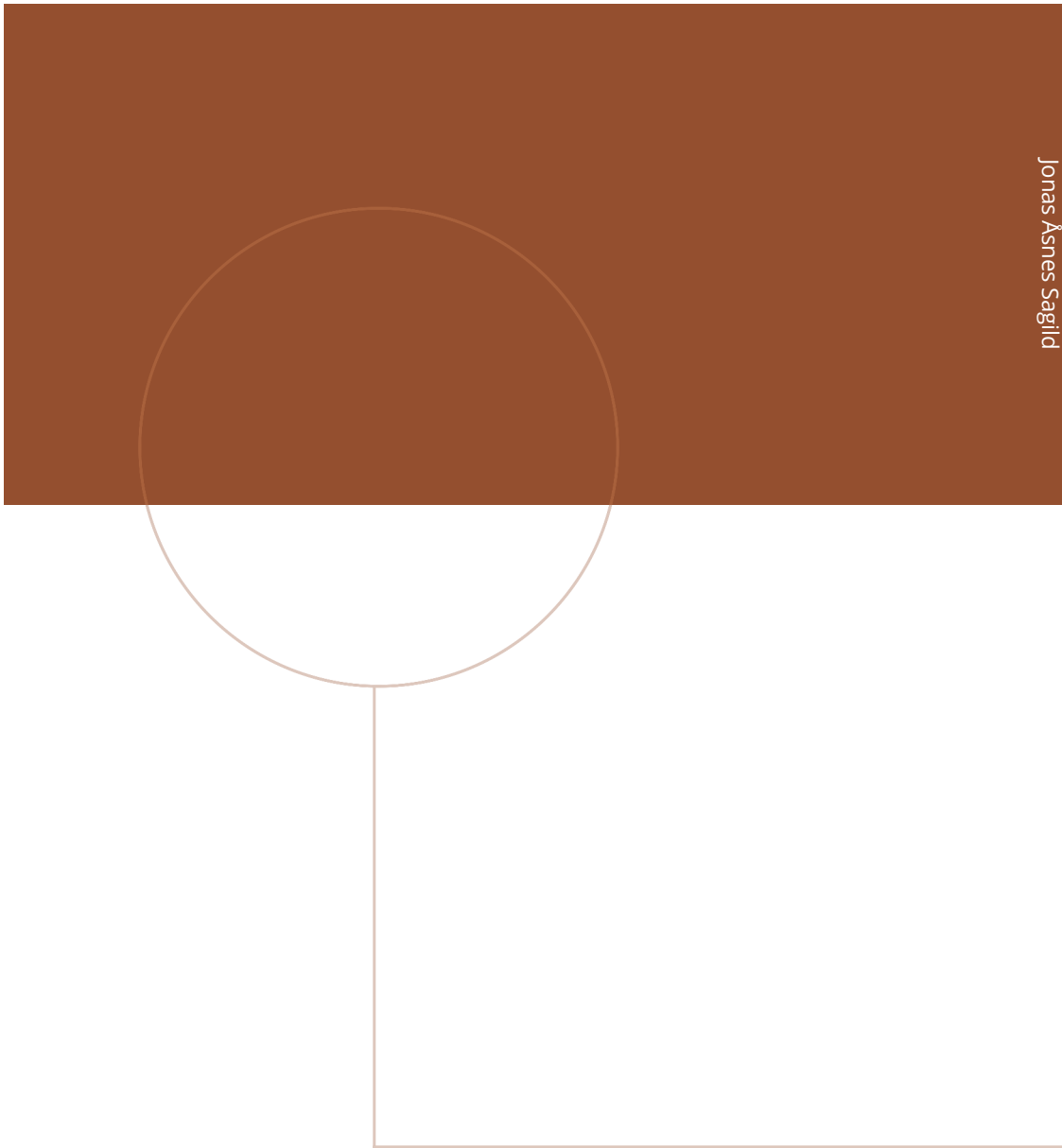

Jonas Åsnes Sagild

NTNU
Kunnskap for en bedre verden